CHALMERS
UNIVERSITY OF TECHNOLOGY

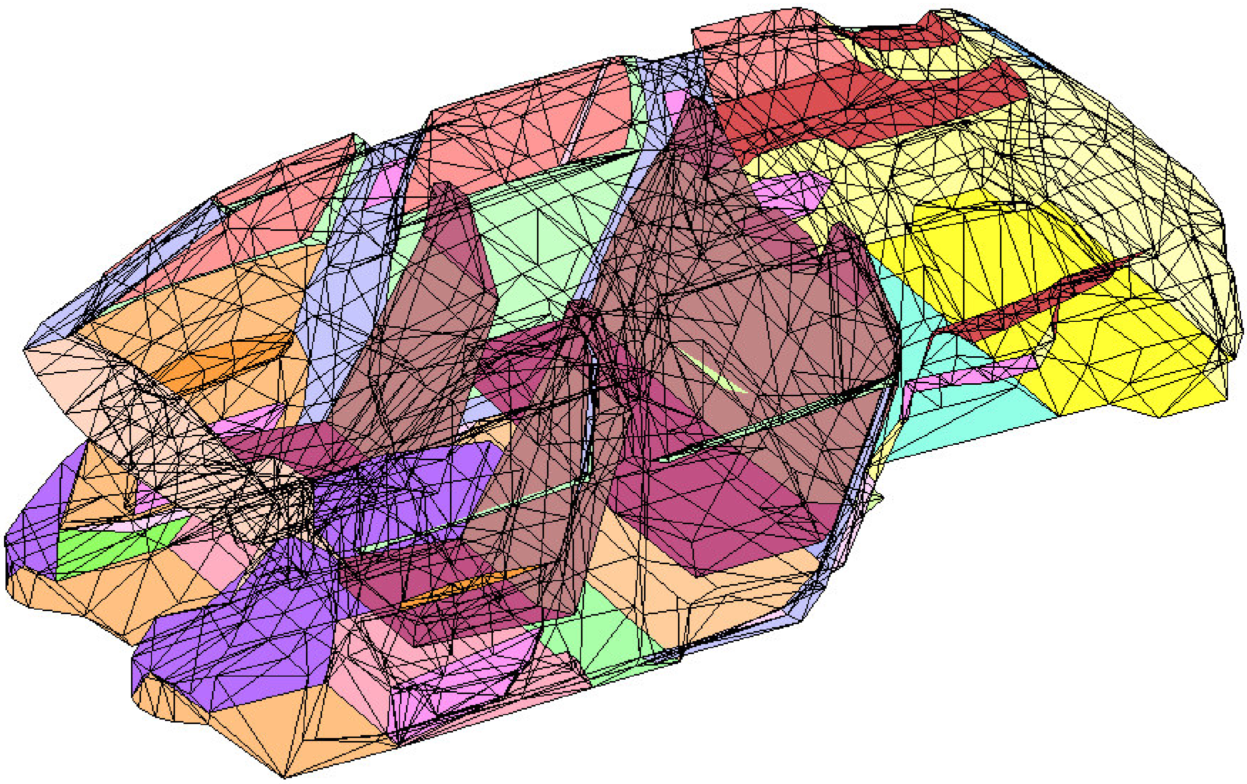

High frequency modelling of a car audio system

Master's thesis in Sound and Vibration

ALEKSANDRA PYZIK

Department of Civil and Environmental Engineering
CHALMERS UNIVERSITY OF TECHNOLOGY
Gothenburg, Sweden 2016

MASTER'S THESIS 2016:79

High frequency modelling of a car audio system

Master of Science Thesis in the Master's Programme Sound and Vibration

ALEKSANDRA PYZIK

Department of Civil and Environmental Engineering
Division of Applied Acoustics
Room Acoustics Group
CHALMERS UNIVERSITY OF TECHNOLOGY
Göteborg, Sweden 2016

High frequency modelling of a car audio system
Master of Science Thesis in the Master's Programme Sound and Vibration

Master's Thesis 2016:79

Department of Civil and Environmental Engineering
Division of Applied Acoustics
Room Acoustics Group
Chalmers University of Technology
SE-41296 Göteborg
Sweden Tel. +46 31 772 1000

Cover: *CATT-Acoustic* model of XC90.

Printed by Department of Civil and Environmental Engineering
Göteborg, Sweden 2016

High frequency modelling of a car audio system
Master of Science Thesis in the Master's Programme Sound and Vibration
ALEKSANDRA PYZIK
Department of Civil and Environmental Engineering
Division of Applied Acoustics
Room Acoustics Group
Chalmers University of Technology

Abstract

Geometrical Acoustics is a widely used room acoustic modelling tool. It is based on the assumption that sound energy travels along the rays, that can be treated as in optics. GA neglects the wave phenomena and is applicable only at high frequencies relative to size of the models. Since GA is commonly used for the large rooms simulations (e.g. concert halls, churches, auditoria) the method can be safely applied in the entire audible frequency range. The use of this methodology in cars is still scarce and opened to research. Due to their size it is restricted to higher frequency range.

The scope of the thesis was to study the feasibility of using the GA method for high frequency simulations of the car loudspeakers. The units of interest were midrange and tweeter of the Bowers&Wilkins Premium Sound System, the top level audio system offered by Volvo XC90. The opportunity to supplement the FE based predictions of the low frequency loudspeakers with reliable GA simulations for the high frequency loudspeakers would speed up the designing process and move it to the earlier stage of the car development projects.

The investigation was conducted at three trim levels with increasing complexity: Body-in-Blue, trimmed body without seats and trimmed body with seats. The GA models of the car compartment for all three stages were created, based on the CAD data provided by Volvo. Those were read into *CATT-Acoustic*, the GA based software that was chosen mainly due to the advanced support available on-site from the developer. The investigation on the input data was carried out. It included the *in-situ* measurements of the car material parameters using the Microflown PU probe and the measurements of the directivity of the loudspeakers in anechoic conditions. The FRF measurements were carried out in XC90 cars for all three trim levels to provide verification data. In subsequent simulations several different algorithms and settings available in the GA software were tested. The results were compared with the measured data and assessed based on the collected responses. The aim of the work in a long run would be to create the sound files that can be subjectively assessed by the Audio Team engineers.

Keywords: room acoustics, Geometrical Acoustics, sound field in small rooms, FRF, IR, absorption coefficient, impedance, scattering coefficient, loudspeaker directivity

Contents

Acknowledgements

This thesis was carried out in the NVH department of Volvo Cars Corporation. Therefore, I would like to thank all the colleagues from Volvo who were involved in the work: Vito Di Fonzo, Andrzej Pietrzyk and Magnus Taskinen for initiating the project, and Henrik Törnqvist, Parinaz Sedarati and Erik Nyström for help with the measurements.

Special thanks to Bengt-Inge Dalenbäck from *CATT-Acoustic* for his great knowledge input and technical support with the GA software.

I would like to thank Wolfgang Kropp, my supervisor at Chalmers University of Technology, for his help and patience during those rare moments when I was completely lost. Also, thanks to Lars Hansson for help with measurements conducted at Applied Acoustics.

Thanks to Andrzej Pietrzyk, my supervisor at Volvo Cars, for help and for stressing me out in order to motivate me to work even harder. And Lisette for distracting me so I was not stressed too much.

Last but not least, I would like to express my gratitude to all my family and friends from Poland for their endless long-distance support and encouragement. In particular to Krzysiek, Antosia and my parents.

Notations

ALG1	Algorithm 1 in *CATT-Acoustic v. 9.0* software
ALG2	Algorithm 2 in *CATT-Acoustic v. 9.0* software
BEM	Boundary Element Method
BIB	Body-in-Blue
CAD	Computer Aided Design
FE	Finite Element
FEM	Finite Element Method
FRF	Frequency Response Function
FFT	Fast Fourier Transform
GA	Geometrical Acoustics
HF	High Frequency
IP	Instrument Panel
IR	Impulse Response
ISM	Image Source Method
LF	Left Front
LOD	Level of Detail
NVH	Noise Vibration Harshness
RF	Right Front
SPL	Sound Pressure Level
TF	Transfer Function

A1	Omnidirectional source - position 1
A2	Omnidirectional source - position 2
B1	LF midrange loudspeaker
B2	LF tweeter loudspeaker

1. Introduction

Geometrical Acoustics is a geometry based room acoustic modelling method. The principle of the method is that the sound wave is approximated by the concept of the sound ray. The sound ray undergoes the same laws as ray in the geometrical optics, apart from different propagation velocity. The rays carry the specific amount of sound energy and when they hit the surface a defined part of the energy gets absorbed, reflected or transmitted. The GA method is applicable for high frequencies. The low frequency limit is stated by the surface dimension. It has to be larger than the shortest wavelength of interest [1].

The aim of the project was to study the possibility of GA usage in high frequency modelling of the Volvo audio system. Currently, Volvo uses well developed FE based methods to support most of the design processes. During work on the sound system design the Audio group is supported with FE calculations for low frequency part of the project. That means the sub-woofer or woofer design. The high frequency part is only evaluated during subjective listening tests in the prototype vehicles and actual cars. Both of them have restricted availability. In a long run the purpose of the thesis is to help the Audio group in creating the virtual environment, when the high frequency loudspeakers (midrange and tweeter) can be evaluated before building the real car structure.

The idea of the project was to create the virtual testing environment allowing subjective evaluation of the system in the whole audible frequency range. The low frequency part would be provided by the FE methods that are developed at the company. The high frequency part would be covered by the GA simulations. The prediction results could be then merged and the sound files for the Audio team could be created using the auralization principle. Such a solution would help to create the new design in much shorter time and without the massive use of the Volvo vehicles.

However, there are many aspects that has to be studied in order to develop the high frequency modelling tool at the company. The focus of the thesis was on verification if the GA based method could be used for this purpose. In order to create the realistic GA models the study on the input conditions had to be done. It included the research on boundary conditions and the source directivity. The GA simulations were conducted using a GA software developed in Göteborg: *CATT-Acoustic v. 9.0c 3.01*. The verification of the predictions by physical measurements was the final step of the work. Also, different possibilities of the results improvement were investigated, discussed and suggested in a scope of the work.

Generally, the tasks included in the thesis were:

- Measurements of normal impedance of materials using Microflown PU probe
- Normal incidence impedance to random incidence absorption coefficient conversion (locally reacting structures are assumed) for the GA simulations
- Creating the GA models of the three trim levels of a car compartment
- Investigation on influence of scattering coefficient in the GA simulations
- Measurements of directivity of the car audio system loudspeakers
- Measurements of FRFs in the car cavity excited with HF speakers in order to obtain verification data
- Simulation of the car compartment sound filed
- Analysis and verification - comparison of modelled and measured data

Possible further work could cover the following problems:

- Further investigation on influence of scattering coefficient
- Investigation on the diffraction model in GA simulations to see if it can improve the results
- Further tuning of GA model
- Creating the FE model for low frequency part
- Merging results of GA with FEM
- Study on the influence of the passengers in the car on the sound field
- Auralization
- Listening tests to assess the quality of auralized binaural signals

2. Background

Since 1950 many publications dealt with the challenge of the realistic simulation of the reverberation time of the rooms. The theoretical basis of the impulse response in time and frequency domain was derived by Bolt (1947), Schroeder (1954), and Kuttruff and Thiele (1954). Also, the simple analog feedback loops were used to create an artificial reverberation time. In 1960 the first computer aided simulation tools were used based on the Geometrical Acoustics theory. First application used ray tracing techniques [2] and soon the image source techniques were in use as well. Presently, there is a number of commercial modelling tools that are the hybrid programs, combining ray tracing, image source and beam tracing techniques. The most known and world widely used packages are *CATT-Acoustic*, *ODEON* and *EASE* [6].

Although, the GA cannot capture wave phenomena of the sound as it is approximate energy-based method, it is considered valid for high frequency range. Meaning, frequencies that have smaller wavelength than the modelled elements. It might not be a problem for large concert halls, but makes it difficult to realistically model the small interiors. Therefore, the application of Finite Element Method at low frequency range was suggested in 1990, when the computers started to be powerful enough to solve room acoustic problems. Currently, the combination of FE-based and GA-based methods seems to be the solution for prediction of a sound field within whole audible frequency range.

In the scope of this project the GA-based simulation was studied with the aim to continue the work in order to combine the results with FE modelling. The extension of classical GA with wave based methods would allow to obtain the IR of the car compartment interior. The final stage of such a prediction could be an auralization and subjective evaluation of the obtained sound files [6].

Within the last decades the two large projects were conducted with exactly this aim: to simulate the sound field of a car compartment in the whole audible frequency range using the FE-based and GA-based methods. The following chapter includes the explicit description of these two projects conducted for automotive clients. These two projects were the basis and the inspiration for the following master thesis.

2.1. Chalmers Univeristy of Technology project

A first extensive study on the acoustical prediction of a car compartment was done in 1993 by Granier in collaboration with Renault-Volvo company and the Department of Applied Acoustics, Chalmers University of Technology [5]. The project aimed for prediction of sound system design in early stage of car production was conducted.

In general, Granier stated that audio system simulations have two main functions: understanding the acoustical behaviour of a sound system and predicting the sound field in a specific car volume. He divided the sound field analysis into three stages: model of the sound source, model of the room (car compartment) and influence of the listeners presence in the car. In a scope of his work he focused on one of the problems the influence of car model on the results. As a result the source model was simplified to a point source and the human head was replaced by omnidirectional microphone. The resulting impulse response was therefore called monoaural impulse response and this stage of the study was named monoaural prediction.

2.1.1. Methods

The acoustical model used in a scope of work was a hybrid model: FE method for low frequency range and GA for high frequency range. The FE calculations were conducted using *SYSNOISE 4.4* software and for GA computations *CATT-Acoustic* software developed partially at the department of Applied Acoustics was used. *CATT-Acoustic* evaluated the main acoustic parameters and the impulse response of the volume. The cross-over frequency between the two analysis was set to Schroeder frequency (see Equation 3.1). However, it was stated that this frequency may change due to the level of detail - as the GA cannot take into account the fine details of the model. At the end, the cross-over frequency was chosen experimentally. The simulation data was later verified with data measured in the existing models and the accuracy of the method was studied. Three different models were examined.

The input data needed for the simulations was prepared in the following way:

- **Geometry and mesh** - for GA models the element size was set to be larger than the smallest wavelength (that is around 1.7 m at 500 Hz) and for FEM models the restraint was 6 nodes per wavelength.
- **Material characteristic** - for GA models the absorption coefficients per octave band were needed. The absorption coefficients were measured using Kundt's tube and reverberation chamber methods and the normal impedance values were obtained from the two microphones method. The limitations of the methods were discussed. For FE models the "locally reacting" materials that can be completely defined by normal impedance were specified with *SYSNOISE*.
- **Directivity of loudspeaker** - the directivity of a loudspeaker was measured in an anechoic chamber.

2.1.2. Results

The simplest considered model was a rectangular 1:3 scaled model built with 10 mm thick plastic walls - the full size model dimensions were 1.5x2.3x1.8 m. One microphone and one speaker position was used in the measurements. The comparison with the

FEM calculations for the rectangular box with rigid and absorptive walls (with porous material mounted) was satisfying. The GA simulation was run only for the absorptive walls, no scattering was assigned in the model, as it was not introduced in the software yet. The results of GA calculation for such a simple model were very good - especially for higher frequencies. Though, due to strong flutter echo and strong first modes the model was not suitable for listening.

In order to remove these effect more complicated shape was used - the car compartment outline. Again a 1:3 scaled model was built and the materials were chosen so that they corresponded more to the real car compartment. The speaker was placed in the same way as in a real car and the microphone positions corresponded to the driver's and passenger's ears. Similarly to the simpler model, the FEM calculations matched well the measurements - except the neighbourhood of the first mode. Impulse response simulated by GA software matched only the frequencies between 500 to 2000 Hz and for 4000 Hz the results mismatch the calculations. However, this was explained by the strange behaviour of the porous material chosen to cover the walls.

The last model used in the scope of work was an estate car Volvo 850. The measurements of impulse response were conducted for 3 locations of the loudspeaker and 6 microphone positions. The BEM results did not match the measurements and the reason was though to be too many rough approximations such as:

- The material of known impedance covering the door panels was assumed to be backed up by rigid walls - in reality more energy could dissipate due to coupling between the air and the structure. The suggested improvement was to measure the real impedance of the door panels treated as a whole.
- The coupling between the car cavity and small volumes (i.e. inner space between the headliner and the car body) was not taken into account - and in reality it could cause significant differences at low frequencies.
- The influence of the internal behaviour of the seats was not considered and the possible sound leakage at the dashboard near pedals was ignored.

Generally, a more complex geometry model was suggested as a solution to improve BEM results, but that was hard at this stage of work due to long computation time.

The GA method provided good global results for complex model, but the detailed results, such as transfer functions, differed from the measurements. So, the only data that could be evaluated for the complex model was for example level per octave or very general shape of the decay. As expected, the accuracy of the predictions increased with frequency.

The main outcome of the work was that the amount of data needed for both simulation methods was very big project in itself. The simulations required very good databases of material parameters, model geometries and source descriptions. Since, the FEM gave satisfying results for simple models, the further work on complex models was suggested. The GA methods were recommended only for obtaining a general idea of the sound behaviour in the higher frequency range. However, a number of approximations influenced the predictions to extent that the evaluation of details was impossible.

2.2. RWTH Aachen University project

In 2012 the PhD dissertation on the extensive work of Aretz was published. It was conducted at the Institute of Technical Acoustics at RWTH Aachen University and covered a research on combined wave and ray based room acoustic simulations of small rooms. A part of the study was devoted to the car compartment sound filed and was carried out together with a car company partner. There were three main questions that were dealt by Aretz in his PhD dissertation [6] and papers (Part I [7] and Part [8]):

1. Which data is required in the FE and GA domain and how does the different input data in both domains relate to each other?
2. Which measurement methods or calculation models exist to determine the required data?
3. What are the conclusions from the results and their uncertainties in the case of the car materials and loudspeakers?

In the scope of his work Aretz investigated two different goals. One of them was the influence of particular aspects on the different method simulation accuracy. These aspects were:

- Potential of image source method used in a low frequency range of a Room Transfer Function to predict its modal characteristics.
- Study of efficient modelling of porous absorbers in FEM domain.
- Study on the possible low frequency coupling of the excitation velocity of a loudspeaker to the sound field at the loudspeaker membrane.

Another goal of the project was to explore the overall potential in the combined approach in room acoustics modelling. It was done by extensive subjective and objective comparison of measurements and simulation results for three types of small spaces: a scale model of a reverberation room, a recording studio and two car compartments (Model 1 and Model 2). In the following report only the part covering research on car compartments is discussed. Aretz conducted and extensive study of the parameters of the materials and source data used in the spaces that are later used in the simulations [7].

Aretz remarked that the general challenges of car compartment simulations are similar to those met in the predictions of small rooms such recording studios. However the car compartment faces additional difficulties.

- First of all, a car compartment is not primarily designed for music listening such as control rooms are. This is not a problem itself in the room acoustics simulation, though it conveys very little or none a priori information on acoustic characteristics of boundary materials and sound sources in the compartment.
- The materials used in studios are usually carefully chosen so that the sound field in the room provides good listening conditions. Meanwhile, in the car compartment the materials are not only not designed to satisfy these conditions, but also they are not accessible to easy determination of the acoustic characteristics, as they are mostly inhomogeneous and have curved shapes.
- Additionally, the GA simulations in the car compartments face limitations due to diffraction at the edges of the seats (including the seating, back and head rest parts and curved surfaces).
- Also high geometrical details in the car cavity call for the very exact modelling that raises the lower frequency range limit for GA or for the high approximation level for FE.
- The proximity of the sound sources to the receivers and all the surfaces (both reflective such windscreen or windows and absorptive such as seat or trim materials) can cause errors in simulations.
- Another question arises when it comes to inclusion of receivers in GA and FE models, since the car compartment has a very small volume and it is not clear how far the presence of passengers influence the sound field [6].

2.2.1. Simulation methods, tools and settings

Aretz et al provided a combined simulation approach that used frequency-domain FE method to calculate the mode dominated low frequency part of the TF and time-domain GA algorithms for the high frequencies of the TF. The FE simulations were conducted with *LMS Virtual Lab Rev 9-SL3* and the GA part was run using the hybrid tool *RAVEN* developed at *ITA of RWTH Aachen University*. It combines image source method for low order reflections and stochastic ray tracing for late part of the impulse response. The results were fused together in the frequency domain using a cross-over filter. Low-pass filter for the FE simulations and high-pass for GA simulations. The cut-off frequencies were set at the same frequency for both filters. To generate true binaural results in the FE model a dummy head (without body) was included, as the test measurement in a real car was conducted with use of a dummy head as well. In GA model however the geometry of the head was not included, but the binaural cues were effectuated using head related transfer functions (HRTFs) measured in the scope of the work.

The FE model was built with elements of 80 and 40 mm that correspond to the simulations up to 1250 and 4000 Hz respectively, when the element size is to be set as 3 times smaller than the shortest wavelength of interest. 4000 Hz has exceeded the rule, but the actual cross-over frequency between FE and GA was set one octave below the highest FE simulation frequency. Around 4000 Hz the slight errors in the FE simulations were already attenuated by the filter roll-off. The GA models consisted of 188 and 585 planar polygon surfaces what allowed a maximum image source reflection order of 2 using *RAVEN*. Also, for ray-tracing a number of 500000 particles was used, time resolution of the energy histogram set to 1 ms and the diameter of a receiver sphere was 14 cm.

Over the past decades several methods for measuring acoustics surface complex impedance Z_S or absorption α of the material have emerged. During his work Aretz used several methods to collect boundary data and compared the reliability of different methods. He used ISO standard methods such as ISO 10534-2:1998 for impedance tube measurements and ISO 354:2003 for the reverberation room measurements as well as the Microflown PU probe and two-port network models. Details about the measurements and broad comparison between results obtained with different methods are fully discussed in his PhD thesis [6].

Since the absorption coefficient can be successfully obtained out of the acoustic surface impedance but not necessarily the other way around, in a scope of the discussed thesis the aim was to obtain the consistent data for bot FE and GA simulations from broadband impedance data. Therefore, whenever it was possible the boundary data was determined using methods measuring the acoustic surface impedance rather than purely energetic methods (e.g. described in ISO 354:2003) that totally neglects the phase shift upon reflection. Eventually, the data used in simulations was: for car seats - absorption and impedance data from the two-port network model (absorption and impedance values was calculated for field incidence conditions as described in [9]); for car mats and floor carpet in the foot space - two-port network model; for headliner: reverberation chamber data; for dashboard, door lining and back shelf: reverberation chamber data (it is suggested after [10] that Microflown PU might not give reasonable results); for windows: the windows could be considered as acoustically rigid, though the two-port network was provided again in order to capture small damping at low frequencies; for console and dashboard: due to difficulties in conducting the reliable impedance measurement and due to similarities of the material to those of the dashboard the boundary data of the dashboard was used; for other materials: back sides of the seats and the areas under the seats were not expected to strongly contribute to the overall damping in the car compartment, so due to lack of any measured data the absorption coefficients of 0.15 and 0.3 relatively were assigned to those surfaces, an according real-valued impedance was calculated on the basis of the estimated broadband absorption value [7].

In a scope of his work Aretz decided to not to go deeper regarding the possibilities to measure and evaluate reasonable values of scattering coefficient inside the car body. Instead he suggests to assigned the scattering coefficient of 0.05 for window surfaces and 0.3 for all other materials.

The sound sources had to be modelled differently for both FE and GA methods. In the FEM domain the source could be modelled as an effective membrane surface moving with certain normal velocity v_n. The normal velocity v_n was measured at 1 V input voltage with a Laser Doppler Vibrometer. In the GA domain the loudspeakers were modelled as point sources emitting rays in every direction. To properly model the source the directivity of the speakers should be measured to adjust the distribution of energy sent in all frequency bands. Also, the free-field sound pressure at 1 m distance and 1 V at the loudspeaker input should be known. These data were measured in line with the standard "IEC 60268 - 5:2003 + A1:2007: Sound system equipment - Part 5: Loudspeakers" [7].

The receivers were placed at four positions corresponding to the potential passengers' heads. The results were presented only for the driver position as the other results supported obtained conclusions. Moreover, the preliminary subjective assessment of simulations and measurements was conducted in the course of the small listening test. 10 workers of ITA were asked to compare the measurements to the auralizations and to freely write their comments regarding the differences they could perceive (artifacts, localization, coloration, reverberation). While this kind of subjective evaluation was not a real listening test with all statistical information, it helped to find out what were the most important aspects for subjective assessment of sound simulation quality.

2.2.2. Results and findings

The comparison of the test measurements and the combined FE and GA simulations included: SPL values for narrow and third octave bands, reverberation time T20 and spectrograms. As mentioned before two different car compartments provided by car company partner were studied. Comparison presented in the report included monaural results for a small dodecahedron source in car model 1 and monaural and binaural results for car speakers in both car compartments.

The following guidelines and conclusions were drawn from the number of comparison of simulation and measurement results:

- In the FE model the dummy head geometry should be included if high quality prediction is required. For a higher frequency range even an inclusion of the geometry of the ears would benefit.
- FE model should be run to at least 3000 or 4000 Hz if the diffraction effects are to be captured. This can be done only with a very fine model. The GA simulation generally neglects the diffraction effects. In high frequency range the method works well and captures the frequency dependent distribution and reverberation characteristic very well, as diffraction in this region is not dominant and is modelled as scattering.
- In case of car model 1 excited with dodecahedron source the FE simulations exhibited big underestimation of SPL values in frequency range from 800 to 1200 Hz. The GA method provided much better results. This raised a question if FE method can deliver better results than GA in the frequency ranges with high modal overlap, especially when there are big uncertainties about the boundary conditions. As a result, FEM can provide a similarly stochastic results as GA,

since the approximations in boundary conditions lead to random phase relations between overlapping room eigenmodes. Realistic prediction can be obtained only if high quality complex impedance of all surfaces are known.

- In GA domain small errors in positioning and orienting the sound source may have a major effect on a lot the direct sound at the receiving position due to short distance between source and receivers. That is why it is of a particular importance to be very exact with source position and orientation.
- Precise prediction of the modal structure using FE simulations is impossible above Schroeder frequency (that is around 400 Hz in a car compartment). This is due to the fact that in higher frequency range with high modal overlap even small geometry changes lead to completely stochastic reformation of the room eigenmodes. So in such a small volume as car compartment every slight geometry change (e.g. seat regulation, steering wheel or back mirror adjustment) leads to a change in the sound field. Therefore, the best sound prediction is the sound decay and sound energy level in a room.

In general, the study revealed that the simulation can give a good insight in energy distribution in time and frequency domain even in rather complex cavities. Although, the big limitation are uncertainties regarding modelling boundary surfaces (as mentioned above) and realistic sound sources. These problems indicates that in order to improve the sound field predictions the measurement techniques determining material properties should be improved and the sound sources representation should be as exact as possible.

3. Theory

The chapter describes the room acoustic methods, especially Geometrical Acoustics. It also explains why GA can be superior to FEM in particular cases. Then the theory behind the boundary conditions and the representation of the sound sources and the receivers in GA is presented. Finally, a brief description of signal processing tools is included. It covers the basis of the impulse response, Fourier Transform, filtering and auralization.

3.1. Room Acoustics

Computerized room acoustics modelling has been practice for almost 50 years now. Today, this type of modelling plays important role in the room acoustic designs. Also, it can help in creating virtual sound field for applications such as computer games, cognitive research and training [18].

Room acoustic modelling provides acoustic parameters that characterize the sound field. It also enables the possibility to listen to the acoustic of the space under design, which is called auralization. The basis of auralization is presented below in Section 3.3. There are two main approaches of room acoustic modelling. One is based on representing the room response in frequency domain, modelling it as the superposition of many decaying harmonic eigenmodes and numerically solving the wave equations (e.g. FEM). Another is based on the assumption of Geometrical Acoustics (GA) where the room energy echogram is modelled as a temporal succession of sound pulses reaching the receiver after several reflections [6]. In principle, wave-based calculations yield more accurate results, but are computationally more expensive especially for higher frequencies. GA on the other hand is faster and more approximate energy-based technique. The Finite Element Method (FEM) is a technique for finding the numerical solution of partial differential equations for given boundary conditions and is used in many engineering applications. In acoustics it is mostly used for modal characteristic prediction of a structure borne, airborne or coupled sound fields in enclosures. In GA, all the wave properties of sound are neglected and sound energy is assumed to propagate along rays. This concept is similar to the concept of geometrical optics. Such simplification is valid for high frequencies, where the wavelength is short compared to the surface dimensions. At lower frequencies the approximation errors increase as wave phenomena play a larger role [18].

However, high computational time for FE methods seems to be a vague argument nowadays when new computer technologies are introduced and faster and faster machines are available. Another advantage of GA method over FE in high frequency range is a possibility to capture a physical behaviour of boundaries, receivers and sources using approximations. To properly model the sound field in high frequency in FEM the extremely fine mesh would be required. At some point the model would have to include the porosity of the materials and very precise representation of receivers and sources. The approximate energy-based GA method makes it possible to model their general behaviour. GA enables to represent the physical aspect of the boundary by defining its absorption, scattering and transmission coefficients. And the source behaviour can be described with its directivity pattern.

Eventually, for the full audible frequency range simulation a hybrid methods linking FE and GA could be a solution, as suggested in previously presented projects. The general idea is shown in a Figure 3.1 below.

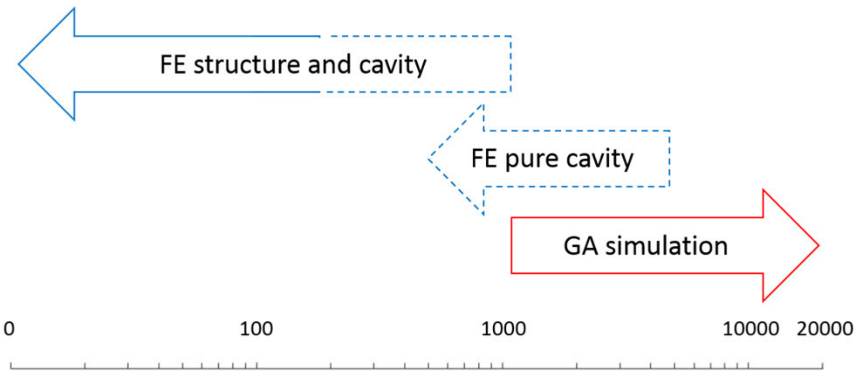

Figure 3.1.: Whole audible frequency range covered by the FE and GA methods.

The definition of the boundary frequency between the two methods is somewhat vague, but generally it is associated with number of modes at certain frequency. At low frequencies the modal overlap is smaller and the characteristic of the sound field in the cavity can be studied mode by mode independently. So the FE method can be used. At higher frequencies complicated modal superposition occurs and studying frequency curves in rooms are no longer useful for solving practical problems. Overlapping room modes are presented in Figure 3.2. The frequency range where this high overlap of modes occurs start above Schroeder frequency (where V denotes an enclosure volume in m^3 and T denotes reverberation time in s) [1]:

$$f_S \approx 2000\sqrt{\frac{T}{V}} \tag{3.1}$$

Above this specific frequency limit, numerous modes interfere with each other in the quasi-stochastic processes. This produces a characteristic features of the room transfer functions, that is sound pressure ratio between the source and the receiver. Essentially, our listening to the sound in the rooms can be hardly related to the room TFs. That is comparing the sound pressure at one point to the other. Room recognition is rather related to the subjective listening impression at one point in the room, the receiver location. And at that location the room impression is described mainly by the time-domain effects, reverberation.

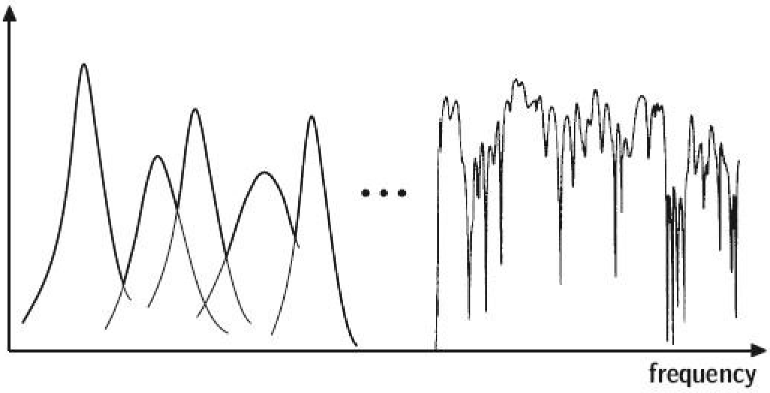

Figure 3.2.: Overlapping modes at low and high frequencies (borrowed from [17]).

The general formulation of room reverberation time was proposed by Sabine in 1898 (where T is reverberation time, V - volume of the room, α - average absorption coefficient, S - wall surface and m - air attenuation) [1] :

$$T = \frac{55V}{c(\alpha S + 4mV)} \tag{3.2}$$

3.2. Geometrical Acoustics

The main objective of GA is to provide time-energy decay and IR of a room, that are used to study a reflection, energy distribution and can be used to compute various parameters such as reverberation time (RT, $T30$, $T20$, $T15$), clarity ($C80$), sound strength (G) etc. The IR can be thought of as a particular signature of the room. The measurement method of the IR is described in the international standard ISO 3382-1 [4] and requires the information collected for at least two source and five receiver positions.

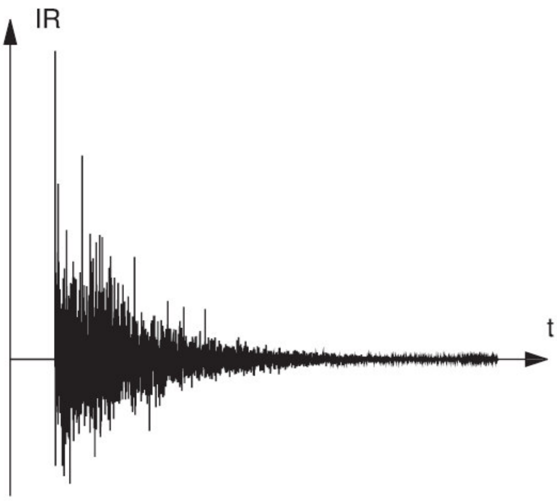

Figure 3.3.: A typical IR (borrowed from [17]).

A typical room IR (measured or modelled) is shown in Figure 3.3. It presents the propagation of the sound pressure from the source to the receiver. Such IR carries the information about three separate parts: direct sound, early reflections and late reverberation. Figure 3.4 presents the schematic reflection diagram, where all the parts of the echogram are highlighted. Each peak presents a single reflection path starting from the direct path that does not undergo any reflections. In the early part of the response most of the reflection paths can be seen separately and then over time they start to overlap. The reflections occurring in the room can be divided into specular or diffuse parts. A diffuse reflection propagates in any direction from the reflecting surface and specular reflection is as from a mirror. The amount of diffusely reflected energy is specified by a scattering coefficient. Also, the magnitude of the peaks depend on the absorption and transmission coefficients that describe the surface (all coefficients are discussed below in Section 3.2.1) [1].

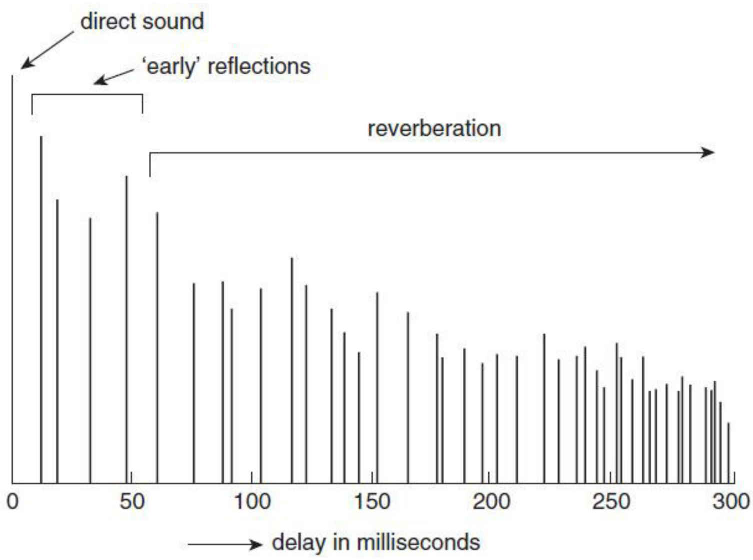

Figure 3.4.: Schematic reflection diagram (borrowed from [1]).

The GA is believed to be applicable if the wavelength is shorter than the smallest dimension of the surface used in the model. Usually, the GA models are prepared with element size no smaller than 0,5 m it corresponds to the frequency around 700 Hz. When special cases are to be discussed the smaller elements can be modelled. For example the wavelength of 5 cm already corresponds to frequency of 7000 Hz. Usually a lower range is of interest and that is because of the following reasons [17]:

- The spectral content excited by natural sources (voice, musical intruments) is small above 7000 Hz
- In broadband signal situations, masking will not allow humans to identify details of low levels at high frequencies

In the scope of this thesis mainly the high frequency modelling is of interest. As a car compartment volume is fairly small it was a plan from the very beginning to look especially at high frequencies. An XC90 model volume (just a cavity) is assumed to be around 5 m^3. If the smallest element is 10 cm then the reliable results can be obtained from around 3500 Hz and for 20 cm elements from 1700 Hz.

Most known modelling techniques used in the Geometrical Acoustics are:

- Ray tracing
- Image source
- Beam tracing

Ray tracing

In ray tracing technique the source emits number of rays. The ray travels throughout the room carrying a specific amount of sound energy. When it hits the surface part of the energy gets absorbed and transmitted through the boundary. The rest of it gets reflected. The ray can be reflected in a specular or a diffuse way. What happens to the ray hitting the surface is defined by the material parameters, usually given in frequency bands. Some of the rays eventually hit the receiver. Those rays contribute to the echogram, that describes the amount of energy reaching the receiver in time [26].

Ray tracing can be seen as a stochastic method, where the space is covered with rays, but never can be really filled, since the number of rays is finite. Increasing the number of rays in general shall improve the simulation results. That is also a reason for modelling the receiver as a sphere. In the ideal case the receiver should be an infinite point, but the detectors need to have a volume to be hit by the rays [18].

Image source

Image Source Method (ISM) is another modelling technique. The image sources are created by mirroring the sound source on the outer side of the room walls. Each of these sources emit the sound just like the original source does. From the receiver point of view the image sources create the first orders reflections from the surfaces. The path of the ray is reconstructed as the path from receiver starting towards the image source, and when the reflecting surface is hit, continuing towards the original source.

The disadvantage of the ISM is that the number of mirrored sources grows exponentially with the number of reflection orders. That is because the second order image sources mirror the first order sources and so on. Therefore, the ISM is possible only for low reflection orders [26], unless the geometry of the rooms is simple (e.g. rectangular room).

Beam / Cone tracing

Beam or cone tracing techniques make it possible to speed up the ISM. Instead of starting the rays from the sound source, the beam (cone) is sent. Ideally the sphere around the source is filled with the number of beams (cones), so that they do not overlap each other. The source is the apex of the beams (cones). Then, when the beam (cone) hits the surfaces it is reflected as in ray tracing. But it is at the same time flipped, so the apex of the new beam (cone) corresponds to the image source. When the beam hits multiple surfaces at the same time it is split into different beams. They are further flipped and traced. The reflection paths are examined by tracing backwards from the receiver. The beam tracing allows to compute a higher order of reflections in the same time when compared to the ISM [26].

In commercial modelling tools the hybrid methods are developed. This combination allows to capture different phenomenas and decrease the computational time.

3.2.1. Material parameters

Sound energy in an enclosure drops due to natural absorbers - properties of the materials in the building, air absorption (though in small rooms sound attenuation by air is small in comparison to other losses), objects in a room and people. Additionally, some part of the energy is transmitted through the boundaries and gets lost. The energy that reflects can be described as specularly and diffusely reflected rays. In GA simulations the reflections from the room boundaries are characterized by assigning the random absorption coefficient α_{diff}, scattering coefficient s and sometimes transmission coefficient τ. Figure 3.5 presents the principle of reflection for one ray. As Aretz presented in his work [6] characterization of boundaries is very important for the simulations accuracy.

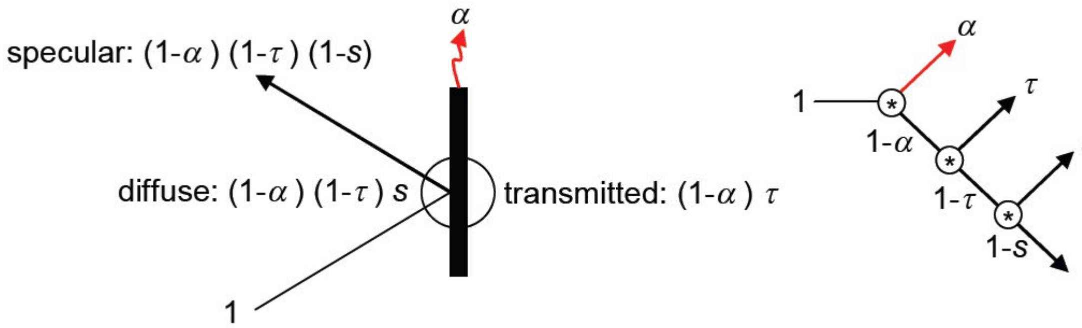

Figure 3.5.: Principle of reflection - including absorption, scattering and transmission coefficients (borrowed from [13]).

Absorption coefficient

Usually, the GA based software requires random absorption coefficient values given in frequency band averages (octave or third-octave bands). This means that both phase-shift at the boundary reflection and the angle dependence of the reflection coefficient are disregarded in typical GA simulations. It is concluded that at least for the late part of the IR this simplification is acceptable. It can be explained by the immense reflection overlap in the late part of the IR. In the late part the perfect reconstruction of a temporal structure of the IR is impossible anyway. Only in the early part of the IR, which may be modelled by the image source method at low reflection orders (in hybrid based software), the benefit from the angle dependent reflection coefficient can be achieved.

However, in this project as well as in Aretz [6] the car compartment is investigated. That means that the reliable results will be obtain at rather high frequencies and the IR is dominated by direct and first reflections. However, it can be a case also for the large rooms that are damped and equipped with controlled directive sound system. Although, strong scattering and diffraction effects occur at the car body boundaries [7] and they blur the IR shape in the late part anyway. The absorption coefficient should be given as values between 0 to 1 (or sometimes as percentages, 0 to 100%).

Scattering coefficient

The scattering coefficient is defined as ratio between energy that is reflected from a surface in non-specular way to the total reflected energy. The energy portion that is scattered can be determined in the following way [17]:

$$s = \frac{1 - E_{specular}}{E_{total}} \tag{3.3}$$

Similar reasoning as for absorption coefficient angle limitations applies to the scattering coefficient. The major difference here is that in contrast to the absorption coefficient, the scattering coefficient itself already constitutes a huge simplification of the scattering processes at a structured or rough surfaces. In a strict sense it only applies to ideally diffuse reflecting surfaces [7]. In GA software the angle dependence of scattering coefficient is typically dealt with according to the Lambert distribution [1].

In a scope of the work the scattering was not measured since it can be a big project in itself. Instead the specific values were proposed to simulate the detailed geometry of the car interior. The proposed values were comparable to the one proposed by Arezt (see Section 2.2). The specific values used in the GA models are presented later in method description in Section 4.2.2.

Transmission coefficient

The transmission coefficient describes the amount of acoustic energy that is transmitted through the boundary when the ray hits the surface. It is relative to an incident wave. In the GA software used during the project the inclusion of the transmission coefficient is optional. If not stated otherwise the transmitted part of the energy is included in absorption coefficient α. In the report this coefficient is not discussed any further.

3.2.2. Source and receiver conditions

As mentioned, GA method allows to capture the physical behaviour of the sound source. It is done by modelling it as a point source emitting rays in any direction into the room. In order to realistically model the directional sources (e.g. loudspeakers) the so-called directivity function D should be applied. It specifies the amount of energy that is sent with rays in particular direction around the source. The directivity function at any angle $D(\theta, \gamma)$ is defined as a ratio of frequency response at this angle to the on-axis response, when both are determined at the same distance from the source in a far field [6].

The directivity handling can be done with several available file formats. The one used in a scope of the project was SD0 supported by the GA software. It interpolates the data from values given in octave bands entered for a horizontal and vertical polar with resolution of 15 °. It is very approximate format, but was for this project the simplest to measure. The most detailed source representation of the source directivity is CF2. In CF2 the third-octave bands data is given at an equiangular grid of 5 ° [24].

The receivers on the other hand are modelled as spheres in the selected GA software. They collect the information about the sound energy when they got hit by the incoming ray. The information is saved in time domain as an IR.

3.3. Signal processing fundamentals

3.3.1. Impulse response

If a source and a receiver are assumed to be immobile, the acoustical space can be considered as a Linear Time Invariant system. Such a system can be characterized by the impulse response $h(t)$ in time domain and transfer function $H(\omega)$ in the frequency domain. IR can be described as the output of the system when it is excited with an ideal Dirac impulse (where $x(t)$ is an input signal and $y(t)$ is an output signal):

$$h(t) = \frac{y(t)}{x(t)} = \frac{y(t)}{\delta(t)} \tag{3.4}$$

And Dirac delta function is defined as:

$$\delta(t) = \begin{cases} 0 & t \neq 0 \\ 1 & t = 0 \end{cases} \tag{3.5}$$

The principle of IR is presented in Figure 3.6.

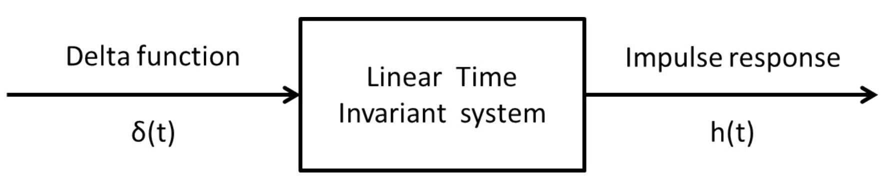

Figure 3.6.: Impulse response principle.

The IR of a room is its particular signature. And Fourier Transform (see Section 3.3.2) of the IR is the room transfer function. In room acoustics the accurate measurement of IRs is of high importance, as many objective acoustic parameters are derived from it (e.g. reverberation time, clarity, sound strength). Moreover, in present applications when the IR is known it can be convolved with any input signal in a complete auralization process in order to obtain the output signal [1].

Ideally, the response of the room should be frequency independent so none of the frequency components are exaggerated or boosted. However, it is very hard to achieve especially in small rooms due to sound reflections from the walls and objects and the formation of the modes within the audible frequency range. Therefore, the transmission path from the sound source to the receiver differs from point to point and is frequency dependant [3].

3.3.2. Fourier Transform

Sound is characterized by the pressure fluctuations, particle velocity, medium density etc. Therefore, it is a function of time. The GA based tools usually provide the characterization of the room as an IR. And as mention before the subjective impression of the room is commonly correlated to the IR. However, it is questionable if in such a special environment as a car compartment the subjective listening really corresponds to the IR.

The interior of the car is highly damped and its reverberation time is around 0.02 s. That may imply that the subjective listening impression could be described better by the room TF, since the human ear cannot recognize the changes in the IR in such a short time. Also, every small head movement in a car changes the sound perception. The time function IR can be transformed into the frequency domain signal using Fourier Transform. That is because time domain signal is at its basis a sum of harmonic functions. The Fourier Transformation of any signal is define as [17]:

$$S(f) = \int_{-\infty}^{\infty} s(t) \cdot e^{-j2\pi f t} \, \mathrm{d}t \tag{3.6}$$

$$s(t) = \int_{-\infty}^{\infty} S(f) \cdot e^{j2\pi f t} \, \mathrm{d}f \tag{3.7}$$

It is not only mathematical description of a signal, but it is said that human hearing can be described as transformation from time to frequency domain.

3.3.3. Filtering

While the measured or modelled IRs includes all frequency components, the main focus on the thesis is on the high frequency simulations. Since the GA method has its limitations the low frequency predictions can be erroneous. To make it possible to directly compare the measured and modelled IRs they have to be filtered so that the IRs do not include the contribution of low frequency part of the spectrum.

In signal processing a filter is a process of removing or suppressing unwanted components from the signal and extracting the important part of the data. In terms of frequency response of the filters there are several types of the filters, for example: low-pass, high-pass, band-pass and stop-band. In order to remove the low frequency components of the IRs the high-pass filter can be used. The high frequencies are passed and low frequencies are attenuated. Also, the band-pass filters can be applied to study the IRs for example within certain octave band.

3.3.4. Auralization

Auralization is a technique for creating sound files from the numerical data (measured, modelled or synthesized) that can be assessed over headphones (preferably) or speakers. In room acoustic applications basically the simulated binaural IR of a source room is convolved with an input sound file in order to obtain an auralization. Binaural IR corresponds to the IR at the two ears. Auralization of an acoustic space can be considered as analogous to visualization in optics [17].

The signal processing basis of auralization is convolution. Generally, the so-called dry source signal $s(t)$, that is free of reverberation and location cues is used in auralization. When the relevant IR $h(t)$ of the system is known from simulation or measurement the output signal $y(t)$ can be obtained by convolving the dry input signal with the IR of the room:

$$y(t) = \int_{-\infty}^{\infty} s(\tau)h(t-\tau)\,\mathrm{d}\tau = s(t) * h(t) \tag{3.8}$$

The procedure of convolution is the basis of signal analysis and processing and it applies only to linear time-invariant systems. The principle of convolution is presented in Figure 3.7. The convolution can be done in various ways - either directly in time domain as described by above Equation 3.8 or by using FFT convolution. Basically, convolution in time domain corresponds to multiplication in frequency domain So when room TF $H(f)$ is known then it can be multiplied with the FFT of an input signal $S(f)$ to obtain an output signal $Y(f)$.

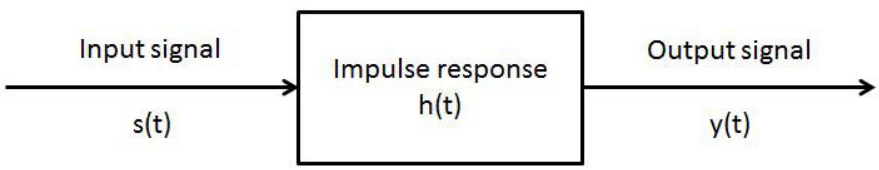

Figure 3.7.: Processing of an input signal with a room (filter) IR to obtain an output signal.

Input signals are related to the specific sources, typically musical instruments, human voice, electro-acoustic sources or noise-generating machines. Modelling and auralization of these sources are usually based on the sound signal recorded at a specific point (in the direction of main radiation or on the symmetry axis). For some of the sources such data can be found. The other possibility is to assume elementary radiation conditions or to measure the directivity in an anechoic situation (as described in Section 3.2.2) or in the near field [17].

Binaural hearing

Binaural cues of sound are introduced to the ear canal sound pressure due to sound diffraction, reflection and scattering over the pinna, head and torso. Usually, a plane wave is considered as the reference. The amount of that diffraction is described by the function called head-related transfer function (HRTF). It is defined as a fraction of the sound pressure measured at the ear drum (or at the entrance of the ear canal) and the sounds pressure measured at the position corresponding to the centre of the head when the listener is not present. The perceived differences between left and right ears can in a simplified way be described as interaural time differences (ITD) and interaural level differences (ILD).

The principle components of the HRTF are in the frequencies higher than 200 Hz. The head and shoulder affect the sound transmission into the ear canal at mid frequency range and the shape of the ear (pinna) contributes to the distortion at higher frequency range (around 3000 Hz). At this point HRTFs are dependent on the individual anatomic dimensions and can differ from person to person, as captured in Figure 3.8 [17].

The HRIRs (head-related impulse response) and HRTFs basically describe the filter. So to obtain the output signal either the input signal should be convolved with the impulse response HRIRs or it should be multiplied with the transfer function HRTFs.

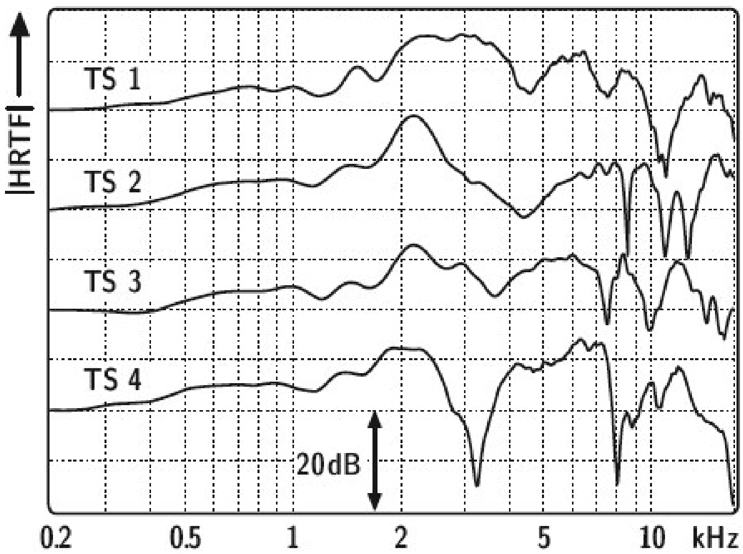

Figure 3.8.: Head-related transfer functions for four people, frontal incidence (borrowed from [17]).

4. Methods

The following chapter reports the methods used in the scope of the thesis to model the sound field in a car compartment. There is a presentation of input data measurements, simulations and the real car FRFs measurements. The measurements and the simulations were conducted at the passengers' ear positions, though the results are presented just for representative examples or, for some cases, as an average over all receiver points. The reason of such spatial averaging is that this method of sound field simulation is the first try in the company and there are still number of uncertainties regarding the input data measurements and use of the GA software. The main goal of a study is to show that the GA method can be successfully used for sound field simulation in a car. However, some improvements in obtaining the input data still have to be done.

The first part of the following chapter describes the methods used to obtain the input data. It includes the section on material parameters. In a scope of the project the independent measurements of the absorption coefficient were conducted, therefore there is a short description of the methods used. It explains how the Microflown PU probe works and the conversion of measured normal incidence impedance to random absorption coefficient needed for GA software. Then, the section on loudspeaker directivity explains how the measurements of the midrange and tweeter loudspeakers were conducted.

Second part of the chapter includes the brief characterization of the GA based software *CATT-Acoustic v. 9.0c 3.01* and its two calculation algorithms used in a scope of this project. Additionally, short explanation of possible settings in *CATT-Acoustic* calculation module *TUCT 1* is included. As well as brief information how the simulation data was post-process in *MATLAB*. Finally, the GA models of a car compartment are depicted. For modelling the sound field in a car compartment three trim levels were chosen. Body-in-Blue which is glass and metal interior. Trimmed body without seats, that is a car in final stage, just without the seats to simplify the geometry. And trimmed body with seats as a most complex case, representing the real car.

The last part of the chapter reports the measurements of the frequency response functions in a car compartment for all three cases. A number of different sources were used to excite the sound field and 10 receivers to collect the response. The receivers were located at both ears of potential five passengers. The simulated and modelled responses were normalized to the same input.

4.1. Measurements of input data

The input data needed for GA simulations include the boundaries conditions (absorption, scattering and transmission coefficient) as well as the information about the source. The input data measured in the scope of this thesis covered the absorption condition measurement, as scattering coefficient was decided to not be measured at this stage of the project. The sources used in the simulation were assumed to be omnidirectional for two special cases:

- Long tube opening mounted to the driver provided by Volvo
- Six drivers mounted on each side of a cube provided by Chalmers

Additionally, the directivity of audio system speakers from Volvo XC90 was measured in Chalmers anechoic chamber to collect data for GA simulations.

4.1.1. Material parameters

In a scope of the thesis the aim was to conduct the measurements of the absorption coefficient values. The scattering coefficient was not measured during the project. There was only a study done how alternation of scattering values change the results.

For the absorption coefficient measurements the newly bought Microflown PU probe was used. The impedance setup provided by Microflown as a package is presented in Figure 4.1a. The impedance gun consists of the calibrated loudspeaker, vibration isolated structure and a PU sensor. The quantities measured by the sensor are the particle velocity and pressure very close to the structure that enables direct calculation of complex surface acoustic impedance [20]:

$$Z = \frac{p}{v} \tag{4.1}$$

For the material parameters measurements the following equipment was used:

- Impedance gun (loudspeaker, vibration isolated structure and PU sensor)
- Scout 422 Data Acquisition
- Signal conditioner MFSC-2 channel
- Laptop with *Impedance 3.2* measurement system
- Cables (lemo probe cable, jack speaker cable, 2 BNC signal conditioner cables to sound card amplifier, USB sound card cable to laptop)

The provided software *Impedance 3.2* allows to obtain quantities such as sound intensity, acoustic impedance, reflection coefficient and absorption coefficient of not only the first layer of the structure but the whole structure. The characteristic of the material is defined by two measurements. One is taken as far as possible from any reflecting surfaces and is called calibration measurement. This measurement describes the behaviour of the loudspeaker and the general environment close to the specimen. The second measurement is taken very close to the sample. The incident and reflected pressure and velocity are collected by the PU probe and this data is an actual characteristic of the material. The measurement data is later post-processed in order to remove the room effects (signal ”smoothing” options). Three computational methods, based on point source model combined with free field and spherical wave fronts corrections, are given to get the impedance [21]:

- Plane wave reflection model - the simplest model assuming that the material under test is exposed to a plane wave.
- Mirror source model - more complicated model combining the mirror source concept and the plane wave reflection factor. This approach needs to be given source-to-probe and probe-to-sample distances.
- Q term method - including the spherical reflection coefficient. Requires source-to-probe and probe-to-sample distances.

All the methods are described broadly in [22]. In the scope of the thesis the second calculation method was chosen to obtain impedance and absorption coefficient. That is because during the test measurements the first model gave unreasonable result and second and third gave the very alike values, so the simpler model was chosen.

(a) (b)

Figure 4.1.: Microflown PU probe: (a) Microflown $^1/_2$ inch PU regular probe (borrowed from [20], (b) measurement *in-situ*.

The main reason for choosing Microflown PU measurement method was the possibility of conducting measurements *in-situ* (see Figure 4.1b). This is possible thanks to calibration measurements that is used for actual measurement ”smoothing” in post-processing. Also, this method determines the complex acoustic surface impedance that can be needed for FE models. Another method taken into account was absorption measurement in the reverberation chamber. But the purely energetic methods neglects the phase shift upon reflection and the collected data could not be used in FE modelling. Moreover, the materials used in a car interior are very often complicated and consist of several layers. The PU probe is supposed to describe the parameters of the whole structure of the material, not only its upper layer. Last but not least, the specimen can be relatively small in comparison to reverberation chamber method and it does not have to be destroyed as it is in case of Kundt's tube measurements. Although, as it is shown in [10] the most reliable results for Microflown PU method are obtained when the specimen size is around 30 x 30 cm. PU probe measurements provide normal incidence absorption data which should be converted to random absorption coefficient.

Microflown method can give unsatisfactory results at some specific conditions. To test the limitations of the the method a short comparison of the Microflown and Kundt's tube measurements were conducted during the preliminary work over summer. The findings are presented in Sections 5, but they generally support the statements given by Aretz [6]:

- Very high uncertainty for reflective surfaces when the velocity is close to zero. It causes high SNR and the incidence and reflected wave is not recognized properly by the probe.
- Close reflections give unreasonable results - especially for low frequencies. Aretz dealt with the problem by placing additional absorptive material around the measurement point (when possible). In case of this work the measurement points were chosen very carefully to be far from additional reflections, but the results may be unreliable.
- The curved shape of a door trim makes the measurement unfeasible due to close interfering reflections.
- In case of headliner the measurements are blurred with diffraction effects caused by the unevenness of the headliner and close reflections from other surfaces.

Further limitations of the Microflown PU probe method are studied in detail by Gemmeren in his master thesis. The findings are discussed broadly and published in [10].

During the preliminary work over summer, apart from the study on the limitations of the method, the first database of material parameters was created. During the master thesis work most of these absorption coefficients were used, but for some of the materials new measurements were conducted, as the values seemed to be incorrect. The questionable measurement was for example the foot area, that is highly influenced by close reflections. The measurements were repeated for the problematic materials taking special care about coherence and IR shape (so that only direct sound and no other reflections are included in the calculations).

As mentioned above GA software requires random incidence absorption coefficient data that can be obtained out of purely energetic measurement methods (such as in reverberation chamber). This is because the sound rays in the room travel in different directions and the random absorption coefficients illustrates better the overall behaviour of the sound when hitting the surface from any possible angle. As the Microflown PU probe provides the impedance and absorption coefficient data collected from normal incidence the conversion to random absorption coefficient was needed. A formula to obtain the random absorption data from normal incidence acoustic impedance data measured in Kundt's tube is proposed by London [19]. In the paper the sound absorption coefficient α_θ for a wave incident at angle θ on a material with acoustic impedance Z is defined as (where ρc is the acoustic impedance of the air):

$$\alpha_\theta = 1 - \left| \frac{(Z/\rho c)cos\theta - 1}{(Z/\rho c)cos\theta + 1} \right|^2 \tag{4.2}$$

Presenting normalized acoustic impedance as a complex number (where r is a real part, x is an imaginary part):

$$Z/\rho c = z = r + jx \tag{4.3}$$

Equation 4.2 can be written as:

$$\alpha_\theta = \frac{4rcos\theta}{(rcos\theta + 1)^2 + (xcos\theta)^2} \overset{\theta=0}{=\!=} \frac{4r}{(r+1)^2 + x^2} \tag{4.4}$$

From customary reverberant sound field statistics the random sound absorption coefficient $\bar{\alpha}$ is defined as:

$$\bar{\alpha} = 2\int_0^{\pi/2} \alpha_\theta cos\theta sin\theta \, \mathrm{d}\theta \tag{4.5}$$

The resulting equation for the random incidence sound absorption coefficient is (obtained by substituting Equation 4.5 into Equation 4.4 and integrating):

$$\alpha_{random} = \frac{8r}{r^2 + x^2}\left(1 + \frac{r^2 - x^2}{x(r^2 + x^2)}\, tan^{-1}\left(\frac{x}{1+r}\right) - \frac{r}{r^2 + x^2}\ln\left[(1+r)^2 + x^2)\right]\right) \tag{4.6}$$

Equation 4.6 is used for computing the data out of normal incidence measurements given by Microflown PU probe. The selected values are discussed in Section 5 and all used data is given in Appendix A.

4.1.2. Loudspeaker directivity

The measurement of the tweeter and midrange units of the Premium Sound system of Volvo XC90 provided by the company was conducted in an anechoic chamber of Applied Acoustics Division, Department of Civil and Environmental Engineering, Chalmers University of Technology on 2016-02-10. The units mounted in the trim door panel are captured in Figure 4.2.

Figure 4.2.: Trim door panel of Volvo XC90 with midrange and tweeter units mounted.

The aim of the measurements was to obtain the directivity of the speakers and their sensitivities. The loudspeaker units were excited separately using white noise signal and the sampling frequency was 51200 Hz. The midrange unit was measured as it was, but the tweeter unit was measured together with the condenser. Meaning the driver with a filter design were together treated as a loudspeaker. For the directivity analysis there were two measurement mountings for each unit. One with units placed in the car doors as depicted in Figure 4.3a and one simplified case with units mounted in a baffle as depicted in Figure 4.3b. Additionally, there was conducted one reference measurement for each driver mounted in a baffle at the distance of 1 m at height of diaphragm centre. After post-processing the data another measurement was conducted in an anechoic chamber at Chalmers on 2016-05-13. This additional measurement was conducted to study the influence of the diffraction from baffle edges on the spectrum. All the measurements were done in consideration of standard IEC 60268-5 suggestions [23].

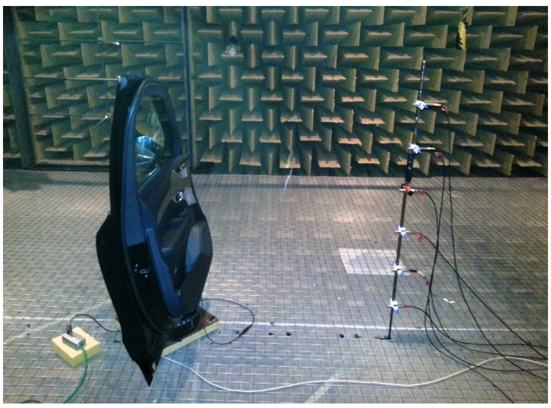

(a)

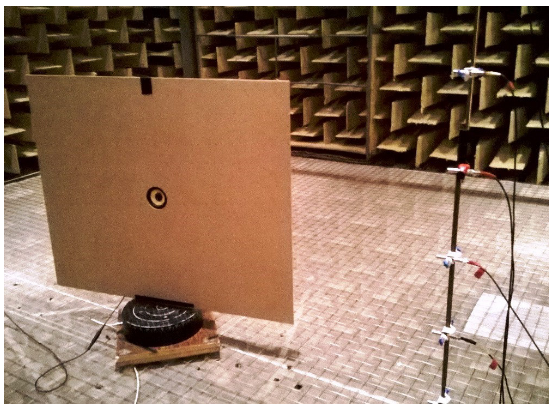

(b)

Figure 4.3.: Drivers mounted in (a) a car door and in (b) a baffle placed on a turntable.

For directivity measurements the following equipment was used:

- 6 microphones: 1/2″ prepolarized free field G.R.A.S. 40 AE
- 6 microphone preamplifiers: G.R.A.S Type 26CA
- National Instruments cDAQ-9178 Compact DAQ USB chassis
- 2 analog input modules NI 9234
- B&K Noise Generator Type 1405
- Low-pass filter
- Automatic electronic turntable Outline ET1
- Computer with *MATLAB* based data acquisition software
- Volvo sound system midrange (working range: 200-5000 Hz)
- Volvo sound system tweeter (working range: 3000-20000 Hz)
- 2 baffles designed for midrange and tweeter (size: 1.2 x 1.5 m)
- Absorptive materials (mineral wool, acoustic foam)
- RMP-01 SP calibrator

The measurement setup consisted of six microphones in a line. The first step of the measurements was to calibrate the microphones using SP calibrator. The transfer function values of all 6 microphones used in the array are shown in Table 4.1. The exact microphones positions regarding the driven loudspeaker are presented for each measurement configurations in the sections below.

Microphone number	1	2	3	4	5	6
Sensitivity (mV/Pa)	44.40	43.69	48.63	49.75	43.08	53.30

Table 4.1.: Transfer functions of the measurement microphones.

Drivers mounted in car door

Midrange mounted in the car door was placed on a turntable. The measurements were conducted every 5° so that the whole front semi-sphere was measured. Figure 4.3a above shows the setup together with the microphone array. The exact position of the microphone array and midrange is presented in Figure 4.4. The dashed line in the picture indicates the net floor of the anechoic chamber. In the left figure the side view is presented and the distances of microphones and midrange from the net floor are marked. In the right figure the view from top is presented in order to show that the array was not located exactly on axis with the centre of diaphragm. That was due to the problems with positioning the car door on the turntable exactly on axis with the microphone array.

The same array setup as for the midrange was used for the tweeter measurements (see picture of a car door in Figure 4.3a). The tweeter is placed higher in the car door than the midrange what is highlighted in the Figure 4.5 below. Also, as the tweeter in a trim

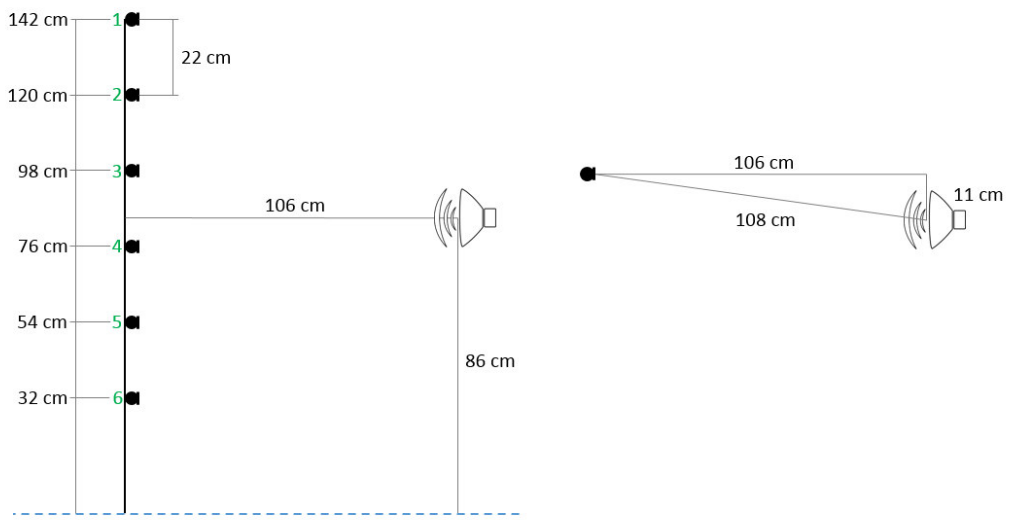

Figure 4.4.: Midrange and microphones positions, left: side view, right: top view.

is located more to the center of the car door, the unit was located closer to the axis to the microphone array. That is depicted in the top view in the figure.

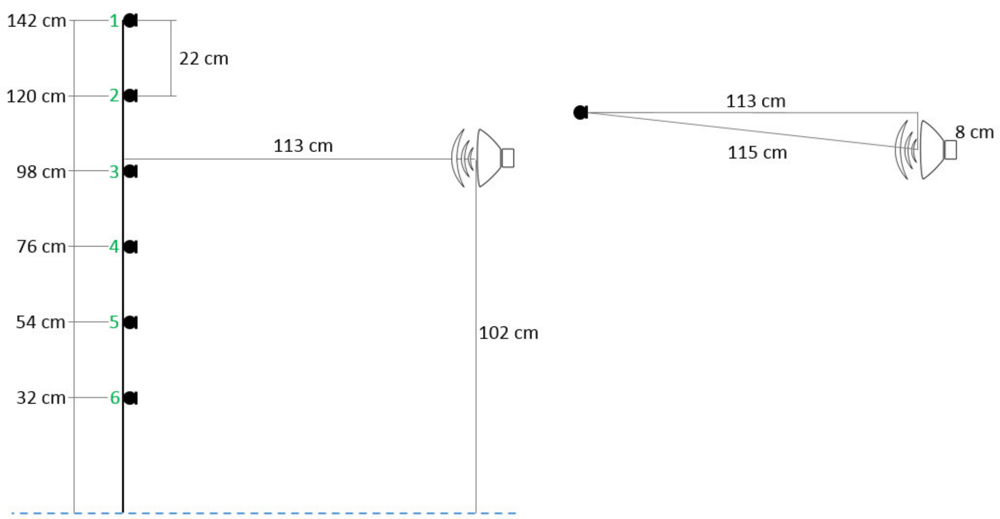

Figure 4.5.: Tweeter and microphones positions, left: side view, right: top view.

Drivers mounted in a baffle

Another measurement was conducted for the midrange placed in the baffle as presented in Figure 4.3b. The baffle was placed on a turntable in a way that the distance between the array and the middle of the diaphragm was 140 cm. That means that the distance was larger than for a car door case. As the direct comparison of the two mountings (car door and baffle) was of the interest the microphones in an array were shifted in order to obtain the same angles vertically as for the case of the unit mounted in the door. The short computation of corresponding heights was done. The new distance of a unit from the net floor was also taken into account. The exact positions for a midrange in a baffle are presented in Figure 4.6.

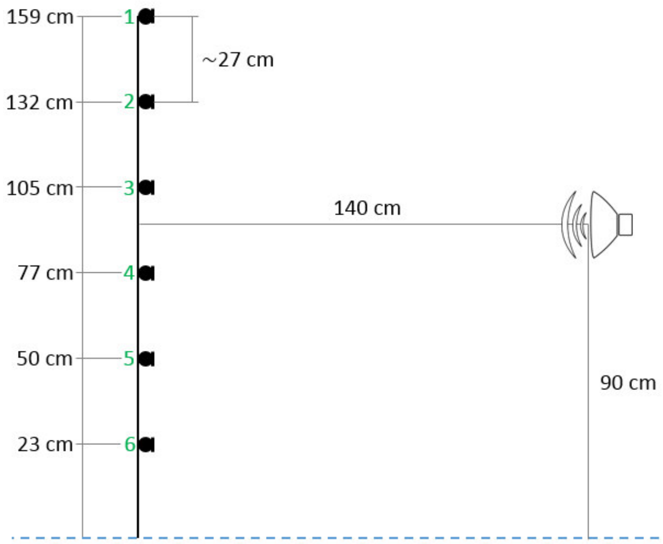

Figure 4.6.: Midrange and microphones positions (side view).

For the directivity measurement of the tweeter in a baffle similar computations were done in order to obtain the sound pressure values at angles corresponding to car door measurement. Also, the new height of the unit relative to the net floor was taken into account. The new setup is presented in Figure 4.7 below.

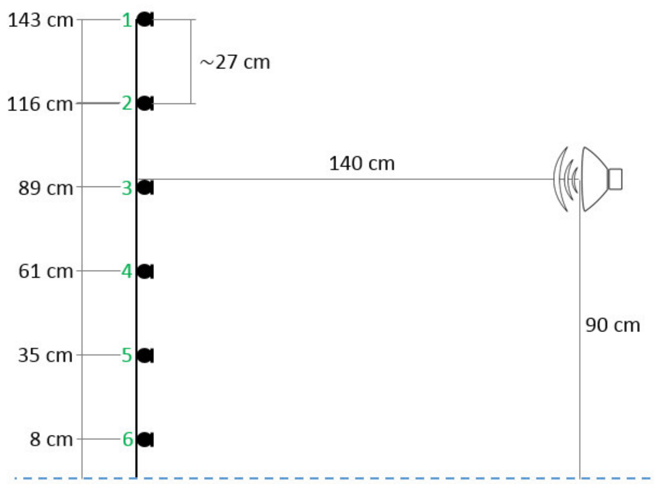

Figure 4.7.: Tweeter and microphones positions (side view).

As mentioned before the midrange and tweeter mounted in the baffle were also measured by placing the microphone exactly at the height of diaphragm centre at 1 m distance as a reference measurement. Picture 4.8 presents one of the drivers during that measurement. This was done because the directivity and sensitivity data needed later for the simulations should be measured in anechoic conditions at 1 m distance from the speaker as stated in GA software manual [12].

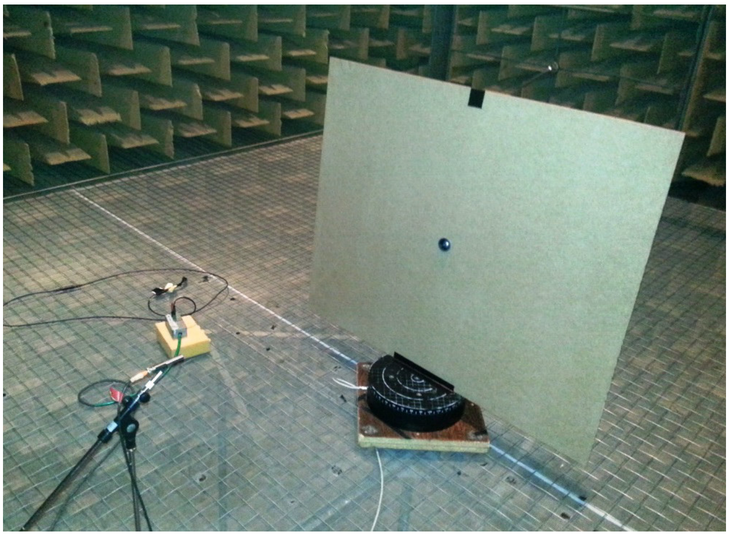

Figure 4.8.: Tweeter sound pressure measured at 1 m distance in free field.

In order to obtain data for GA models from previous measurements the correction of a distance was done in the following way:

$$p_2 \cdot r_2 = p_1 \cdot r_1 \tag{4.7}$$

Where r_1 is known distance, p_1 are the pressure values collected at this distance, r_2 is a new distance (in this case equal to 1 m) and p_2 is a desired distance.

Drivers mounted in different baffles

Additionally, the drivers were measured one more time in anechoic chamber later in the work-flow to study the influence of the edge diffraction on the speaker response. Also, during this repeated measurements the absorption was put behind the baffle to cover the rear of the speaker to ensure that no contribution from this part of the driver influences the measured response. In case of first baffle measurements that was neglected. Three cases were measured. First, just clear baffle as before. Second, with a small amount of absorption (acoustic foam) on the baffle edges. And the last one with large amount of the absorption (mineral wool). The last two cases are presented in the Figures 4.9a and 4.9b below.

As captured in Figure 4.9b this time only one microphone was used to collect the pressure data. It was placed at exactly 1 m distance from the speaker at the same height as diaphragm center. The baffle was again placed on a turntable. The data for each speaker was collected every 15° for a half sphere in front of the baffle. Then the speaker was turned by 90° inside the baffle to check if the drivers are really symmetric. The aim of this measurement was to get the speaker response at the horizontal and vertical arches. This allowed later to model the data in SD0 directivity file format supported by GA software. Figure 4.10 presents how the speaker data are stored in SD0 directivity file. During the measurement the data was collected for the front arch (left to right for

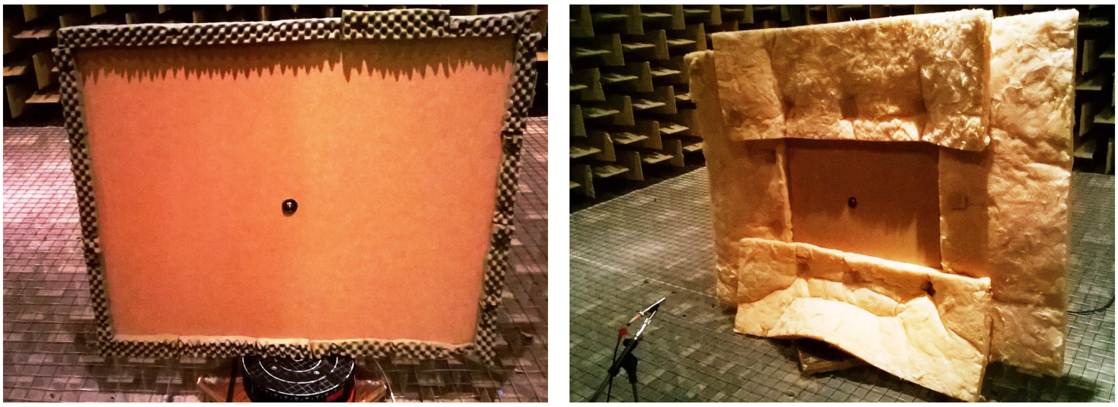

(a) (b)

Figure 4.9.: Driver measured in a baffle with (a) acoustic foam absorption and (b) mineral wool absorption.

top view and top to bottom for side view) and pressure behind the loudspeaker was assumed to be very low.

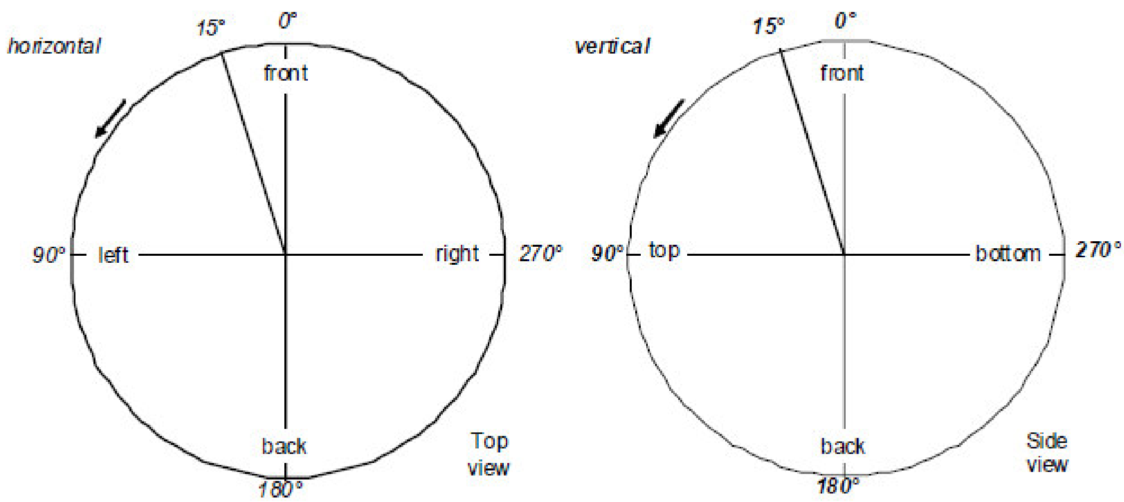

Figure 4.10.: Directivity file SD0 - angle conversion every 15° for top view (right) and side view (left). Borrowed from [12].

The measured narrow band data was post-process using *MATLAB*. The SD0 file requires directivity function and sensitivity data in octave bands. The directivity function values describe the amount of attenuation in dB relative to the on-axis value. Therefore, the value measured at 1 m distance on-axis is always 0. The directivity function in octaves from 125 to 16000 Hz was obtained from the narrow band pressure values. When needed the distance and angle correction was applied. Also, the sensitivity of the speaker was measured and computed to octave bands, as it is a required parameter in SD0 directivity file.

4.2. Simulations

4.2.1. Algorithms

The *CATT-Acoustic v. 9.0c 3.01* GA based software was used in the scope of the thesis. The software allows the user to build the geometry of the room, assign the material parameters such as absorption and scattering coefficients and to model the source parameters in the *CATT-A* module. The software includes the prediction model *TUCT 1* (*The Universal Cone-Tracer*) that offers three different cone-tracing algorithms for source-receiver echograms and IRs and one audience area mapping algorithm. In the scope of the thesis only two algorithms for source-receiver IR were used: ALG1 with max split order of 1 and ALG2. *TUCT* itself does not create the geometry, but reads the geometry and acoustic input data from *CATT-A* files. The principle of GA are discussed in Section 3.2. The general difference between the two used algorithms are explained below in Figures 4.11 and 4.12. The presented ray reflection trees illustrate up to 5 reflections, but the same principle works for later reflections. Each branch split up represents the ray hitting the boundary. The left yellow branch is a diffuse reflection (D) and the right green branch is a specular reflection (S). Also, deterministic paths are solid and the random paths are dashed [13].

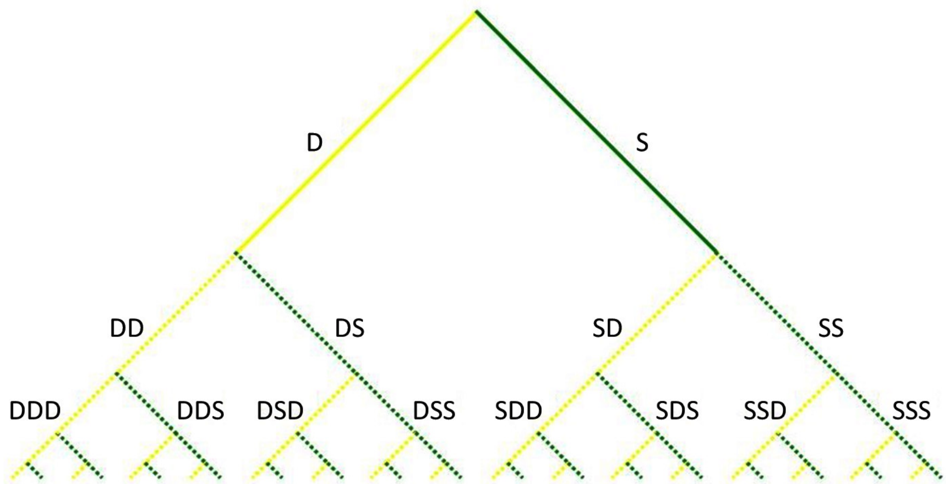

Figure 4.11.: Algorithm 1 principle, showing max split order n = 1. Borrowed from [13].

For ALG1 the diffuse and specular reflections are deterministic until the order of reflection is max split order n. From the order $n+1$ the reflections are randomly distributed from the assigned scattering coefficient s. So for order higher than n, if scattering s is 40% that means that on average 4 out of 10 rays are randomly reflected according to Lambert distribution and 6 out of 10 are specularly reflected [13]. Figure 4.11 presents the ALG1 for max split order of 1. ALG1 due to its random nature never provides two runs that are exactly the same, but for well behaved rooms (with high scattering and even absorption distribution) the two runs are similar enough.

Figure 4.12 presents the ALG2 basis. For all reflection orders the specular-specular (rightmost branch) and specular-diffuse paths are deterministic, while the rest of paths are random as in ALG1. At each solid split-up the energy is divided into a specular part $(1 - s)(1 - \alpha)$ and a diffuse part $s(1 - \alpha)$ and energy α is lost due to absorption. Generally, ALG2 is more complex and provides more reliable results.

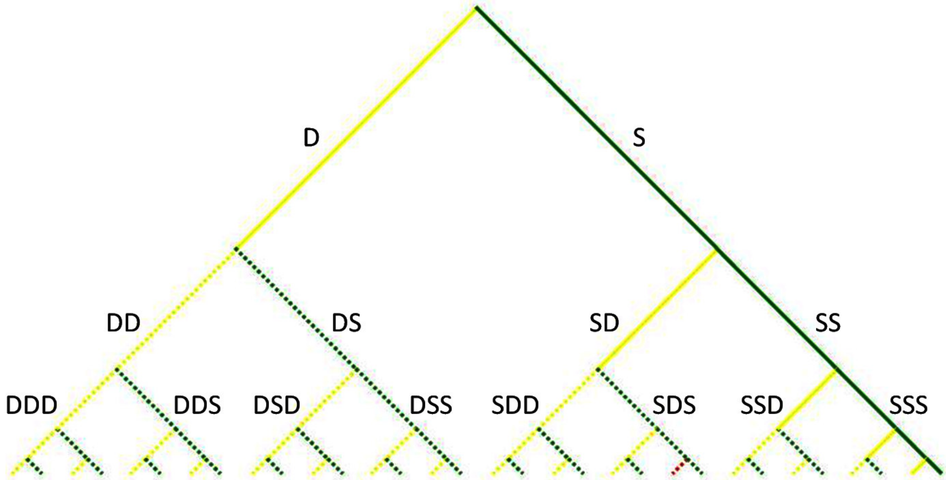

Figure 4.12.: Algorithm 2 principle. Borrowed from [13].

Apart from deciding on calculation algorithm, in GA software calculation module *TUCT* it is possible to set a number of rays/cones. Usually, the higher number the more reliable results (especially in more random ALG1), but that might be not a case in a small enclosure, such as car compartment. Also, the length of the echogram can be set. It states for how long the emitted rays would travel within the enclosure until they die out. The echogram length should be set to at least to half the length of anticipated reverberation time. Furthermore, edge diffraction can be used what is useful when there are hard objects between the source and receiver.

The results extracted from the GA software were source-receiver IRs. The software provides the export of the IRs that are relative to the source transfer function measured on-axis at 1 m distance in anechoic conditions. The user can decide for *MATLAB* file export for different type of receivers (e.g. omnidirectional or binaural). Also, *TUCT* includes the calculation of basic room acoustic parameters (i.e. clarity, sound strength, reverberation time, early-decay time etc.), but in this stage of the work the IRs and TFs were of interest. *MATLAB* was used afterwards to post-process data to obtain the modelled transfer functions that could be compared directly with measured data. It included making sure that both modelled and measured data are normalized to the same input. For BIB it was loudspeaker transfer function measured at 1 m distance in a free field and for the trimmed body it was an input voltage. Also, for direct IRs comparison usually the octave bands filtering was applied.

4.2.2. Simulation models

The geometry models were extracted from *ANSA* files provided by the company. As there is no convenient tool that can automatically create the suitable model for GA with big enough elements, the models were created manually. The larger surfaces of the GA models were created out of fine mesh of the given FE model by connecting the specific nodes in the *ANSA* file. Then, the *Nastran* output files were translated to the *CATT-A* geometry files using a smart Python script provided by the company.

For the absorption coefficient measurements and FRF measurements of the trimmed body the car with panorama roof was used. The same type of car was also modelled in GA software in order to be able to conduct a direct comparison of modelled and measured frequency responses. The three trim levels of the car were modelled and studied:

- First case was so-called Body-in-Blue (BIB). In this stage a car body consists basically of metal sheets and glass. In our case BIB also had trim panels mounted at the doors in order to have the speakers mounted in their usual positions in the car (in door trim panels).
- The second stage was trimmed body without seats. Trimmed body means that the car is at its final stage of production with instrument panel on and all the materials put inside.
- The third stage of a car used in the project was a trimmed body with seats. That means that the car is basically modelled as it appears at the sales.

In the scope of the thesis two levels of details (LOD) were used in modelling and the comparison of the influence of complexity level in creating the models was studied. The two steps were: simple model that was built with relatively large surfaces and detailed model that was built with more precision regarding the geometrical detailing. Having in mind the limitations of GA it is important to expect that the models would give reasonable results from around 1000 Hz in case of the simple model and around 2000 Hz in case of the detailed model.

The outcome of comparison of the selected GA models and real car measurements are presented in Section 6. Additionally, during work on GA models a short study on the accuracy of the receivers placement was done (see Section 6.1). Also, the scattering influence was investigated in order to check how the response differs for the default (10% for all octave bands) and proposed scattering values. Moreover, the usage of different algorithms and different number of rays was compared in order to get the best results in a good computational time.

Body-in-Blue

Figure 4.13 presents the simple and detailed models for the BIB case. The simple model has 216 elements and detailed model has 2628 elements. The model was run for two positions of the omnidirectional source and there were 10 receivers. The positions of the receivers corresponded to both ears of potential passengers. The source positions corresponded to the measurement positions to allow a direct comparison of the modelled and measured IRs. In this model all the surfaces were assigned the same absorption and scattering coefficients. Both, glass and metal were assumed to be highly reflective. The absorption of this model was determined using transformed and simplified Sabine's formula (see Equation 3.2):

$$\alpha = 0.161 \frac{V}{TS} \tag{4.8}$$

Where the reverberation time T was extrapolated from the third octave band values measured from 25 to 1000 Hz (provided by the company), and car volume and wall surfaces were estimated from geometrical model. The air absorption m was disregarded, as it was assumed to be small in such a small room as car compartment. The values of absorption and scattering coefficients used for this model are shown in Table 4.2. Scattering was set lower than default value of 10% for lower frequencies.

Octave frequency	125	250	500	1000	2000	4000	8000	16000
Absorption, α [%]	19.5	17.9	18.4	14.9	12.1	8.6	5.4	3.1
Scattering, s [%]	5.0	5.0	5.0	5.0	10.0	10.0	10.0	10.0

Table 4.2.: Absorption and scattering data used in GA model of BIB.

The BIB creates a very reverberant model so ALG1 was used to find the IRs in the car. This is because the absorption is evenly distributed and the room is closed, but also because the simulation would take very long time for ALG2 in such a reverberant case and it will be overage. The high number of the rays was used to increase the reliability of the prediction.

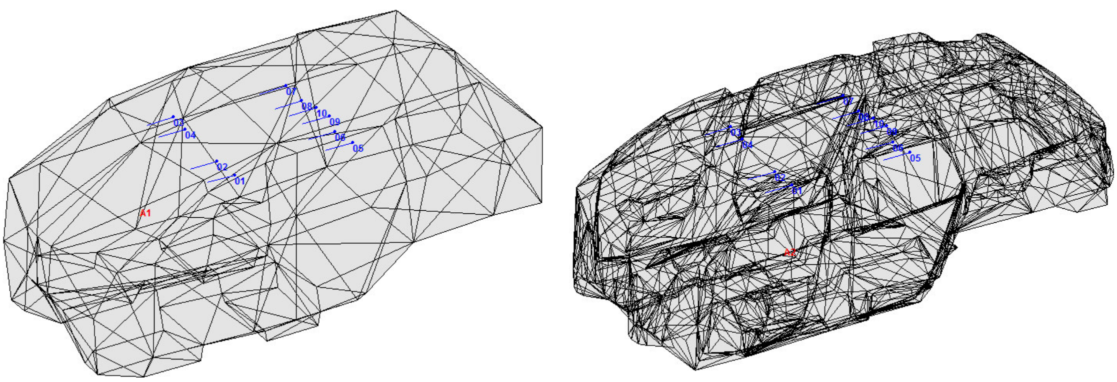

Figure 4.13.: BIB model: simple and detailed LOD.

Trimmed body without seats

Figure 4.14 presents the simple (216 elements) and detailed (2628 elements) models for the trimmed body without seats. The model geometries are basically the same as for the BIB, but the absorption and scattering are different. The absorption coefficient is defined as discussed in Section 4.1.1. The exact values are presented in Appendix A. The scattering coefficient values was differentiated into low and high scattering values. Low scattering was assigned to smooth surfaces, such as windows, and high scattering was ascribed to remaining surfaces. The exact values are shown in Table 4.3.

Octave frequency	125	250	500	1000	2000	4000	8000	16000
Low scattering, s [%]	2.0	2.0	2.0	2.0	2.0	2.0	2.0	2.0
High scattering, s [%]	20.0	20.0	30.0	30.0	30.0	30.0	30.0	30.0

Table 4.3.: Scattering data used in GA model of the trimmed body.

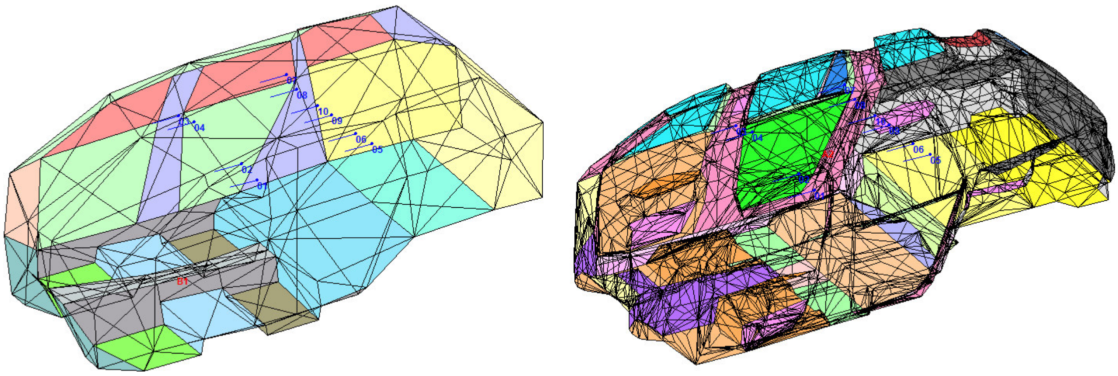

Figure 4.14.: Trimmed body without seats model: simple and detailed LOD.

In case of this model the number of receivers was the same as for BIB, though the source was different. There was no omnidirectional source, but the audio system midrange and tweeter were used to excite the structure. The simulation was done for one speaker at the time. The directivity and sensitivity of the speakers were collected and modelled as described in Section 4.1.2. Generally, the prediction was done with use of ALG2 that includes more deterministically reflected rays. Different number of rays was used to check how much it influences the results.

Trimmed body with seats

In Figure 4.15 the simple and detailed models for the trimmed body seats are given. The simple model consists of 413 planes and the detailed one of 1790. The reason for less elements than in case without seats is that the merging function of GA software was used for a detailed model. In general, the absorption and scattering of the materials were the same as for the previous case. Only now the geometry of the car seats were added. It is important to state that the model without seats is a simpler case for GA and the model with seats can acquire a number of errors due to diffraction over seats. Some of the receivers, corresponding to ears of the rear seats passengers, were not even exposed to the direct sound. Though, this case of modelling is of a big interest for the company as it describes the sound field in a real car at the final stage. If the modelling at this stage agrees until certain extent with the real car measurement, it would be a progress in high frequency prediction of the sound system behaviour.

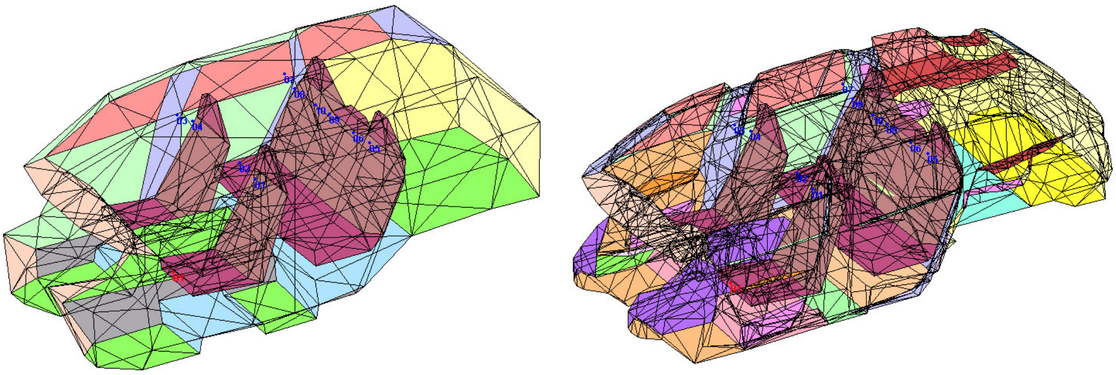

Figure 4.15.: Trimmed body with seats model: simple and detailed LOD.

In this model the sources used were again the midrange and tweeter of the sound system of the car - working one at the time. The directivity and sensitivity data was the same as before. The details about the speakers data are presented in Appendix B. In GA simulation the ALG2 was used mostly, as the absorption is unevenly distributed and the echogram was rather short, what made the simulation shorter as well. And ALG2 was also focused on as it is supposed to give more exact results at this case.

4.3. Measurements of verification data

To evaluate how well the simulation resembles reality, a comparison with real measurement data was conducted. To be able to assess the agreement with reality, the three cases were measured - same as the modelled ones. That is: BIB (glass and metal body structure), trimmed body without seats and trimmed body with seats. In each model particular sources were used to excite the sound field. The measurements of the FRFs in the cars were conducted in Volvo respectively on 2016-02-25, 2016-03-14 and 2016-03-15 in quiet environment. For all the measurements the excitation signal was a white noise from 0 to 20000 Hz, the sampling frequency was set to 102400 Hz. The following sections describe in detail the use of sources and receivers during the measurements for each case.

4.3.1. Body-in-Blue

For BIB measurements the following equipment was used:

- 10 microphones: 1/2″ prepolarized free field G.R.A.S. 40 AE
- 10 microphone preamplifiers: G.R.A.S Type 26CA
- 4 accelerometers: B&K Type 4507
- Laptop with *LMS* measurement system

- NAD Stereo Amplifier 3020 e
- HF source designed by Volvo (presented in Figure 4.16a and 4.16b)
- HF source designed by Chalmers (presented in Figure 4.16c)
- Midrange and tweeter units of Volvo sound system
- 3D Sonic Digitizer model 5230XL
- Cables
- Tape to install the microphones in a car
- Ruler, meter tape

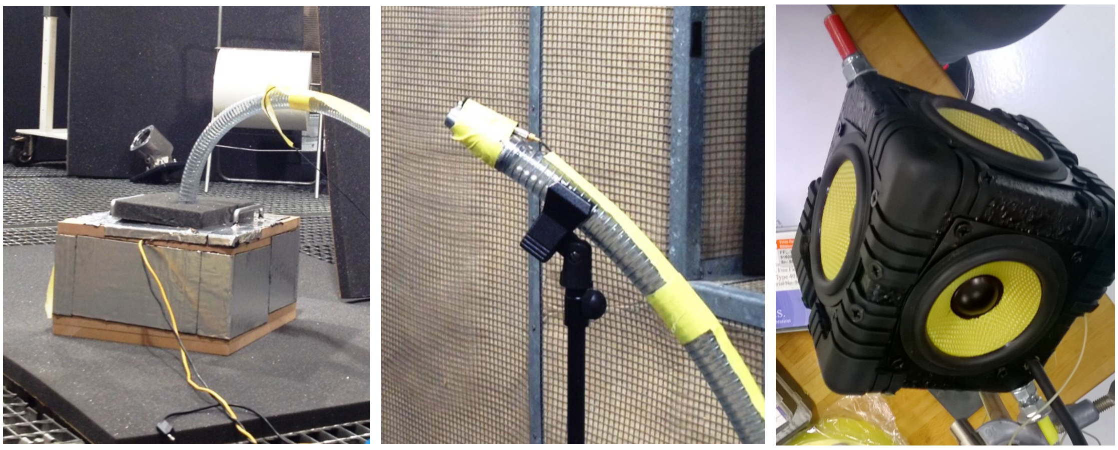

(a) (b) (c)

Figure 4.16.: HF sources: box with driver (a) and hose (b) by Volvo design, Chalmers design (c).

For the BIB measurements 10 microphones were used to collect the response of the car when excited with white noise. The positions of the receivers correspond to so called standard positions and they are placed at both ears of the car passengers. The microphones were mounted in a way that they hung from the headliner, the cables were taped to the roof. It is captured in Figure 4.17 and 4.18. The microphones were situated in the car using a reference frame placed inside. The reference frame have a number of points with known locations relative to the defined coordinate system. The microphone positions were chosen by carefully measuring the distances from the known points using a ruler. To verify the exact positions also the 3D Sonic Digitizer was used. Though, the coordinates measured by 3D Sonic Digitizer were saved in different coordinate system. To obtain the locations in the same system as in GA models, the values were modelled as points in *ANSA* and the function *Transform* was used. The exact positions were used later for receiver positions in GA models. As 3D Sonic Digitizer system has its own limitations and its accuracy relies on user's precision, the correctness of this measurement was checked with couple of known points located on a frame. It turned out that the standard deviation is +/- 4 cm. This mismatch may generate visible discrepancy between measured and modelled TFs and IRs for higher frequencies (above 8000 Hz). As a comparison such discrepancies in receiver locations would correspond to ca 40 cm differences in the large rooms with 20 m long walls. The standard positions and measured positions of all 10 receivers are presented in Table 4.4. The sketch from GA model in Figure 4.19 makes it easier to imagine where the receivers where located during measurements.

Figure 4.17.: Microphones mounted in the BIB (view from the tailgate).

Figure 4.18.: Microphones mounted in the BIB (receivers corresponding to rear passengers' ears).

Additionally, a couple of accelerometers were placed in the car to ensure that the metal and glass plates behave as rigid boundaries. Figure 4.20 presents 2 out of 4 measurement point for the accelerometers. As it was proved that one can treat glass and metal as rigid in high frequency, this vibration data is not discussed in detail anymore.

The sound pressure data was collected for several different sources at different loca-

Receivers	Standard positions			Body-in-Blue			Trimmed body		
Coordinates	x	y	z	x	y	z	x	y	z
mic 1	3.36	-0.49	1.45	3.19	-0.42	1.42	3.31	-0.51	1.42
mic 2	3.36	-0.29	1.45	3.19	-0.21	1.43	3.32	-0.29	1.43
mic 3	3.36	0.49	1.45	3.23	0.43	1.43	3.28	0.47	1.43
mic 4	3.36	0.29	1.45	3.20	0.24	1.46	3.30	0.30	1.46
mic 5	4.16	-0.51	1.45	4.07	-0.44	1.46	4.15	-0.54	1.46
mic 6	4.16	-0.31	1.45	4.05	-0.25	1.44	4.14	-0.34	1.44
mic 7	4.16	0.51	1.45	4.07	0.42	1.45	4.13	0.53	1.45
mic 8	4.16	0.31	1.45	4.06	0.21	1.44	4.09	0.33	1.45
mic 9	4.16	-0.10	1.45	4.11	-0.07	1.47	4.10	-0.10	1.47
mic 10	4.16	0.10	1.45	4.09	0.07	1.44	4.11	0.10	1.44

Table 4.4.: Measurement microphone positions: desired values, coordinates in BIB, coordinates in trimmed body.

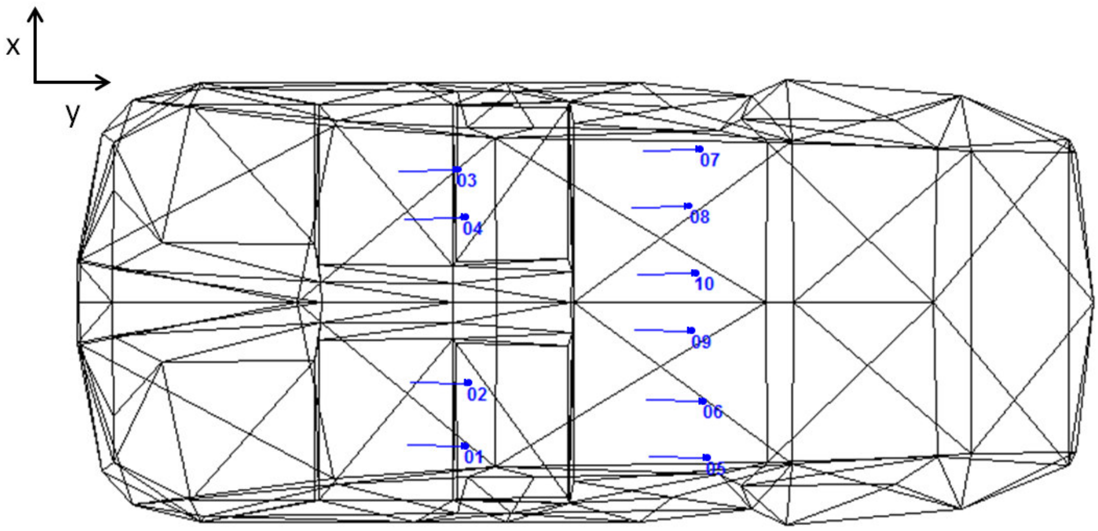

Figure 4.19.: Receiver points with head direction for BIB model in GA software.

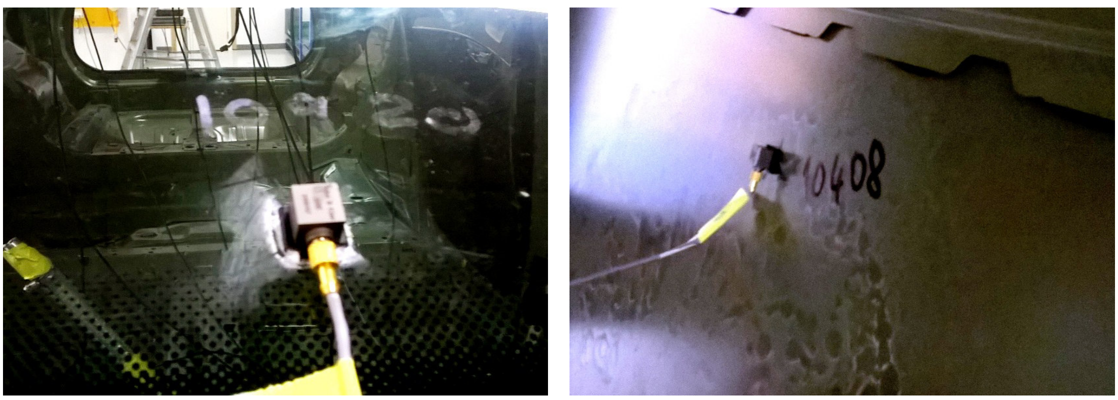

(a) (b)

Figure 4.20.: Accelerometers in the BIB: (a) on a windscreen, (b) on the headliner.

tions. Two positions of omnidirectional Volvo source and two positions for Chalmers source were chosen. The exact positions of the omnidirectional sources placed in BIB are presented in Table 4.5.

Sources coordinates	x [m]	y [m]	z [m]
Volvo A1	2.85	0.23	1.02
Volvo A2	3.23	-0.26	0.93
Chalmers A1	3.68	0.29	1.00
Chalmers A2	3.10	-0.44	1.00

Table 4.5.: Chalmers and Volvo source positions in BIB.

The data was also collected for the case when the sound field was excited with the drivers of the Volvo sound system. The drivers were mounted in a door trim, where they are in a final stage of production. The sources were measured one at the time. All the excitation sources used in response measurements were:

- Volvo omnidirectional source - 2 different positions
- Chalmers ”omnidirectional” source - 2 different positions
- LF tweeter
- LF midrange
- LF midrange + tweeter
- RF tweeter
- RF midrange
- RF midrange + tweeter

4.3.2. Trimmed body with seats

In case of the trimmed body measurement the fully equipped car was investigated. Firstly, the measurement with the seats inside was taken. Again, the receiver positions were chosen to correspond to two ears of the passengers of the car. The microphones were placed in a car using a special wooden skeleton that helped to place the microphones in ear positions. The exact receiver locations in a car are depicted in Table 4.4. The receivers are placed in very similar positions as in BIB (see Figure 4.19). Figure 4.21) present the setup of the microphones during the measurements as well as the wooden frame used for positioning the microphones.

The equipment used during the trimmed body measurements differed a bit from the BIB measurements. As it was hard to put the Volvo source inside the car without causing the doors to be open, only the Chalmers source was used. Also, for this measurement different power amplifier was used. The equipment consisted of:

- 10 microphones: 1/2” prepolarized free field G.R.A.S. 40 AE

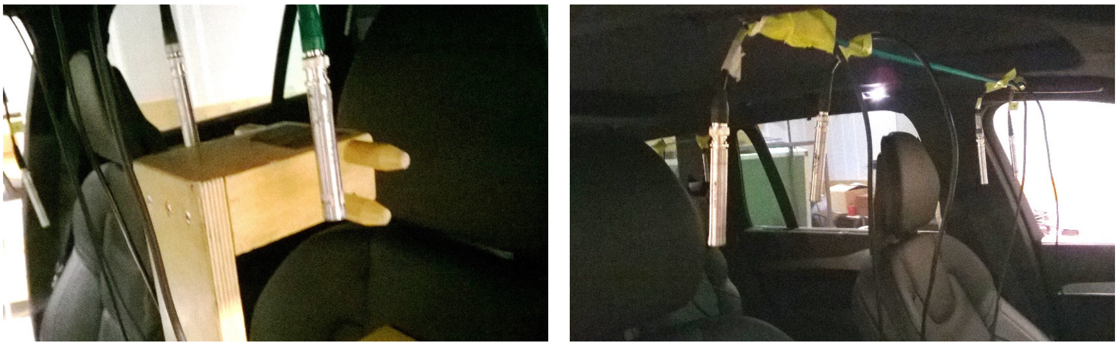

(a) (b)

Figure 4.21.: Microphones placed in trimmed body: (a) wooden frame, (b) front seats.

- 10 microphone preamplifiers: G.R.A.S Type 26CA
- Laptop with *LMS* measurement system
- HF source designed by Chalmers (see Figure 4.16a and 4.16b)
- Midrange and tweeter units of Volvo sound system
- GW Power Amplifier
- Tape and rubber ropes to install the microphones in a car
- Wooden frame for placing the microphones at ear positions
- Ruler, meter tape

Again, the pressure data was collected for different sources. The exact positions of the Chalmers source is presented in Table 4.7. The tweeter and midrange in the door trim on both sides of the car were measured when working one at a time and when working together as one speaker. The car fully trimmed also had an instrument panel (IP) that has a small speaker consisting of midrange and tweeter, placed in the center of the IP. The response of this speaker was measured as well. It consists of both midrange and tweeter. It is shown in Figure 4.22. Generally, the same sound sources were used as for BIB case, apart from adding IP speaker and not having HF Volvo source.

Sources coordinates	x [m]	y [m]	z [m]
Chalmers A1	3.71	0.51	1.41
Chalmers A2	3.14	-0.32	1.29

Table 4.6.: Chalmers source positions in trimmed body without seats.

4.3.3. Trimmed body without seats

The FRFs were also measured in a trimmed body without seats, as this seemed like simplified case to model. The setup was the same as for the trimmed body with seats. Only the seats were removed. The same equipment and the same sources were used (see Section 4.3.2 above). The receivers positions were also the same (see Table 4.4).

Figure 4.22.: IP center speaker by Bowers&Wilkins (borrowed from [25]).

Though, the locations of the Chalmers source were different. The coordinates are presented in Table 4.7.

Sources coordinates	x [m]	y [m]	z [m]
Chalmers A1	3.06	-0.40	1.00
Chalmers A2	3.81	0.27	1.19

Table 4.7.: Chalmers source positions in trimmed body without seats.

Due to time restriction not all of the measured combinations were modelled in GA software. At the end a limited number of measured FRFs was compared to the modelled data. For each stage (BIB, trimmed body without seats and trimmed body with seats) the models with chosen sources were created and compared with measurements. A part of the future work could be then to create the GA models that relate to the all measured data. However, in a scope of the project a numerous predictions with slight changes between the GA models were run in order to find a good match with measured data. To make it clear what settings were used in specific GA simulations, they are noted alongside with selected simulation results in Chapter 5.

5. Input data evaluation

In the following chapter the measurement results of the input data needed for GA modelling are presented. For the sake of brevity only the most representative results are described. The first part presents the absorption coefficient data. The reliability of Microflown PU measurements is shortly discussed and the brief comparison with Kundt's tube measurements is shown. Then the selected absorption coefficient values used in *CATT-Acoustic* models are presented.

The second part includes the source directivity measurements alongside with brief discussion on obtained values. In the final comparison of simulations and real car data only chosen sources were modelled. Therefore, the following part presents the data on those chosen sources. These are the following:

- HF GA speaker designed by Volvo
- Volvo sound system midrange
- Volvo sound system tweeter

5.1. Material properties

The description of material properties data contains short comparative study between Kundt's tube and Microflown measurement as well as brief summary on obtained absorption coefficient values.

5.1.1. PU Microflown reliability

As Microflown PU probe was a newly bought measurement system in the company at first a number of trial measurement were conducted to learn how to use it. Four different absorptive materials were chosen and their normal incidence absorption was measured in Kundt's tube. The material were: Lump, Pur 9295, LF 301 DX and Solomid. Figure 5.1 shows the materials pieces cut to fit the Kundt's tube.

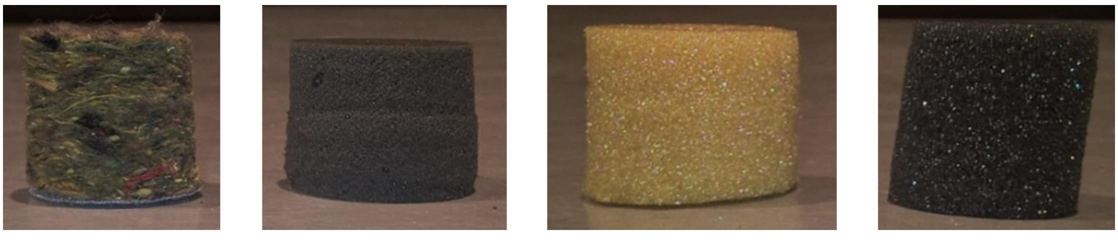

Figure 5.1.: Four pieces of selected materials: Lump, Pur 9295, Solomid and LF 301 DX.

The Kundt's tube diameter was 0.029 m, so the absorption was obtained up to cut-off frequency:

$$f = \frac{c_0}{1.71 \cdot d} = \frac{343}{1.71 \cdot 0.029} \approx 6920Hz \tag{5.1}$$

The Kundt's tube absorption was compared with the normal incidence absorption obtained directly from Microflown measurements. The PU probe measurements were conducted using white noise excitation and mirror source computation model. There were two measurements conducted for each material - one in a usual lab room and one in semi-anechoic chamber. The materials were cut to square pieces ca 20x20 cm. Figures 5.2a and 5.2b present the results with fairly good match between the two methods especially for frequency above 650 Hz. The mismatch at low frequencies may occur due to Microflown limitations - the probe works better at higher frequencies and is prone to any curves and reflections from other materials at low frequencies. Also, the size of the pieces might cause unreliable results. According to Gemmeren the best results of the in-situ measurements can be obtained for flat specimens of size 30x30 cm [10].

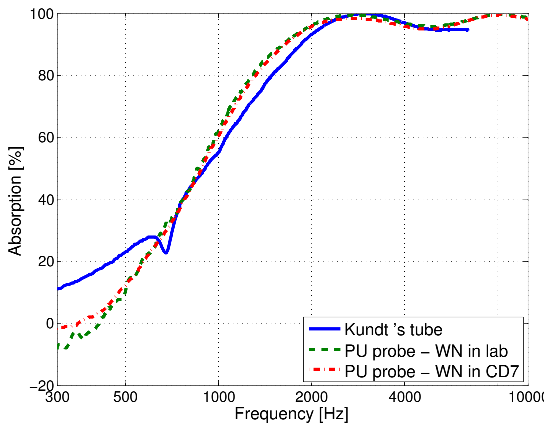

(a)

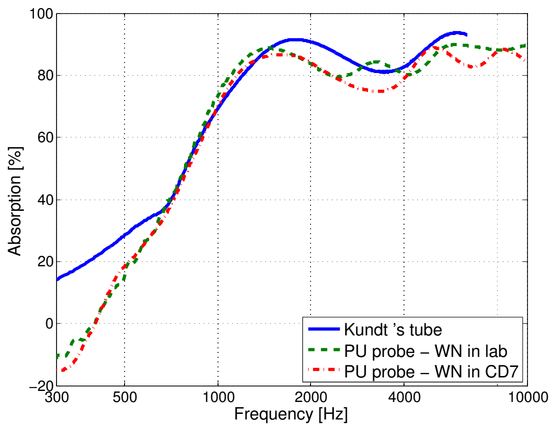

(b)

Figure 5.2.: (a) Lump and (b) Pur 9295 absortpion measured with different methods.

Figure 5.3a and 5.3b present the results for the two materials that gave different results for both methods. The difference below 500 Hz might occur due to the same reasons as for the two previous materials. Though, at higher frequencies the high mismatch may also be caused by the Kundt's tube limitations. The overestimation of absorption may appear for the materials with high flow resistivity and low Youngs modulus and the two presented cases had high flow resistivity. Another thing worth to mention is that the measurements conducted with PU probe showed strong reflection in pressure and velocity graphs just after the first reflection. That means that the results may be also influenced by additional reflections coming from other places. It is therefore good to note that the measurements have to be conducted with special care to not have strong reflections coming just after the one from the measured material. Though, in the real car measurements it is impossible to not to have the later reflection that come from the structures located close to the measured materials. It is highly recommended then to manually remove them using windowing option in *Impedance 3.2* software. It was noticed that not all of the data can be proceed correctly using automatic calibration provided by the software.

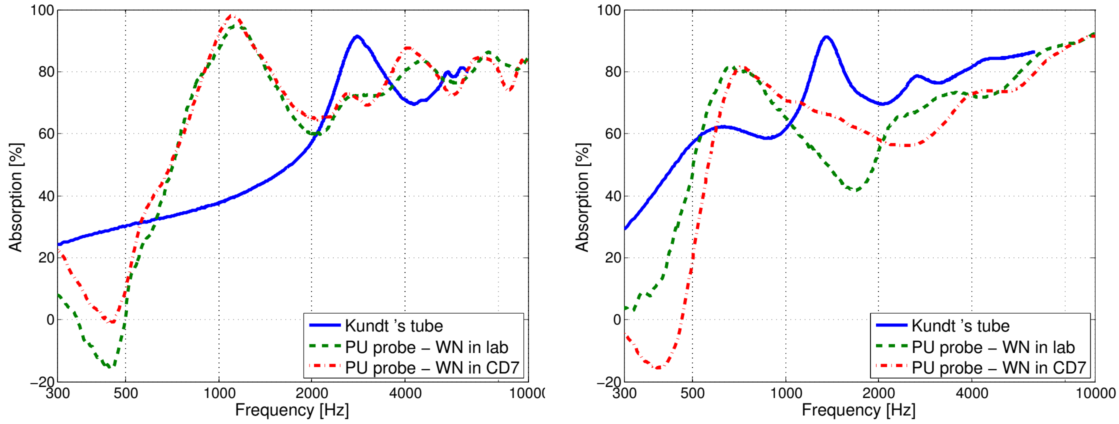

(a) (b)

Figure 5.3.: (a) Solomid and (b) LF 301 DX absorption measured with different methods.

Additionally, some more limitations of the Microflown PU method were found during the scope of the project. They were generally supported by the statements given in Section 4.1.1. Also, it was seen that if the seat material measurement was conducted in the car and when the seat was taken out it was difficult to always obtain the same results. It was again the influence of close reflections coming from the car structure that blurred the results. It happened even though the suggested calibration inside the *Impedance 3.2* software was done. So, as mentioned above it is of high importance to be sure that the material boundary parameters are not altered by other surfaces.

5.1.2. Random absorption coefficient

As described in previous chapters the normal incidence impedance was obtained using the Microflown Impedance Setup. The absorption coefficient data in GA software is random sound absorption coefficient given in octave bands. So the data from *Impedance 3.2* was exported in octave bands and converted to random values using *MATLAB* in a way described in Section 4.1.1. Figures below present the normal incidence absorption (solid line) coefficient for selected materials that were exported directly from the software. A dash-dot line is the random incidence data obtained after calculations. A red dash line presents the random absorption coefficient finally used in GA models. They are slightly different from the computed values. For the Figures from 5.4a to 5.5b the reason is that the Microflown PU provided rather unreasonable values with abrupt changes. As a result of consultation with *CATT-Acoustic* developer the values above 4000 Hz were extrapolated from values at 2000 and 4000 Hz. This is done automatically in GA software when user does not include the values for higher octave bands. Providing data for 8000 and 16000 Hz is optional. For some of the materials the data was smoothed manually - for example when the absorption seemed to be unreasonably high, as presented in Figure 5.4a.

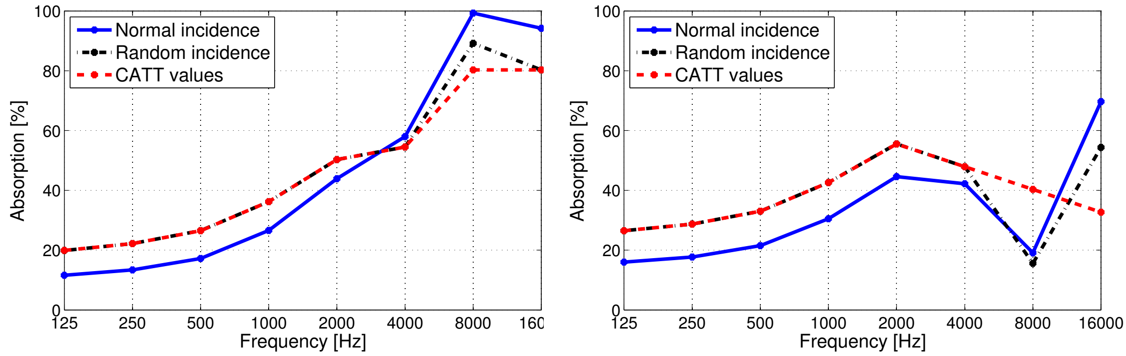

(a) (b)

Figure 5.4.: Absorption for: (a) carpet material on a floor, (b) door armrest.

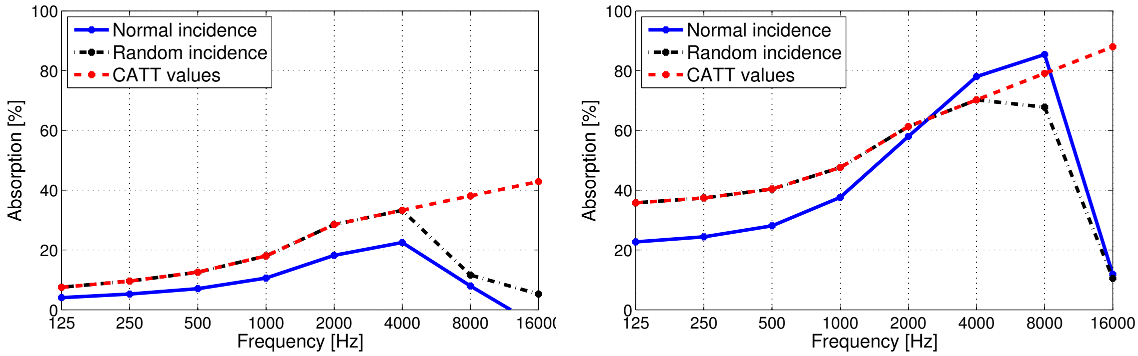

(a) (b)

Figure 5.5.: Absorption for: (a) leather-like material above door armrest, (b) headliner.

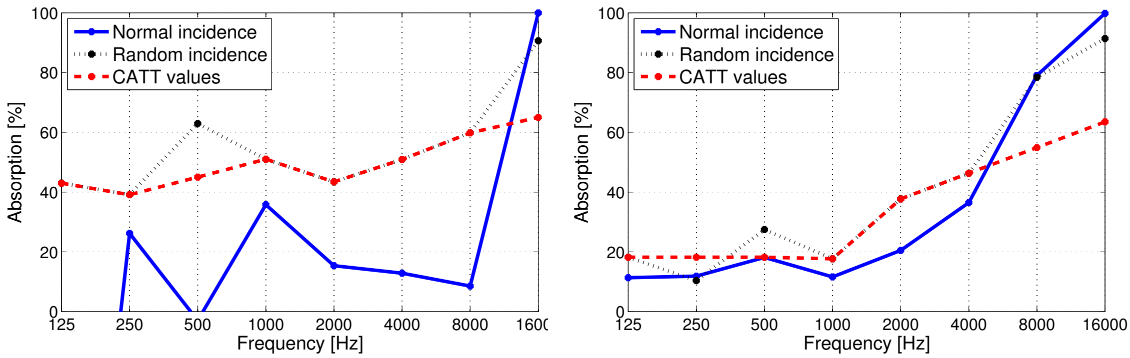

(a) (b)

Figure 5.6.: Absorption for: (a) trim material, (b) floor material under seat.

Figure 5.6 on the other hand presents the examples of the absorption coefficient data that was slightly modified also in lower frequency bands. That was done manually for some of the materials due to the fact that the models are believed to give good results above 1000 Hz. This comes from GA restriction regarding the element size in the model. Since, GA software analyzes the impulse responses in 1/1 octave bands and uses the 1/1 octave bands FIR filters which are not perfectly sharp, the leakage from lower bands is possible if the low frequency reverberation time is too long and/or too high. That is why for some problematic cases with irregular absorption pattern the values were changed for lower bands. It was assigned similar to the value obtained for 1000 Hz.

All the random absorption coefficient values used in the final GA models are presented in Appendix A. Since it was impossible to measure highly reflective materials (e.g. windows) with PU probe for those the literature data was used.

5.2. Source condition

The following section reports the result of the directivity measurements of the audio system high frequency loudspeakers: midrange and tweeter. In the final comparison of measured and modelled sound field data only the selected cases are presented. Basically, the loudspeakers used were Volvo HF loudspeaker and audio system midrange and tweeter. The cubical source designed by Chalmers was eventually not used in the models since its directivity was not known and it was decided that it cannot be assumed omnidirectional at frequencies above 1000 Hz. The data of loudspeakers used in the final GA models is discussed below.

All the measured directivity data presented in the section uses the angle conversion shown in Figure 5.7. It is worth to notice that the angles are differently distributed than in usual SD0 directivity file (see Figure 4.10 in Section 4.1.2). The data for all cases is presented only for the vertical arch. Whereas, the full data that was used in final GA models is included in Appendix B. There are presented horizontal and vertical polar plots for all loudspeakers measured under different conditions.

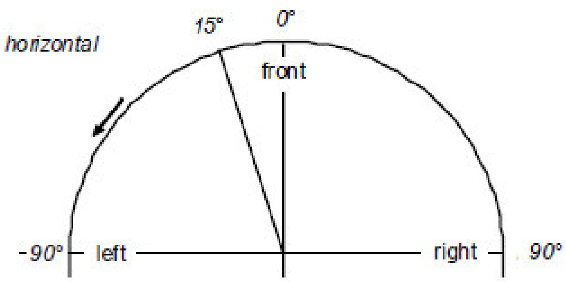

Figure 5.7.: Angle conversion for a vertical arch measured every 15° for measured data.

5.2.1. Volvo omnidirectional speaker

For BIB comparison only the HF omnidirectional source designed by Volvo was used to evaluate the GA models. That was because a highly reverberant room like the BIB took relatively long time to calculate the response even with faster ALG1. And since the trimmed body cases were more interesting for Volvo the main focus was put on their modelling. The measurement data of the Volvo HF speaker was provided by the company. It showed that the speaker is omnidirectional at least until 10000 Hz. Also, the transfer function of the Volvo speaker measured in anechoic conditions at 1 m distance was provided by the company, as this data was needed for a direct comparison of the measured and modelled transfer functions of the car cavity.

5.2.2. Midrange

Measurements in a car door

The sound pressure level at 1 m distance measured in free field for the midrange in the car door is presented in Figure 5.8 below. In the figure the solid line is SPL at 0° that is the measurement taken almost on-axis, in front of the speaker. The other two lines present the drop of SPL measured for -/+ 30° and -/+ 60° off-axis. It is important to emphasize that the results are not symmetric as the midrange is mounted in the door and the car door shape is not symmetric. Also, as mentioned in Section 4.1.2 the speaker was placed a little bit off-axis when measured in car door. In the figure there are visible distinct dips alongside the frequency band that are probably caused by the diffraction effect, that is the strong reflections coming from the edges of the car door. The most profound dips are visible for SPL at -60° at around 650 Hz and 3250 Hz. There are also dips visible for SPL at -30° around 600 Hz and 2000 Hz, as well as for 30 and 60° just above 250 Hz. Also, there is one strong drop at 0° response at 1100 Hz that is rather clearly caused by the diffraction of the waves at the door edges.

Figure 5.9 presents the directivity data with better angle resolution. The four lines present the sound pressure measured at different angles normalized to the on-axis measurement. It is so called directivity function value D. Therefore, is is visible how much the pressure differs from on-axis measurement. The clear peaks around 1100 Hz in the normalized pressure correspond to the dips at 0° caused by diffraction. It is important to remember that the response of midrange in the car was not measured precisely at 1 m distance as described in Section 4.1.2. The values were later corrected for the distance, therefore the dips and peaks would be shifted if the measurement was conducted at 1 m distance. This means that even though the measurement was conducted in a free-field what makes it simple to correct the pressure over distance, the actual measured data might lead to discrepancies between measured and modelled IRs in car compartment. So, part of the future work could be to collect the data which is specifically needed, that is measured at 1 m distance. Another task would be to come up with the idea how to actually measure the directivity in car door without the diffraction effects. In the GA software the pressure normalized to on-axis value is averaged to 1/1 octave bands as seen in Figure 5.10. Still, the influence of the diffraction can be recognized.

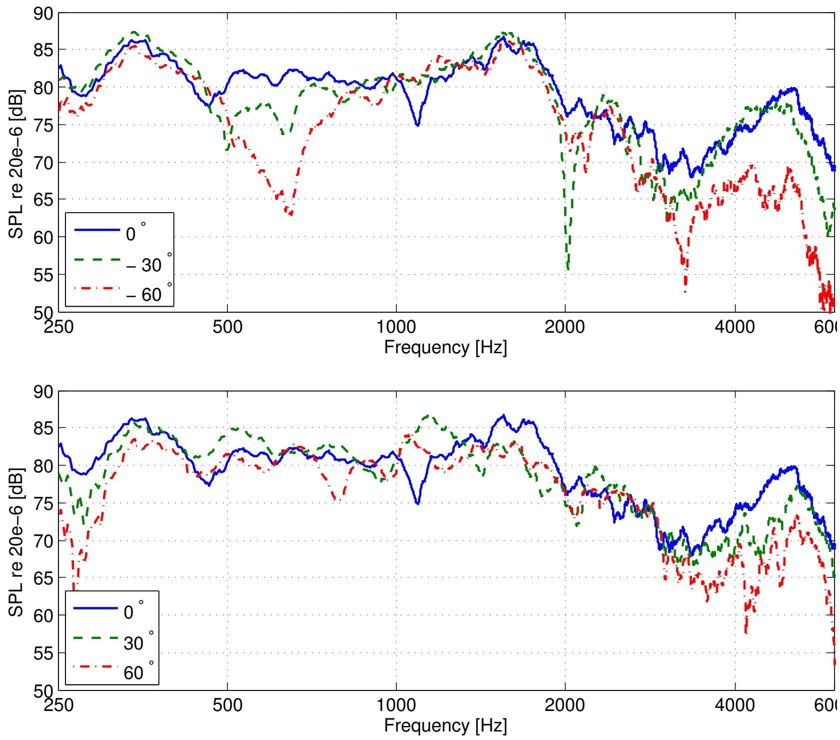

Figure 5.8.: Midrange in a car door: SPL at 1 m in anechoic conditions on- and off-axis (left and right side of a speaker from a top view).

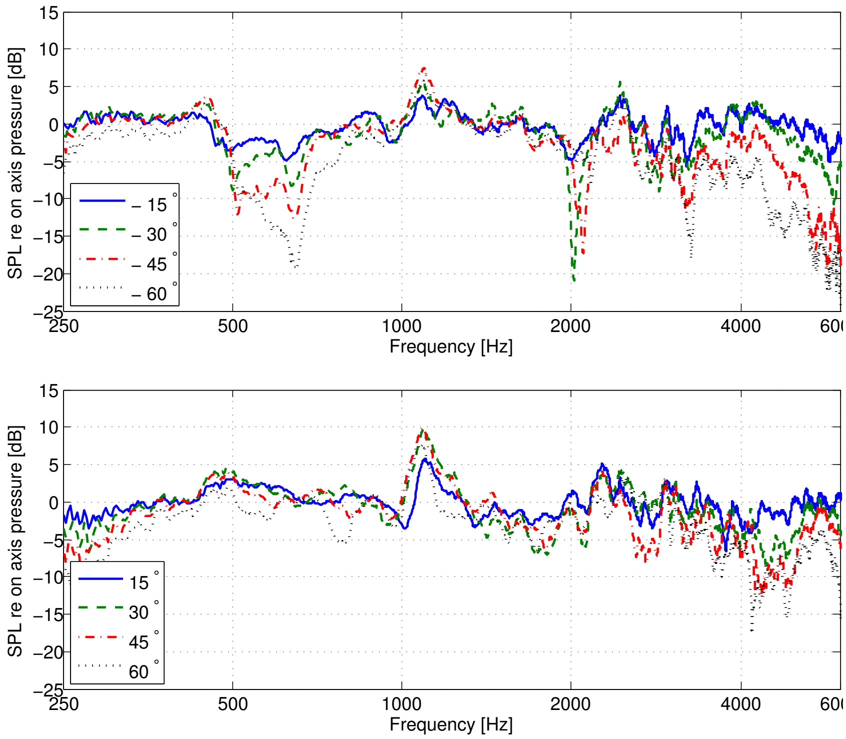

Figure 5.9.: Midrange in a car door: pressure at different angles normalized to on-axis (left and right side of a speaker from a top view).

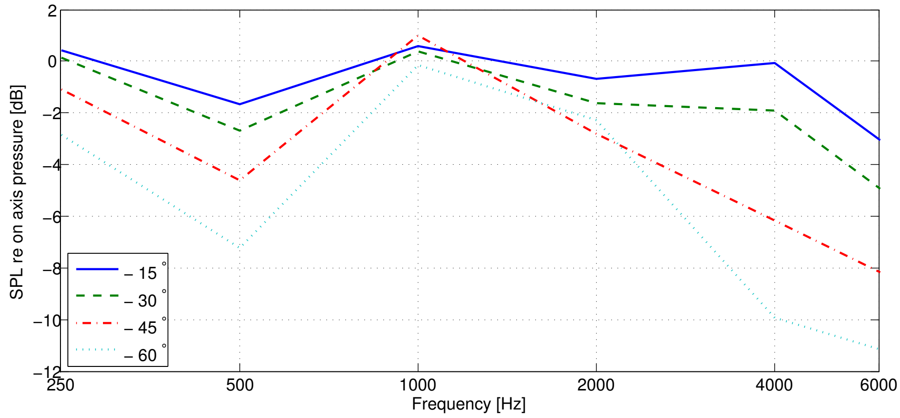

Figure 5.10.: Midrange in a car door: directivity function in octave bands.

Measurements in a baffle

As one could see in the results presented above it is not an easy task to measure the directivity of the speaker when mounted in a car door. The international standard suggests to measure the drivers when mounted in a baffle of specific dimensions [23]. As mentioned before the measurement with midrange in the baffle was also conducted (Figure 4.3b). There were two reasons behind it. First, it is easier to transport only a driver and mount it in the baffle on a measurement scene. Second, the question arises - if the GA model is simplified and it does not reflect small details of the door geometry - should the directivity file also be simplified? Generally, it was of a big interest to see how much the results would differ for car door and baffle cases. And how big difference will they make in GA predictions.

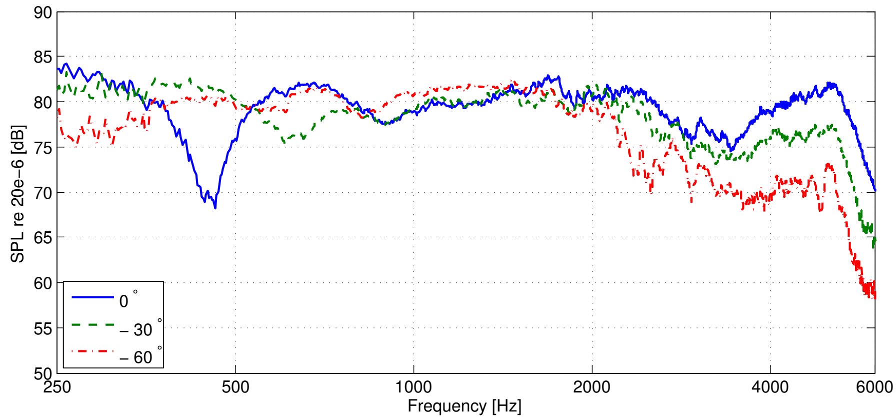

Figure 5.11.: Midrange in a baffle: SPL at 1 m in anechoic conditions on- and off-axis.

Figure 5.11 presents the SPL in a free field corrected to 1 m distance for different angles. Since the midrange in a baffle is rather symmetric, the data only for one side off-axis is shown. The small errors and lack of symmetry could be caused only by not very precise setup. The results are presented for the driver mounted in a baffle without any additional absorption placed on the edges. Therefore, there is a profound dip due to diffraction at 450 Hz and it is reflected in directivity function depicted in Figure 5.12 as a sudden peak for all angles off-axis. The diffraction influence is also visible when the frequency averaging is conducted (see Figure 5.13). Additionally, the octave bands averaged values differ from the door data - especially for 500 Hz, where the difference is 8 dB between the two. Apart from the diffraction issue seen in the figures, the overall directivity of the midrange is captured. The higher the frequency the less omnidirectional the source is.

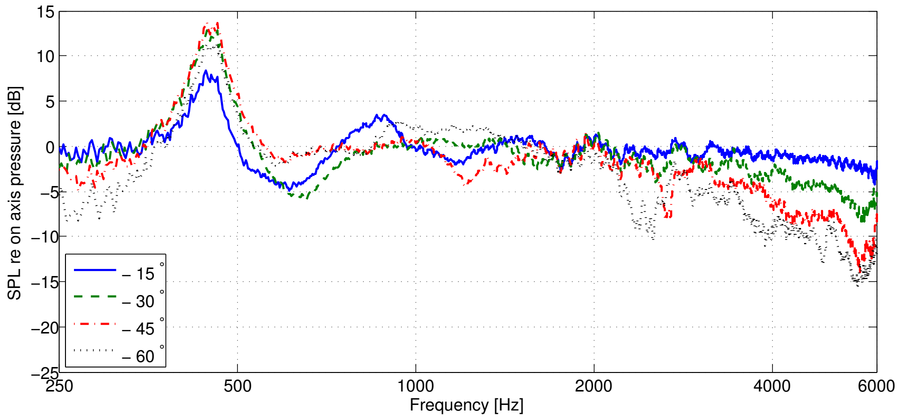

Figure 5.12.: Midrange in a baffle: pressure at different angles normalized to on-axis.

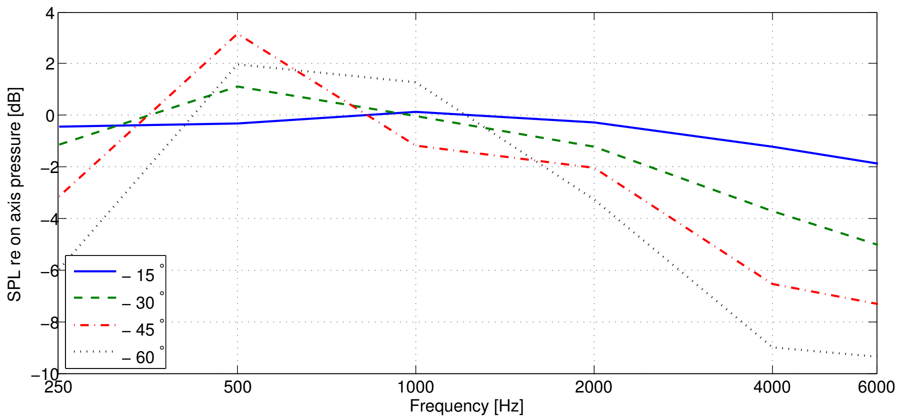

Figure 5.13.: Midrange in a baffle: directivity function in octave bands.

Since, the problems with diffraction issues occurred one more directivity data measurement was conducted after post-processing the previous data. The absorption was added at the edges of the baffle as described in Section 4.1.2. Figure 5.14 shows the results for the midrange placed in a baffle with large amount of absorption (Figure 4.9b). Adding absorption resulted in smoothing out the dip below 500 Hz. Also, since this repeated measurement was taken after post-processing the previous data it was already known that it is better to take the measurements at exactly 1 m distance. It can be seen that the reduced diffraction dip appears at lower frequency (400 Hz) than for the clean baffle case. In general, the average to octave bands transfer function used for modelling is more even than for the two previous cases (see Appendix B).

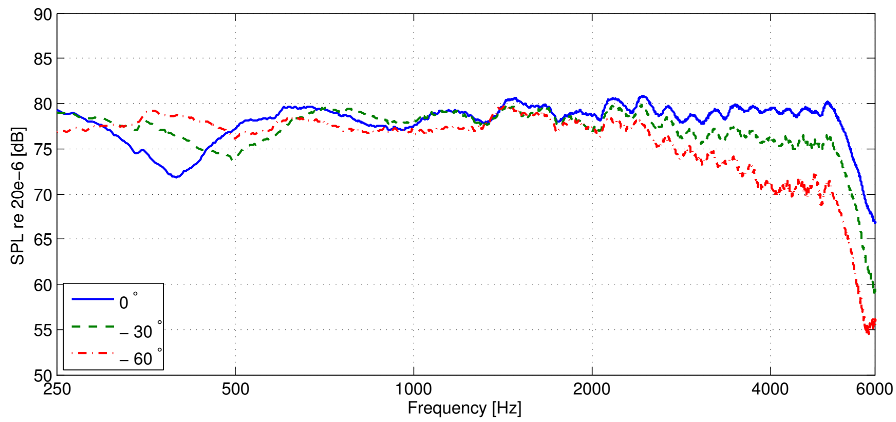

Figure 5.14.: Midrange in a baffle with mineral wool on the edges: SPL at 1 m in anechoic conditions on- and off-axis.

5.2.3. Tweeter

Measurements in a car door

The same set of measurements as for midrange was done for the tweeter. Figure 5.15 shows the transfer functions of the tweeter for different angles. It is interesting to notice that the same angles off-axis give quite different results. The lac of symmetry is most probably cause by the fact that the tweeter was placed not exactly on-axis during measurements. At high frequencies the collected sound pressure is very sensitive to any small geometry differences. Another reason could be the geometry of the car door itself that influences the results. Both graphs capture the fact that the tweeter starts to be omnidirectional already at 4000 Hz when placed in a door. For SPL measured at -30 and -60° a comb filtering occurs. That might be caused by the reflective metal panel on the left to the tweeter (see Figure 4.2). The strong reflection from this panel can cause an interference that is captured as comb filtering.

Due to comb filtering effects on the left side off-axis the directivity function *D* looks very uneven so it is not presented here. Though, the values for right side look rather reliable. Around 3450 Hz a peak due to some diffraction appears. In general the pressure drops until 8000 Hz and then increases again, which is in agreement with data sheet provided by manufacturer. An uneven behaviour of the tweeter mounted in the car door is smeared out when computed to octave bands as seen in Figure 5.16.

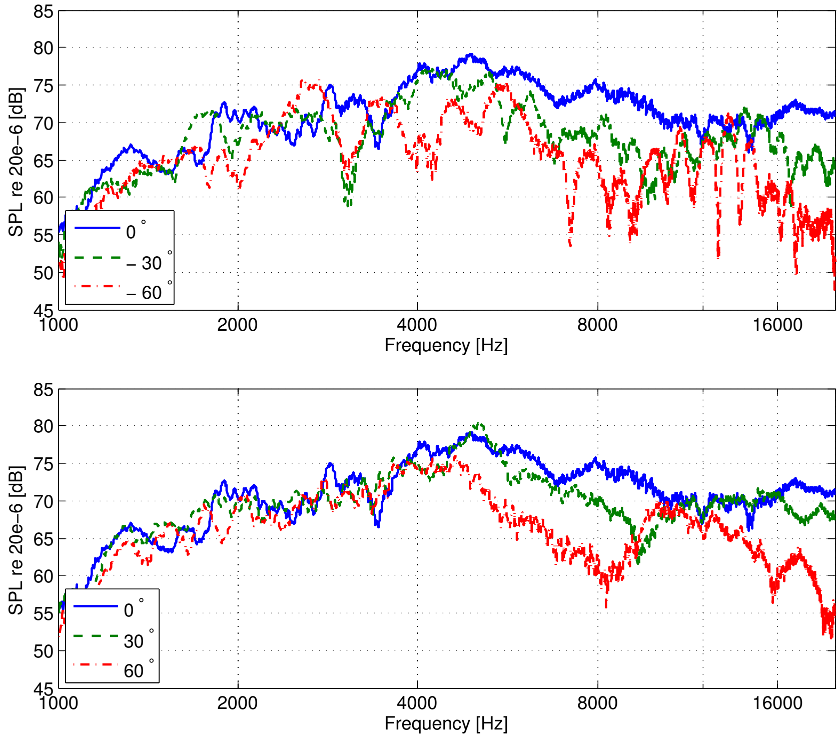

Figure 5.15.: Tweeter in a car door: SPL at 1 m in anechoic conditions on- and off-axis (left and right side of a speaker from a top view).

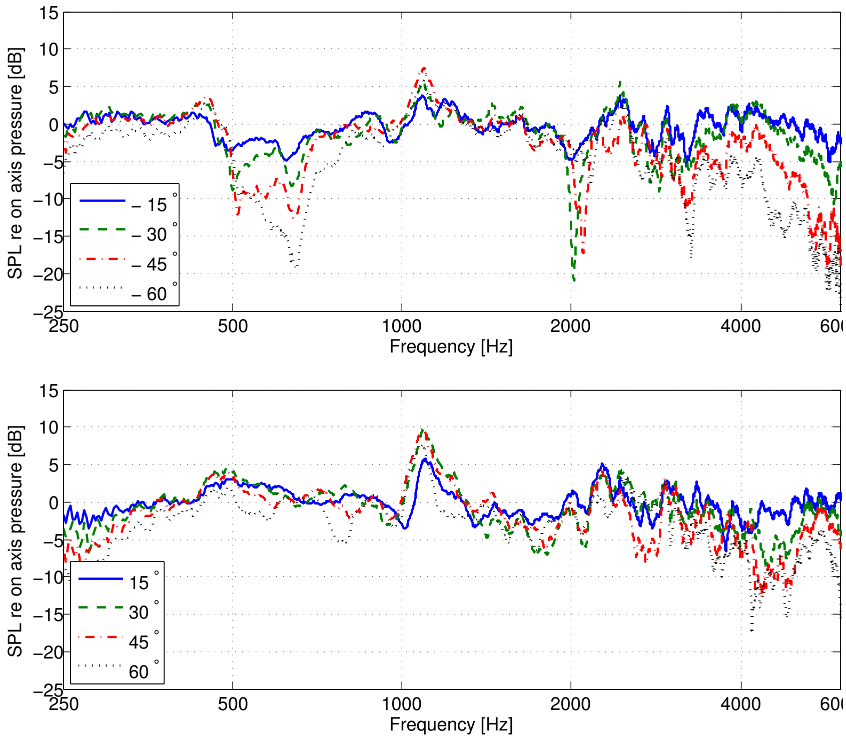

Figure 5.16.: Tweeter in a car door: pressure at different angles normalized to on-axis (left and right side of a speaker from a top view).

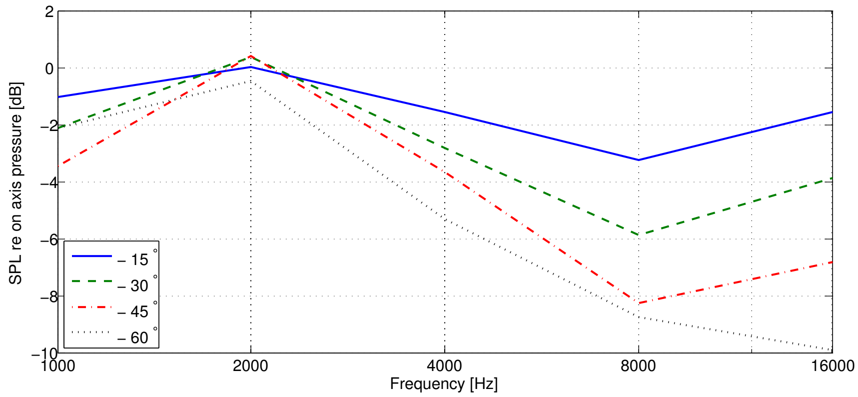

Figure 5.17.: Tweeter in a car door: directivity function in octave bands.

Measurements in a baffle

Again, the measurement was conducted with the tweeter mounted in a baffle as it was assumed to be a simpler case that can fairly enough model the directivity of the unit. Especially since the simple directivity file SD0 was used instead of CLF files (CF1 or CF2) that are much more detailed if it comes to directivity data. Figure 5.18 presents the SPL corrected to 1 m distance. The baffle case was symmetric - more or less the same amplitudes were obtained on left and right side off-axis. In this case there are no comb filtering effects that were observed before. Also, the general shape of SPL for three different angles correspond to the data sheet values given by the manufacturer.

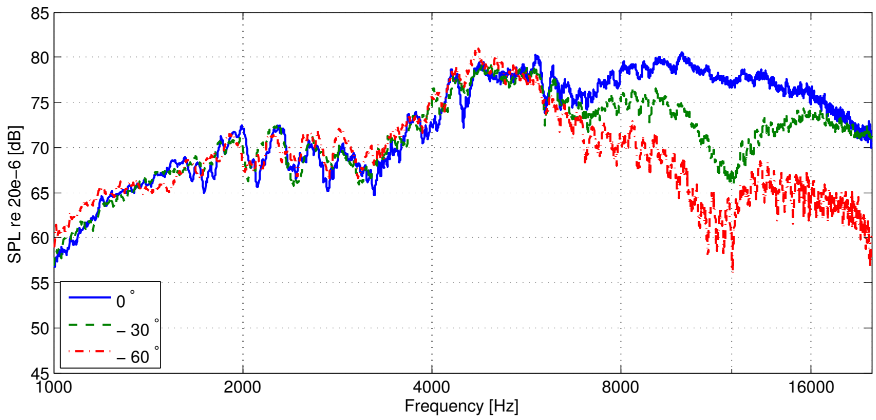

Figure 5.18.: Tweeter in a baffle: SPL at 1 m in anechoic conditions on- and off-axis.

Figure 5.19 presents the directivity function values for selected angles. It captures very well the behaviour of a speaker off-axis. Also, it can be noticed that the tweeter starts to be directive around 5700 Hz which is much higher than for the case of tweeter mounted in a door. So the door geometry influences the speaker transfer function a lot.

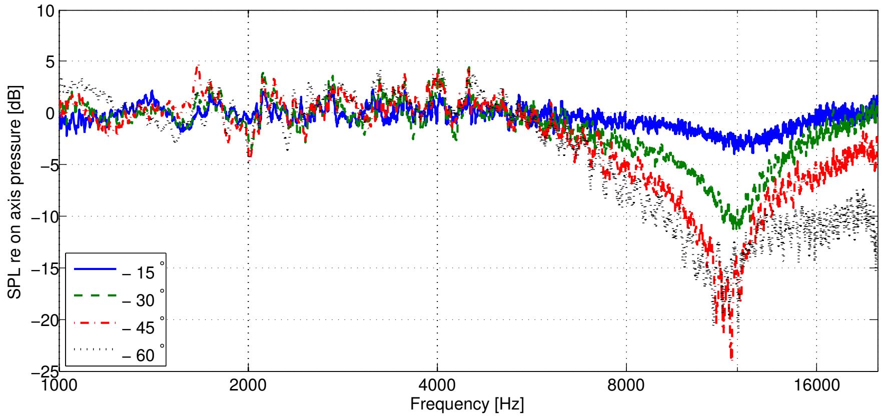

Figure 5.19.: Tweeter in a baffle: pressure at different angles normalized to on-axis.

Figure 5.20 presents the directivity function values already averaged to octave bands, as they are used in GA models. Again, the details of SD0 files for each measurement can be found in the Appendix B. When comparing values in octave bands for door measurement (Figure 5.17) and baffle measurement it can be noticed that they are different, but within +/- 3 dB range. That means that even though the difference in narrow bands seems large the SD0 files do not capture that. The question arises again if more detailed directivity files should not be used to model the source data more realistically. It is worth to mention that in the very first stage of the project the more detailed directivity file format was planned to be used. For example CF2 from *CLF group*. That is why the first measurements were conducted with resolution of 5 °. However, the post-processing of data became rather a large project in itself, so at some point it was decided to use the simpler directivity files. In further work on GA models it would be of great advantage to use better models of loudspeakers. They could be measured by Volvo, bearing in mind all the issues that were problematic during the measurements conducted in the scope of this thesis. They could also be requested from the manufacturer, as directivity data in *CLF* files is widely used by speaker manufacturers.

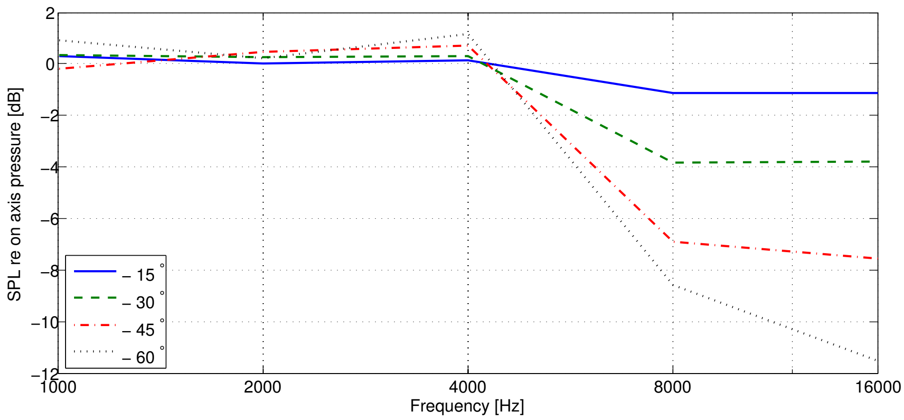

Figure 5.20.: Tweeter in a baffle: directivity function in octave bands.

Figure 5.21 present the SPL measured at 1 m distance arch for the midrange placed in baffle with absorption on the edges. For a tweeter case a smaller amount of absorption was enough to reduce the ringing in frequency response. Figure 4.9a presents the setup. It can be noticed that the peaks are smeared out in comparison to clean baffle when the absorption was used.

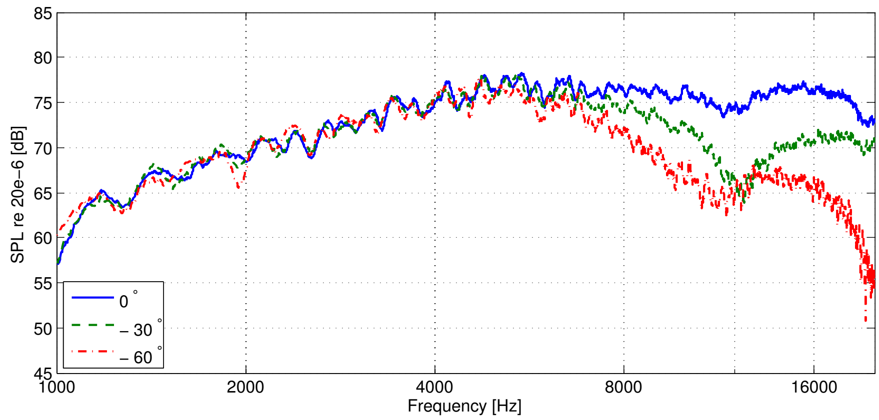

Figure 5.21.: Tweeter in a baffle with acoustic foam absorption on the edges: SPL at 1 m in anechoic conditions on- and off-axis.

As the result of the directivity measurements the three SD0 files for each unit were created and later used in GA models. There were:

- Midrange in a car door
- Midrange in a clean baffle
- Midrange in a baffle with the mineral wool absorption on the edges
- Tweeter in a car door
- Tweeter in a clean baffle
- Tweeter in a baffle with the acoustic foam absorption on the edges

6. Simulations evaluation

Similarly to Microflown measurement method the *CATT-Acoustic* software was newly used at Volvo so modelling the car sound field using GA method was a learning process as well. As a result, within a comparison of GA models with the real car measurements, the study was done on:

- Resolution - how the slight alternations of receiver influence the results
- Scattering coefficient - if and how the results change if the scattering is varied
- Different algorithms and number of rays
- Different level of detail (LOD)

For the sake of brevity not all the results obtained during the project are reported. Instead, the focus is on showing that GA based software can be used to model and predict the sound field in such a specific interior as car compartment at a satisfying level. Mainly, the presented results are the representative results that support the given findings. Additionally, the results that were found unexpected are discussed, as they may lead to better understanding of modelling the car cavity with presented methods.

The chapter contains the comparison of the modelled and measured data for the car in three trim levels. Firstly, BIB was excited with Volvo HF speaker as it was the simplest case. Then, all the cases (BIB, trimmed body without and with seats) were excited with the audio system midrange and tweeter located in the LF door trim panel. Appendix C includes the list of the models that are compared to the measurements within each section of the chapter. Also, the run times for each simulations are noted. The computer CPU was E5-2620 v2 (12 cores).

The results are mostly presented as the FRFs. Only in some special cases the IRs are studied. The reason is that in such a small and absorptive enclosure as car compartment the reverberation time is really low and it is believed that perception of sound may correspond more to the frequency domain than the time domain. The reverberation time was around 30-50 ms. For comparison the reverberation time in a small recording studio can be around 500 ms and in a big church 5000 ms or even more.

In the figures presenting the modelled FRFs of the car cavity there is a green vertical line depicted. It states that above this frequency the GA is supposed to give reliable results. It is roughly 1000 Hz for simple models, though it is good to know that for detailed models this boundary can be higher, around 2000 Hz. That is due to the limitations of GA regarding elements size. The results below 1000 Hz may agree with the measured data, but it is somewhat a matter of coincidence.

6.1. Resolution study in GA models

The aim of a resolution study was to show how the simulation results can be affected by misplacing the receivers in the models. One receiver was chosen to run the model: right ear of left rear passenger, that is receiver 6 in Figure 4.19. Next, 8 receivers were added in a way that they built the vertex of a cube with the original microphone in the middle. It is depicted in Figure 6.1. Distance *d* between the additional microphones was 5 cm in one simulation and 2 cm in another.

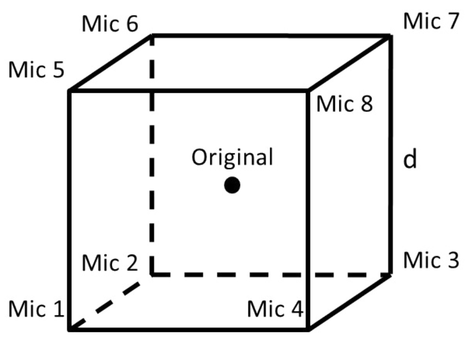

Figure 6.1.: Receivers placement around original microphone (mic 6 in Figure 4.19).

The resolution study was done on the model of trimmed body without seats excited with midrange source. There were several reasons for choosing this particular model for a study. First, the BIB model has the same absorption assigned on all the surfaces and trimmed body already uses the measured absorption in a real car. It was of an interest to see how the results may change for a real car application. Second, ALG2 was tested, as it makes more sense to choose a more deterministic algorithm than ALG1 and since a more absorptive case takes less time to run ALG2 the trimmed body was chosen. Also, the trimmed body without seats was selected simply because it is simpler case than the one with seats inside.

Firstly, the distance *d* between the added microphones was 5 cm - that means that the original microphone was placed ca 8.5 cm apart from the others. The simulation was run using ALG2, 20000 rays and echogram length of 100 ms. The calculation time was 19:02 minutes. Figure 6.2 presents FRFs for all receivers normalized to the input voltage. It can be seen that when the FRFs are averaged to third octave bands, the difference between the receivers falls into +/- 3 dB range. Although, when it comes to comparing the IRs the bigger difference can be noted. Figure 6.3 presents the IRs for 1000 Hz octave band for original microphone and two additional ones. The time plots show that the location of the receiver will affect the IR shape. The question arises if such short time differences can be noticed by the human ear. Maybe, when it comes to subjective listening, the difference between those signals would not be noticeable. Though, they will be reflected in the TF and audible if the auralization is done.

Exactly the same model was run for the receivers placed closer to the original micro-

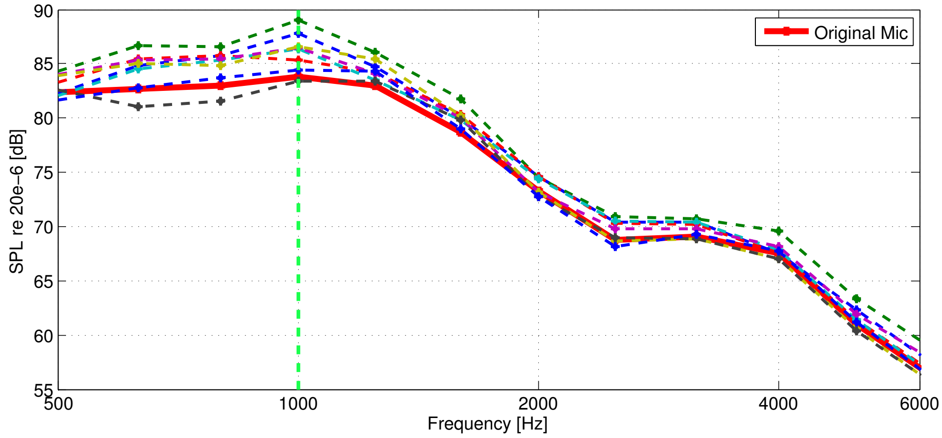

Figure 6.2.: All microphones FRF normalized to input voltage when distance d = 5 cm.

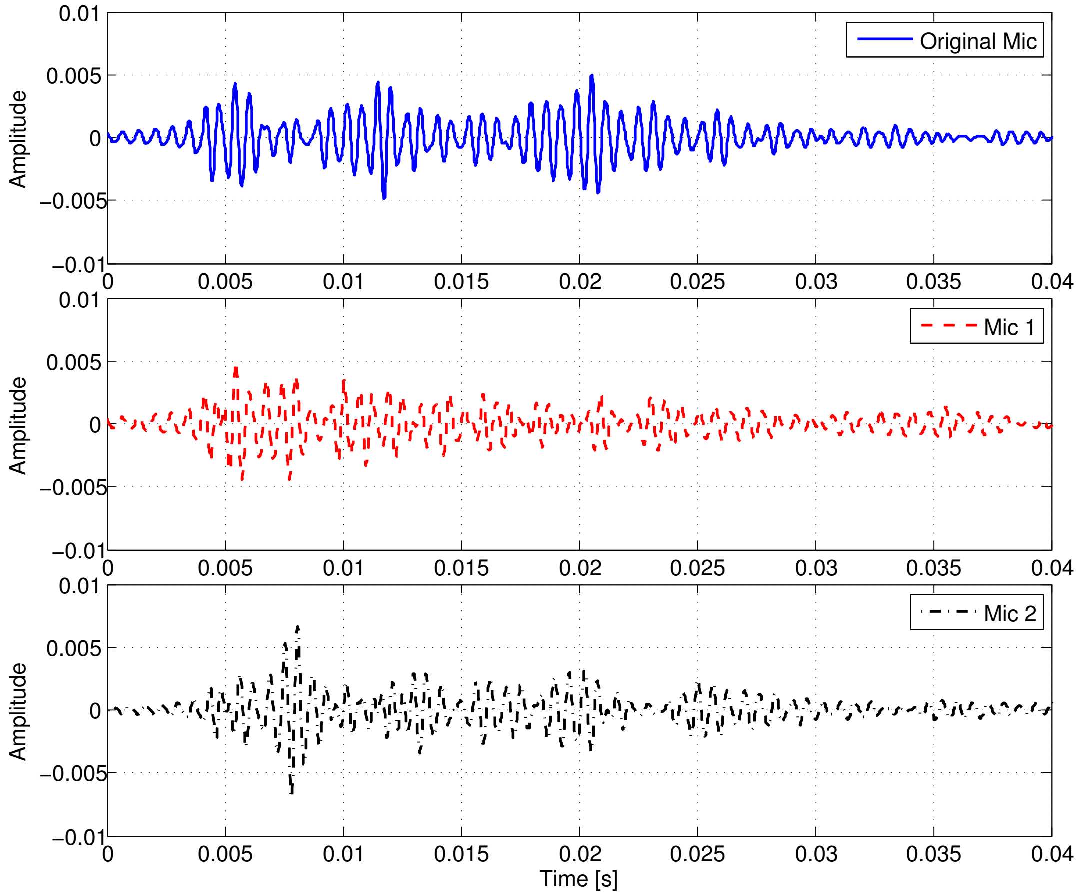

Figure 6.3.: IR for 1000 Hz octave band collected at original microphone, Mic 1 and Mic 2 when distance d = 5 cm.

phone. The idea was to test if the data improves. Now the distance d was 2 cm, making the original microphone placed ca 3.5 cm apart from any other receiver. The simulation was run with the same settings. The calculation time was 17:52 minutes. As expected the FRFs were more alike. Still, the IR plots displayed small differences in time and amplitude.

All in all, it is good bearing in mind that the minor mismatches between actual measurement positions in a real car and receiver locations in the models may lead to discrepancies in results comparison.

6.2. FRF measurements in real car

The FRF measurements were conducted in three different types of cars: BIB, trimmed body without and with seats. Each of this case differs from each other. As mentioned, the reverberation time in all cases is around 20 ms, though for more reverberant case a slightly higher value was observed. Generally when it comes to FRF measurements in BIB the overall SPL values are expected to be higher than in the trimmed body. This is because the BIB has very reflective surfaces (glass and metal) and trimmed body is a more damped structure. In a trimmed body it is expected that the overall SPL is lower when seats are included, as they are quite absorptive. Although, it does not seem to be a case for the microphones located in front of the car. Figure 6.4 presents the case representative for all front microphones for both midrange and tweeter. The BIB case exhibits the expected behaviour. The SPL values are higher than for trimmed body case. However, the SPL in trimmed body with seats for Mic1 to Mic4 is attenuated rather slightly in comparison to the case without seats. And for higher frequencies even a slight boost occurs.

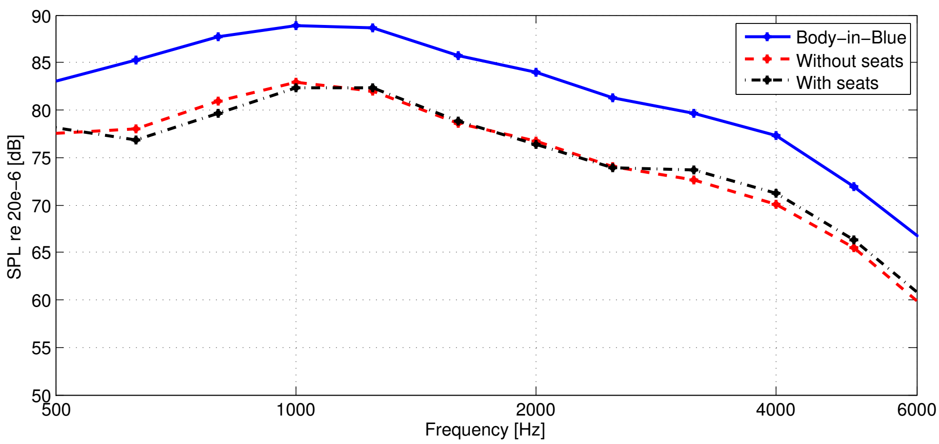

Figure 6.4.: FRF B1xMic4: measurement in trimmed body without seats and with seats.

Though, the microphones corresponding to the rear passengers expose the expected level drop due to the barrier. The sound reaching Mic5 to Mic10 is mostly diffracted over the seats. Figure 6.5 is a representative result for all of the receivers at the back of the car compartment. Again the values for BIB are the highest. Then the big difference occurs for both trimmed body cases. It is shown that the SPL at rear position is lowered by ca 5 dB across all third octave bands due to the front seats. The behaviour was analogical when the tweeter was used in measurements.

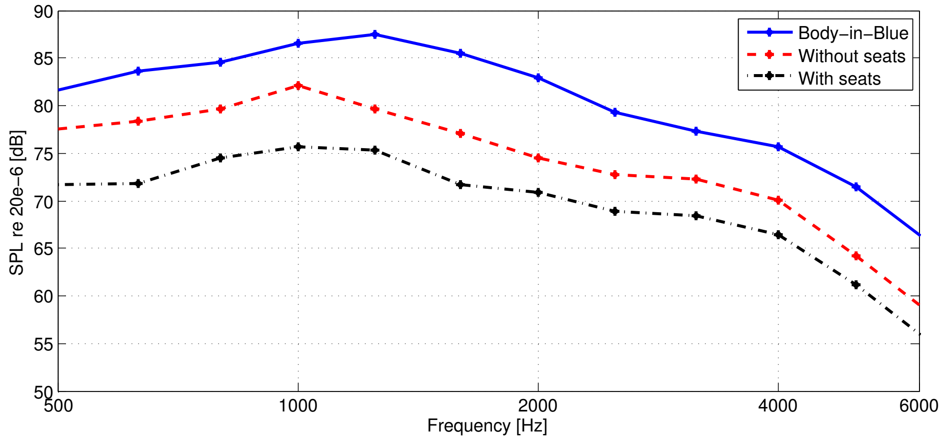

Figure 6.5.: FRF B1xMic6: measurement in trimmed body without seats and with seats.

6.3. Comparison with measurements

The following section presents the simulation data evaluated with the real car measurements obtained as described in Section 4.3.

6.3.1. Body-in-Blue

All the results for BIB excited with Volvo HF speaker are presented as FRFs normalized to the TF of the source measured in anechoic conditions at 1 m distance. This is a default option in GA software, but the measured data had to be compensated for the speaker TF on-axis. The data provided by Volvo allowed to use a correction factor instead of real TF. Although, the correction factor applies only until 10 kHz. Thus, above 10 kHz the measured data might be overestimated.

When the real Volvo audio system loudspeakers are used in the models the presented FRFs are normalized to input voltage. That basically means that the measured FRFs are presented without any further changes. Instead the modelled FRFs had to be corrected for loudspeaker TF measured in anechoic condition at 1 m distance. So during the post-processing all the modelled FRFs are multiplied with adequate measured TF of midrange or tweeter. This means that a phase shift is introduced. Thus, whenever a comparison of measured and modelled IRs is presented, the modelled IRs are corrected for the time shift.

Different levels of detail

As described in Method section there were two GA models built for BIB case. The simple model with 216 elements and detailed model with 2628 elements. Simple model was run with ALG1, 2000000 rays and echogram length of 3000 ms. The run time was 1:46:02 hours for the Volvo source A1. The same setting were used for detailed model. The run time was 18:18:07 hours. The very long calculation time was due to the fact that both sources (A1 and A2) were run in the same calculation. If they are run separately, the calculation would take half the time.

Figure 6.6 presents the third-octave bands values normalized to the TF of a source A1 for Mic 1. In this case it is visible that detailed model matches the measurement better than the simple one even in the region when it was not supposed to give reliable results. In general the results are very satisfying, starting from 1000 Hz the modelled curves follows the measured with +/- 3 dB mismatch. Above 10000 Hz the measured levels seemed to be overestimated what may be caused by the HF Volvo source correction factor which is not correct anymore.

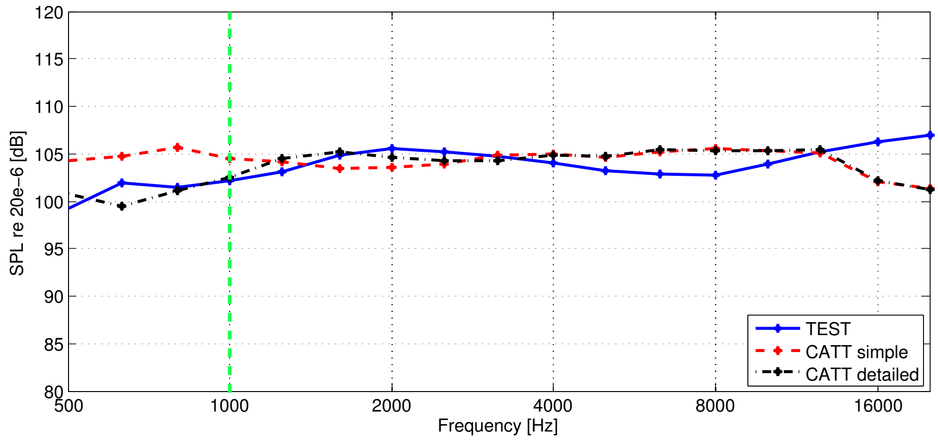

Figure 6.6.: FRF A1xMic1: measurement, simple and detailed simulations run with ALG1 with 2000000 rays.

The biggest differences between the measured and modelled FRFs occur for the receivers in the middle of the car for Mic 9 and Mic 10. The FRFs for Mic 9 are presented in Figure 6.7. The curves for Mic 10 look very similar. Surprisingly, the detailed models capture the behaviour quite well, despite the region from 3150-12500 Hz where the absorption coefficient values seem to be too low, as the small overestimation occurs for all receiver position.

General outcome of this study is that for BIB structure the difference in geometry LOD do not improve the obtained results noticeably. So, it can be stated that the simple model could capture the behaviour of the sound field in the BIB. This means that detailed LOD does not have to be used what leads to shorter computation time for the BIB case.

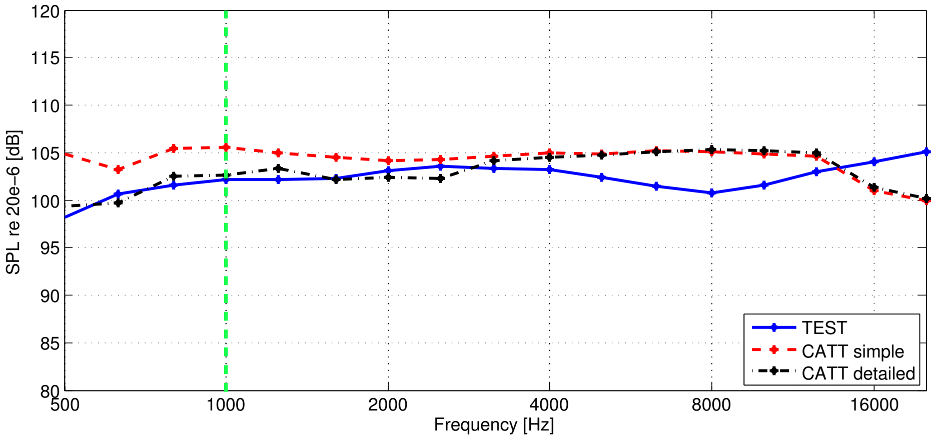

Figure 6.7.: FRF A1xMic9: test, simple and detailed simulations run with ALG1 with 2000000 rays.

Different algorithms

Two different algorithms were used for BIB models to see which one can give better results. Again two models were compared to the measurements. Both were the simple models. First was run with ALG1, 2000000 rays and echogram length of 3000 ms and took 1:46:02 hours. The second one was run with ALG2, 20000 rays, echogram length of 3000 ms and took 1:18:21 hours. Generally speaking, ALG1 is faster than ALG2 and it was suggested by *CATT-Acoustic* developer to use ALG1 for BIB model since it is very reverberant. In this particular case the calculation time for ALG1 is longer as some other runs were started at the same time on the computer. Also, even though the high number of rays in ALG1 generally increase the reliability, the number of rays used seems to be an surplus. Eventually, the number of rays could be lower, as in such a small room they would still manage to cover all the surfaces sufficiently well.

As presented in Figure 6.8 the difference between the ALG1 and ALG2 is not profound. This result is representative for almost all microphones. The biggest discrepancies between the measured and modelled data was observed for Mic 7, as depicted in Figure 6.9. Still, the difference is not big. The highest deviation occurs above 1000 Hz and is less than 5 dB. In the figure it is visible that the ALG2 overestimates the results more than ALG1. This implies that the scattering coefficient might be too low close to this receiver. Very similar results were noted for Mic 5, which is a mirror position to Mic 7. That means that the surfaces on both sides at the back of a car should have higher scattering. General finding is that too low values of absorption at 8000 Hz octave band seem to make the modelled FRFs overestimated. Above 10000 kHz the measured data can be overestimated due to the source correction factor.

Main outcome of this study is that the BIB case can be properly simulated with ALG1 and even the lower number of rays could be used. This means lower computation time. ALG2 can be used as well, but in BIB case it seems unnecessary. Another finding is that the scattering can be increased especially in the vicinity of Mic5 and Mic7.

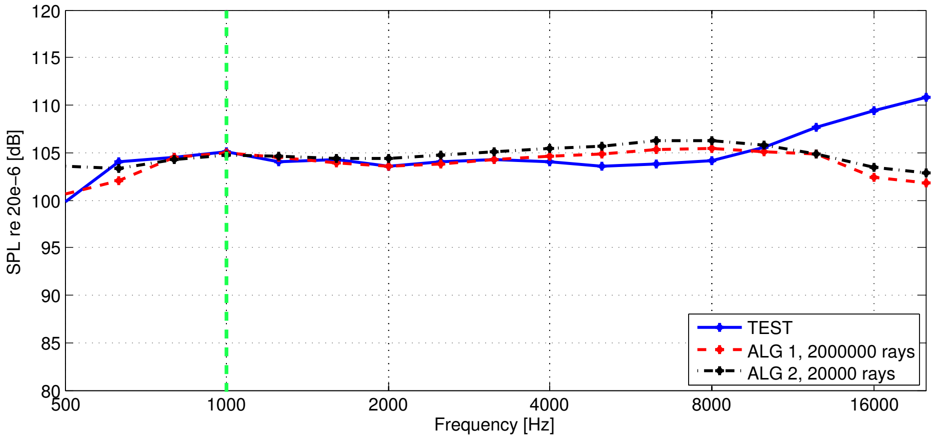

Figure 6.8.: FRF A1xMic3: test, simple simulations run with ALG1, 2000000 rays and ALG2, 20000 rays.

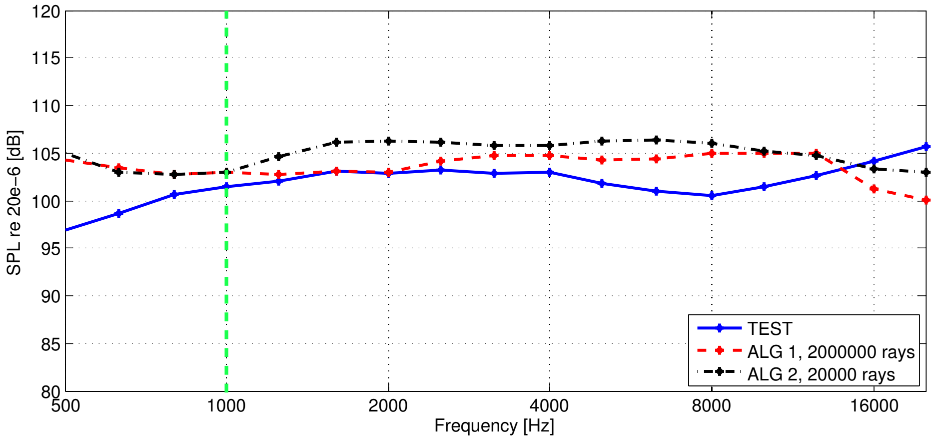

Figure 6.9.: FRF A1xMic7: test, simple simulations run with ALG1, 2000000 rays and ALG2, 20000 rays.

New directivity

As mentioned in Section 4.1.2 due to diffraction effect the new measurement of directivity data was conducted. Basically the problem before was that, especially for the midrange, the diffraction effects were resembled in SD0 files. Meaning that not only the speaker was modelled, but also additional influence of the barrier it was mounted in. Below there are presented the results for the simulations with old and new directivity data. As mentioned, in case of real loudspeakers the FRFs are normalized to the input voltage.

For the case of the midrange the simple model was run with ALG2, 20000 rays. As shown before this could have been done as well using ALG1. Two simple models were compared for different sources. The echogram was set to 3000 ms. The run time for old and new directivity data was around 1:02:00 hours. Figure 6.10 presents results for

Mic6, the shape of the FRFs looks very much alike for all the other microphones. The new directivity data for the midrange agrees with the measurements better than the old data. This implies that the source conditions have to be measured and modelled very carefully in order to provide good results.

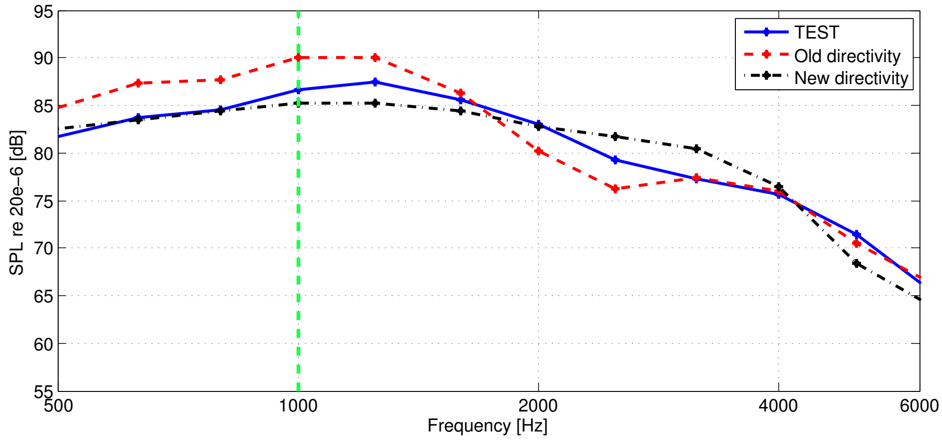

Figure 6.10.: FRF B1xMic6: test, simulations run with ALG2 with 200000 rays for old and new directivity data.

Figure 6.11 presents the FRFs for Mic6 when the BIB was excited with the tweeter. The models with both, old and new, directivity data was run with ALG2, 20000 rays and took approximately 2:25:00 hours. The general difference between the two models were similar for all the other receivers. Again, the new data provides better match. Also, the modelled values above 4000 Hz are overestimated suggesting that the absorption coefficient was too low in the BIB model. So the main conclusion on this study is that the quality of the input data for GA models determines the accuracy of the simulations.

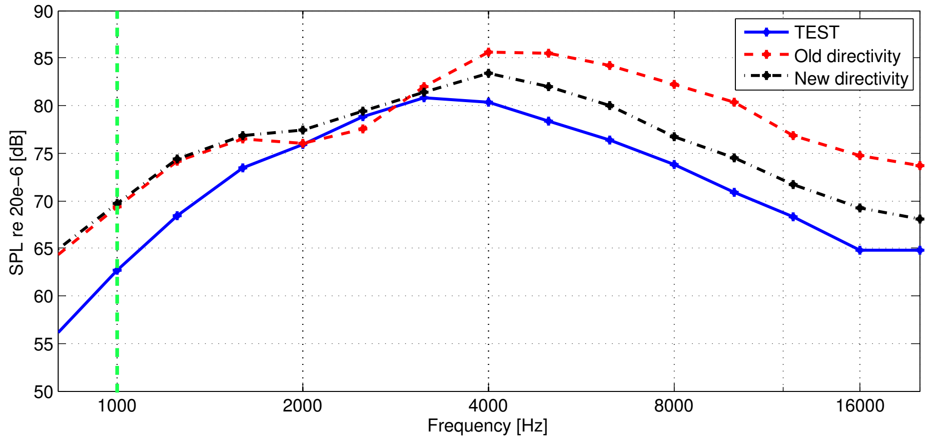

Figure 6.11.: FRF B2xMic6: test, simulations run with ALG2 with 200000 rays for old and new directivity data.

6.3.2. Trimmed body without seats

For all the trimmed body results (both without and with seats) the presented FRFs are normalized to input voltage, since the models were run only for audio system loudspeakers. Generally, in the selected models the directivity files are the ones obtained from measurements in the car door for midrange and for clean baffle for the tweeter. Unless stated otherwise in the model description. That is because mostly the better results were obtained for midrange in car door, since there was no so profound diffraction effect. For the tweeter the better results were obtained for a baffle, since these files did not include comb filtering effects that occurred for car door measurement. At the end of each section there are also reported results for new directivity files, created from measurements in a baffle with absorption on the edges.

Also, in trimmed body cases only ALG2 was used as it is more deterministic and the trimmed cavity is much more absorptive than BIB. That makes it possible to set a lower echogram length in the GA software calculations and that makes the computation faster.

Scattering study

A short study on scattering was conducted in a trimmed body. This was done on a trimmed body case, because it was simulated using ALG2 and it makes more sense to test the scattering influence on the car compartment model with more deterministic algorithm. For one model the scattering was set as described in Section 4.2.2 and for another default values were used for all surfaces apart from windows. That means that all other surfaces had scattering of 10% and windows of 2%. Not much of a difference was noticed in FRFs values averaged to third octave bands neither for midrange speaker or tweeter speaker. Figure 6.12 shows the results for midrange excitation at Mic1, that is a representative example for all the cases.

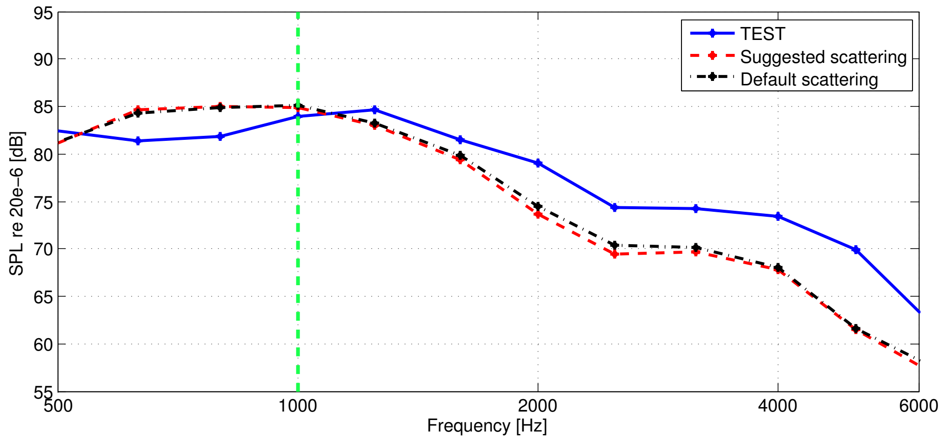

Figure 6.12.: FRF B1xMic1: test, simulations run with ALG2 with 200000 rays for default and suggested scattering values.

Also, the differences between the IRs shape were not easy to catch. It is therefore believed that scattering might not influence the results to a big extent. Although, maybe the difference between the two scattering values was not high enough to notice the change. Thus, it is good to bear in mind that apart from absorption coefficient, scattering values can be always further investigated in order to obtained better simulations.

Additionally, in a scope of further work an investigation on the *auto-edge* scattering is suggested to be done. Generally, when the surface and edge diffraction is used in the GA software the scattering includes the automatic size and frequency dependent values. It is believed that the use of this function would improve the results as it helps to capture the diffraction effects better.

Different number of rays

To test what might be enough number of rays when using ALG2 in trimmed body the different number of rays calculation was done. First simple model excited with LF midrange was run using ALG2, 20000 rays and echogram of length of 200 ms. The run time was 31:16 minutes. Second model was exactly the same only the number of rays was increased to 500000. The calculation time was 2:18:11 hours.

Figure 6.8 presents the example of measured and modelled FRFs in third octave bands. Generally, the difference between the two models is very small, Mic3 is a receiver with the worst mismatch between the models. The other microphones exposed even better match. In the figure, only below 1000 Hz the discrepancies occur what is probably caused by the element size limitation. As a result of this small comparison, it was decided that ALG2 with 20000 rays is enough to model the sound field sufficiently well. The exact same comparison was run for the tweeter excitation and the same conclusions were drawn.

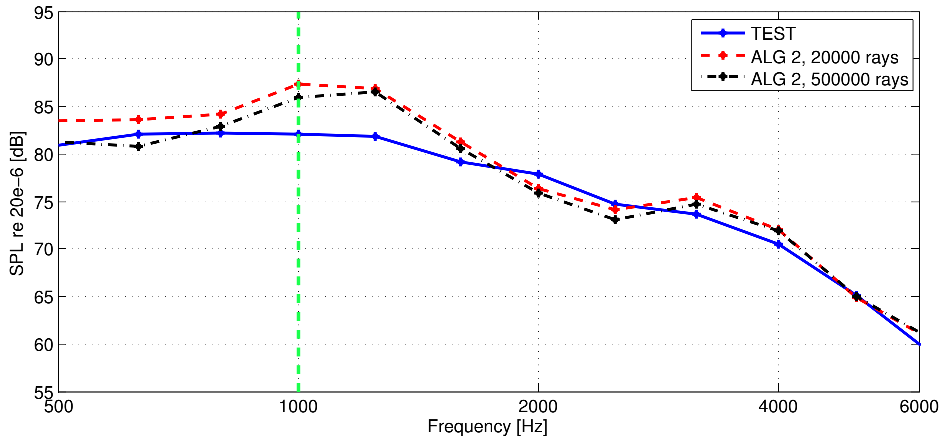

Figure 6.13.: FRF B1xMic3: test, simple simulations run with ALG1, 20000 rays and 500000 rays.

Different levels of detail

The study on LOD was conducted as well. The simple and detailed models were compared. Both were run with ALG2, 20000 rays and echogram of 200 ms. Simple model took 31:16 minutes and detailed 15:28:15 hours. When looking at the FRF averaged over all measurement points presented in Figure 6.14 the two models do not differ much in the range above 500 Hz. In general both models underestimate the results above 2000 Hz, what may be general issue with too low absorption assigned in this frequency band.

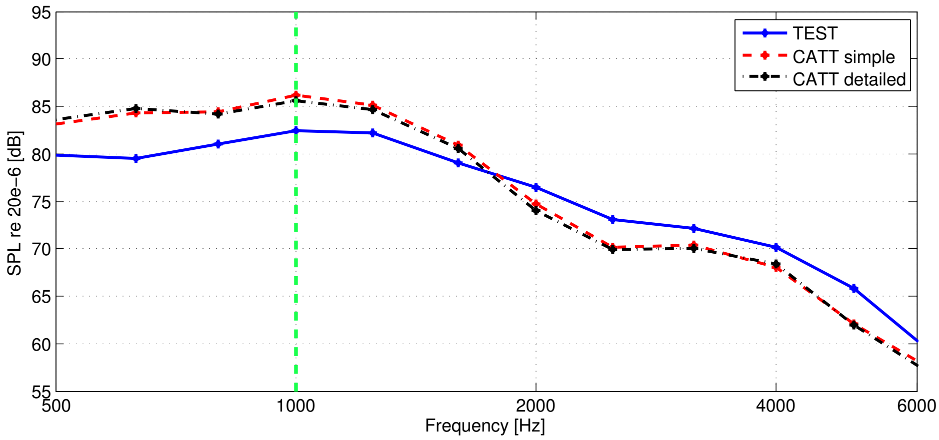

Figure 6.14.: Averaged FRF B1: test, simple and detailed simulations run with ALG2 with 200000 rays.

Generally, the detailed model captures the behaviour at high frequencies better than the simple model as presented in Figure 6.15. For lower frequencies, below 2000 Hz, the modelled FRFs are different from measurements what suggest that at this frequency the model might not work.

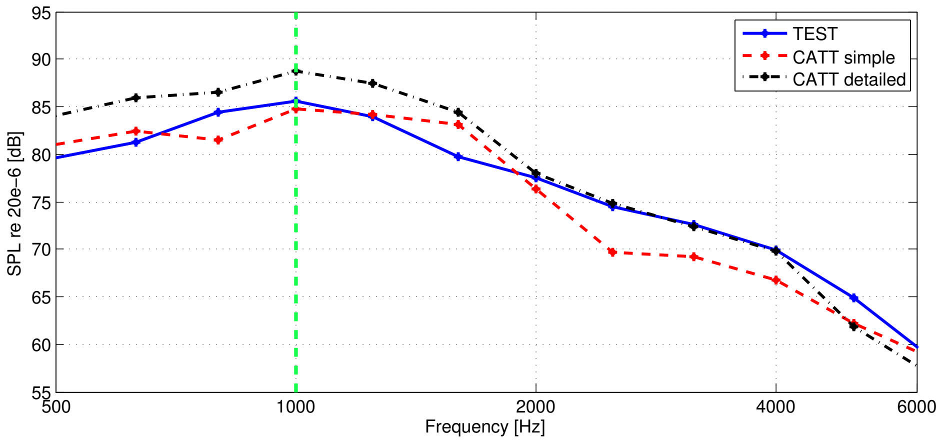

Figure 6.15.: FRF B1xMic7: test, simple and detailed simulations run with ALG2 with 200000 rays.

Although, for two specific receivers the response is better for the detailed model below

2000 Hz. This is a case for Mic2 and Mic4 that are located close to the gear console in the middle of the car. Figure 6.16 presents the FRFs for Mic2 (the curves for Mic4 look fairly similar). There is visible peaking around 1000 Hz in simple model case. Figure 6.17 shows the IRs for 1000 Hz octave band. It can be seen that that there are strong first reflections in the simple model in comparison to reality and the detailed model. In the GA software the ISM module allows to check where the first reflections come from to the receiver. It turned out that the discrepancy appears due to the fact that different absorption was used at the trim panel in both models. Now, in the simple model the reflection from the trim door is very weak and strong early reflections come from the windows and the headliner. Meanwhile, in the detailed model the front door trim seems to capture the sound behaviour better. But that behaviour appears only for the two microphones. The question is if is it not somewhat a matter of coincidence that the detailed model worked better so low in the frequencies. Anyway, the solution could be to model the front trim panel a bit differently, maybe rearranging the geometry in a way that the first reflections reproduce the reality better.

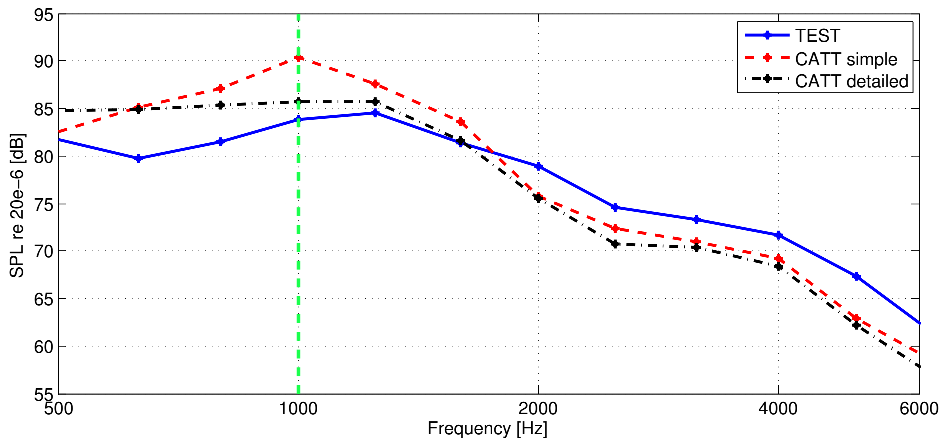

Figure 6.16.: FRF B1xMic2: test, simple and detailed simulations run with ALG2 with 200000 rays.

The same comparison was conducted for higher range loudspeaker. The simple model excited with tweeter was run with ALG2, 20000 rays and it took 48:08 minutes. The detailed model with the same setting run for 6:59:38 hours. Although the front microphones (Mic1 to Mic4) do not exhibit a big difference between the two models, as seen in Figure 6.18, the improvement was noticed for the rear receivers. Figure 6.19 presents the results for Mic6. In general for tweeter simulations slightly better results were obtained when using detailed model, what is logical since GA works better when the elements are larger than the wavelength.

Overall conclusion is that both models can capture the behaviour of the sound in a car compartment with an advantage of more precise models when it comes to high frequencies. Thus, for the future work the split could be suggested. The simple model could be run for the midrange and detailed model for the tweeter simulations.

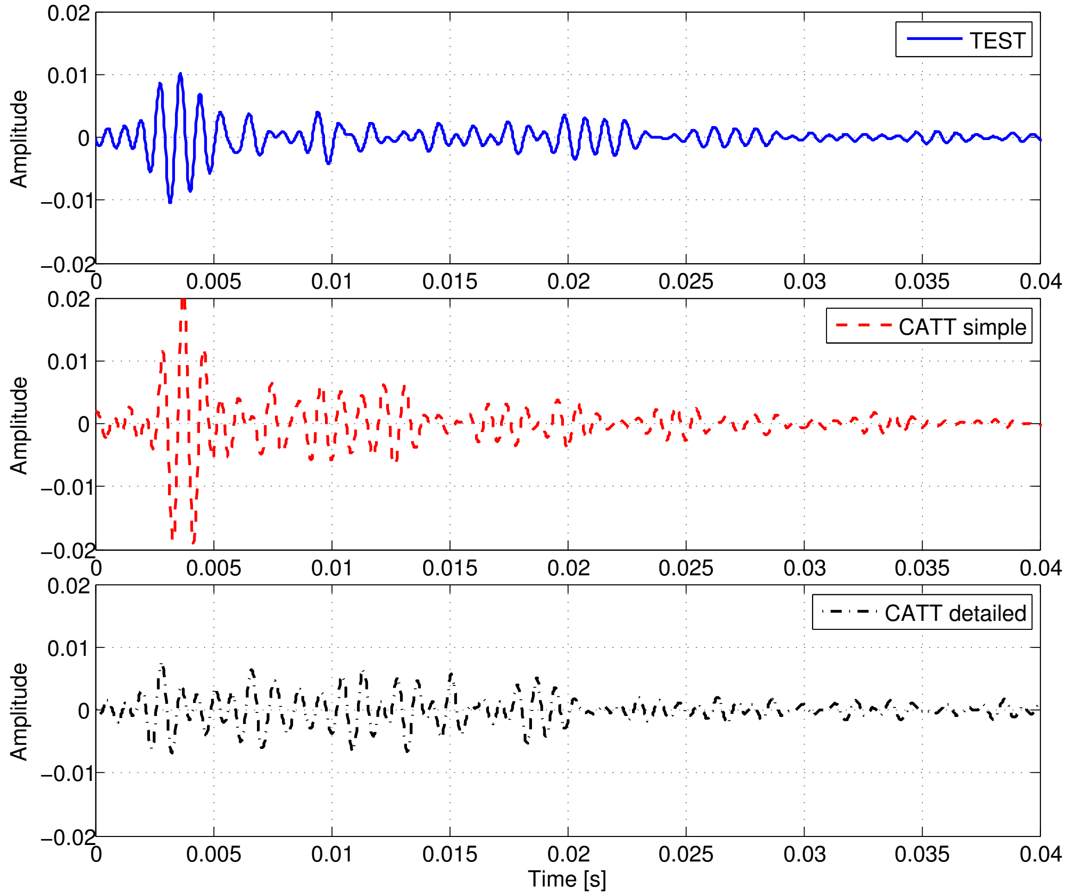

Figure 6.17.: IR B1xMic2 for 1000 Hz octave band: test, simple and detailed simulations run with ALG2 with 200000 rays.

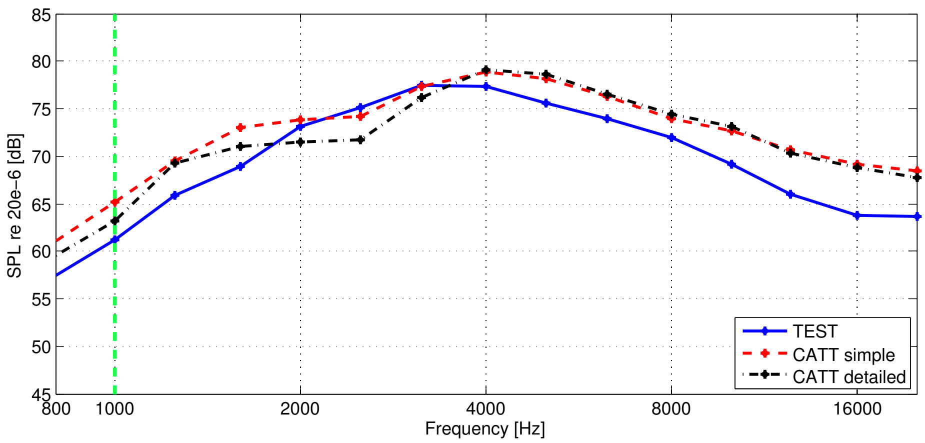

Figure 6.18.: FRF B2xMic3: test, simple and detailed simulations run with ALG2 with 200000 rays.

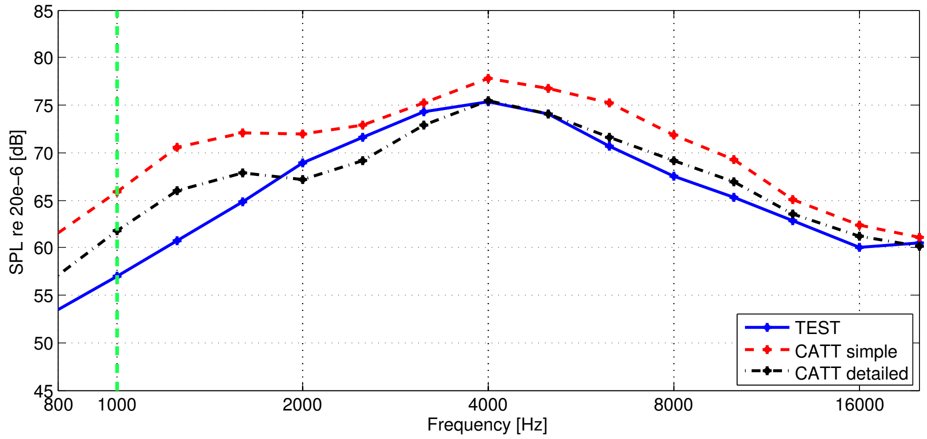

Figure 6.19.: FRF B2xMic6: test, simple and detailed simulations run with ALG2 with 200000 rays.

Additionally, the better correlation with the measurements was seen for two particular receiver positions in the car. This may be treated as a hint for reconsideration of surfaces modelling in front of the car in simple model. That may include altering the front trim geometry as well as the absorption and scattering coefficient values.

New directivity

Again, the old and new directivity data was tested in trimmed body case. For the midrange comparison the two simple models were chosen. Both of them run with ALG2 and 20000 rays. The models run for roughly 21:00 minutes. Figure 6.20 presents the FRFs in third-octave bands for a representative receiver Mic5. The solid line is a measurement and there are two curves showing the averaged responses for old and new directivity files. The discrepancies with measured data fall within +/- 3 dB range. Only above 4000 Hz the absorption coefficient seems to be too high or the source is not properly modelled, as the models overestimate the results. The responses, when using new source data, for the most of the receivers are as good as presented example.

Generally, the new directivity data gave better results than the old directivity data. It means that the high quality input data is of a prior importance. In the scope of the future work an inclusion of more detailed source data would be a benefit.

Figure 6.21 on the other hand shows the worst mismatch, that happened at Mic7. It is interesting to notice that Mic5 and Mic7 are the mirror receivers placed at two different side of the car axis. That suggests that the mismatch does not come from the surface properties data close to the receivers. It can be seen in the impulse response plot presented in Figure 6.22, showing the IRs for Mic7 filtered for 1000 Hz octave band, that the direct sound and early reflections are very weak in comparison to measured data. After studying the first reflections in ISM module in GA software it was confirmed that in both models the first reflections are the same. Therefore, the directivity of the speaker could be incorrectly modelled at one angle corresponding to Mic7 position.

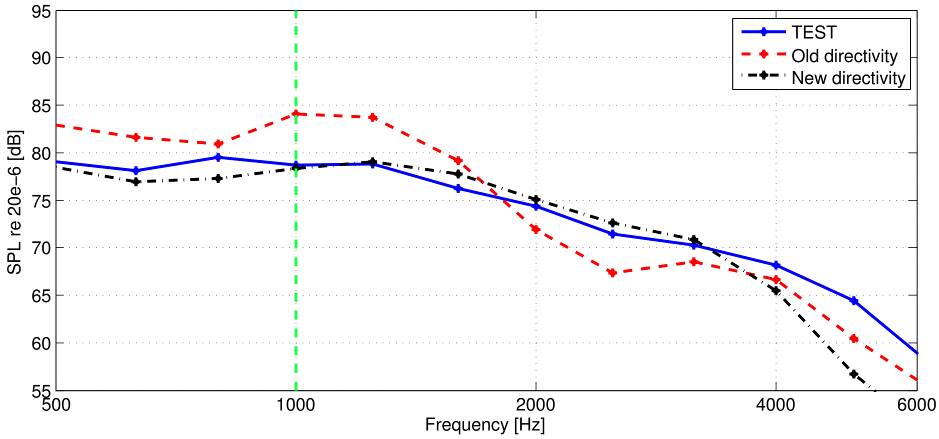

Figure 6.20.: FRF B1xMic5: test, simulations run with ALG2 with 200000 rays for old and new directivity data.

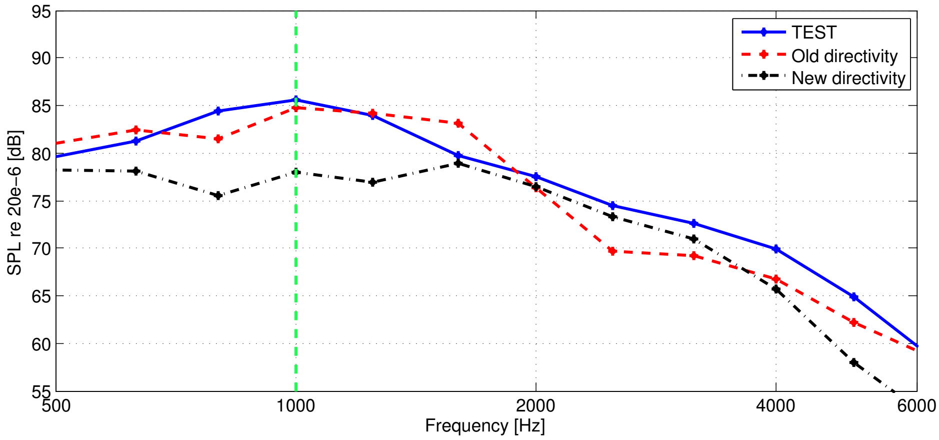

Figure 6.21.: FRF B1xMic7: test, simulations run with ALG2 with 200000 rays for old and new directivity data.

The same comparison was conducted for the tweeter. ALG2 was used with 20000 rays and computation times for both models were around 21:00 minutes. Figure 6.23 presents the averaged values of FRFs for all the receivers. It represents the behaviour of all the microphones very well. While both models agree with the measurements quite well, it is clear that discrepancy above 4000 Hz occurs due to differences in directivity. For an old source the levels are too high, since for the new source the levels in SD0 file are too low (see Appendix B). The mismatch below 2000 Hz seems to be caused by the car geometry data, since for lower frequencies both source files look fairly similar.

The outcome of this study is that the directivity measurements conducted with the special care to remove the edge diffraction effect improved the simulations. It means that the input data regarding source conditions should be modelled as good as possible

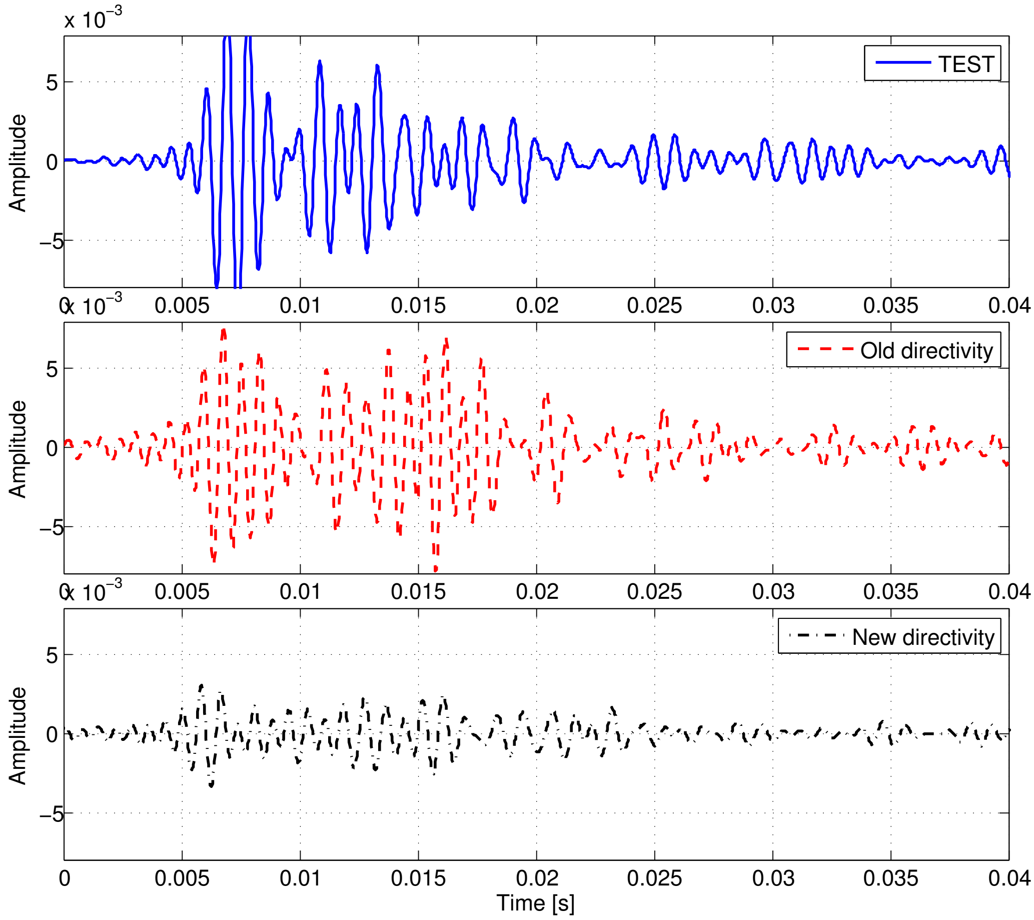

Figure 6.22.: IR B1xMic7 for 1000 Hz octave band: test, simulations run with ALG2 with 200000 rays for old and new directivity data.

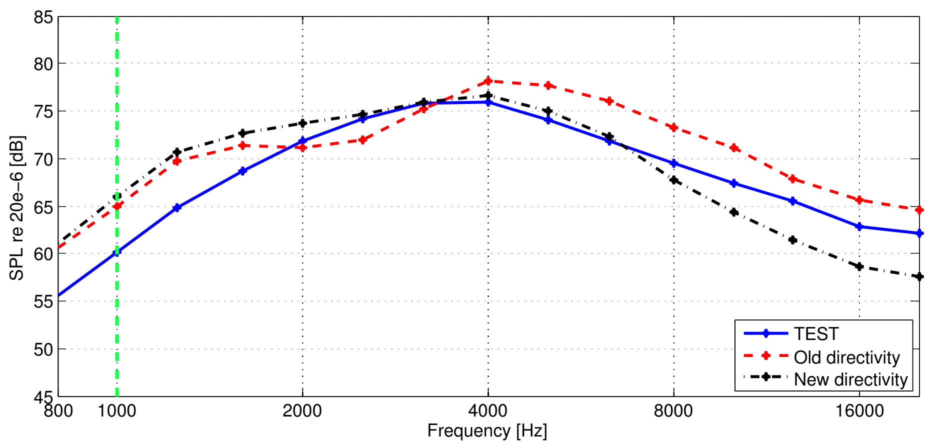

Figure 6.23.: Averaged FRF B2: test, simulations run with ALG2 with 200000 rays for old and new directivity data.

in order to improve the results even more. Although, the predictions give very good match with the measurements for almost all the receivers even though the approximate SD0 directivity format was used.

6.3.3. Trimmed body with seats

As mentioned above the comparisons of the measured and modelled data for trimmed body is done in a way that the modelled FRFs are compensated for the source TF. ALG2 is used in all the models. Generally, the trimmed body with seats is a more complicated case for modelling than the case without seats. That is because there is no direct path between the source and receiver for some of the microphones. It is generally quite hard to capture the diffraction over the obstacle in GA. The problems may occur especially for receivers Mic6, mic9 and Mic10 since they are not visible from the source in the GA models. All the models were run in *TUCT* calculation module with diffraction function switched on.

Different number of rays

For a trimmed body with seats the same study on different number of rays was conducted and the findings were generally the same as for the case without seats. The responses for both models were pretty much the same. The models in such a small room as car compartment may be run with ALG2 with 20000 rays and the response will essentially be the same as for 500000 rays. Figure 6.24 presents Mic8 response. Mainly, the behaviour of both models was similar for all other receivers. The model with smaller number of rays calculated for 34:27 minutes and with higher number of rays for 1:15:23 hours.

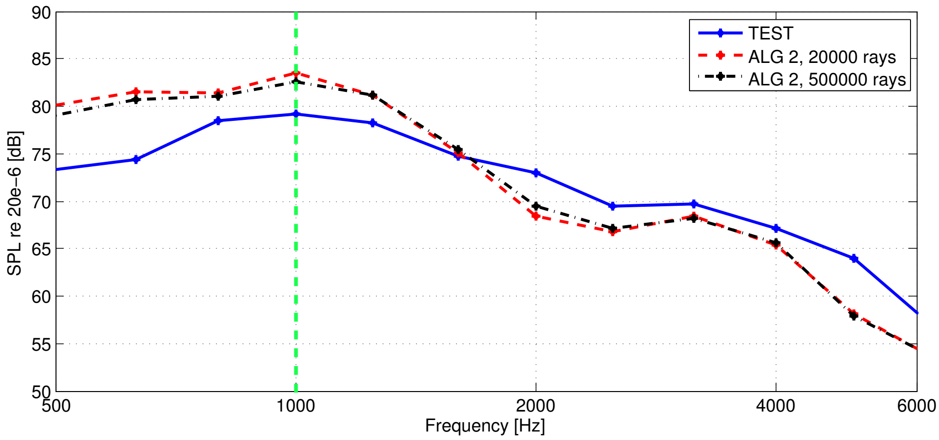

Figure 6.24.: FRF B1xMic8: test, simple simulations run with ALG2 20000 rays and 500000 rays.

The general behaviour for the tweeter is represented by Mic6 shown in Figure 6.25. The model with 20000 rays calculated for 1:18:37 and the one with 500000 rays for 1:14:08. The agreement between the two models using different number of rays is very good.

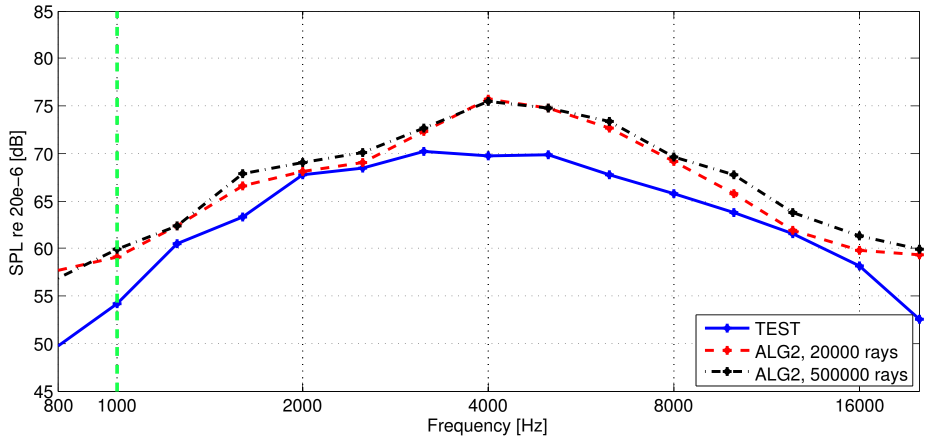

Figure 6.25.: FRF B2xMic6: test, simple simulations run with ALG2 20000 rays and 500000 rays.

The only difference between the two models occurred for Mic5 position. It happened for both sources - midrange and tweeter. Figure 6.26 presents the discrepancy for simple models excited with midrange. The general shape of the modelled values agree with measured values above 1000 Hz with underestimation at around 4000 Hz. Though, below 1000 Hz the mismatch between the models is quite surprising. This might be caused by the fact that in the model the seats geometry is included. This geometry actually has a smaller elements size than the rest of the elements what may increase the frequency from where the GA works properly.

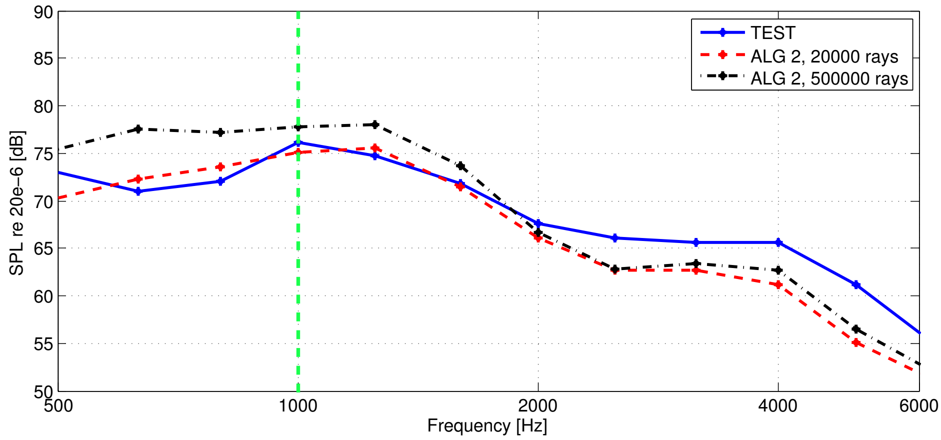

Figure 6.26.: FRF B1xMic5: test, simple simulations run with ALG2 20000 rays and 500000 rays.

Although, it does not seem to be a case for a tweeter simulation. Figure 6.27 shows

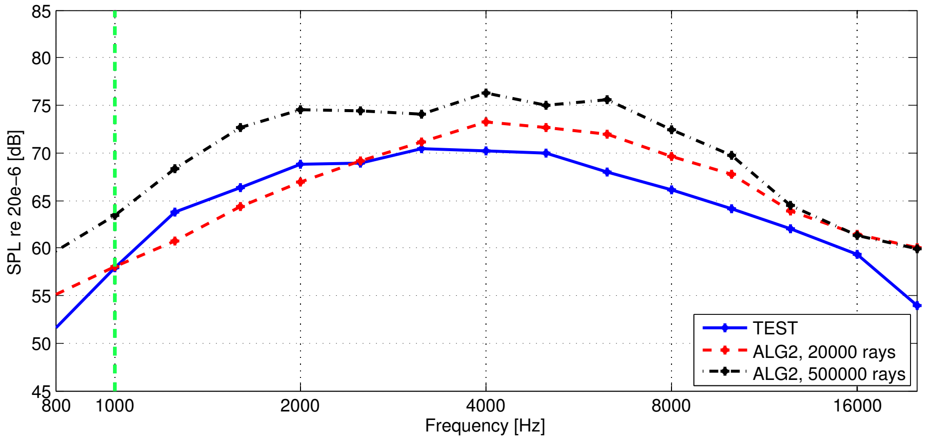

Figure 6.27.: FRF B2xMic5: test, simple simulations run with ALG2 20000 rays and 500000 rays.

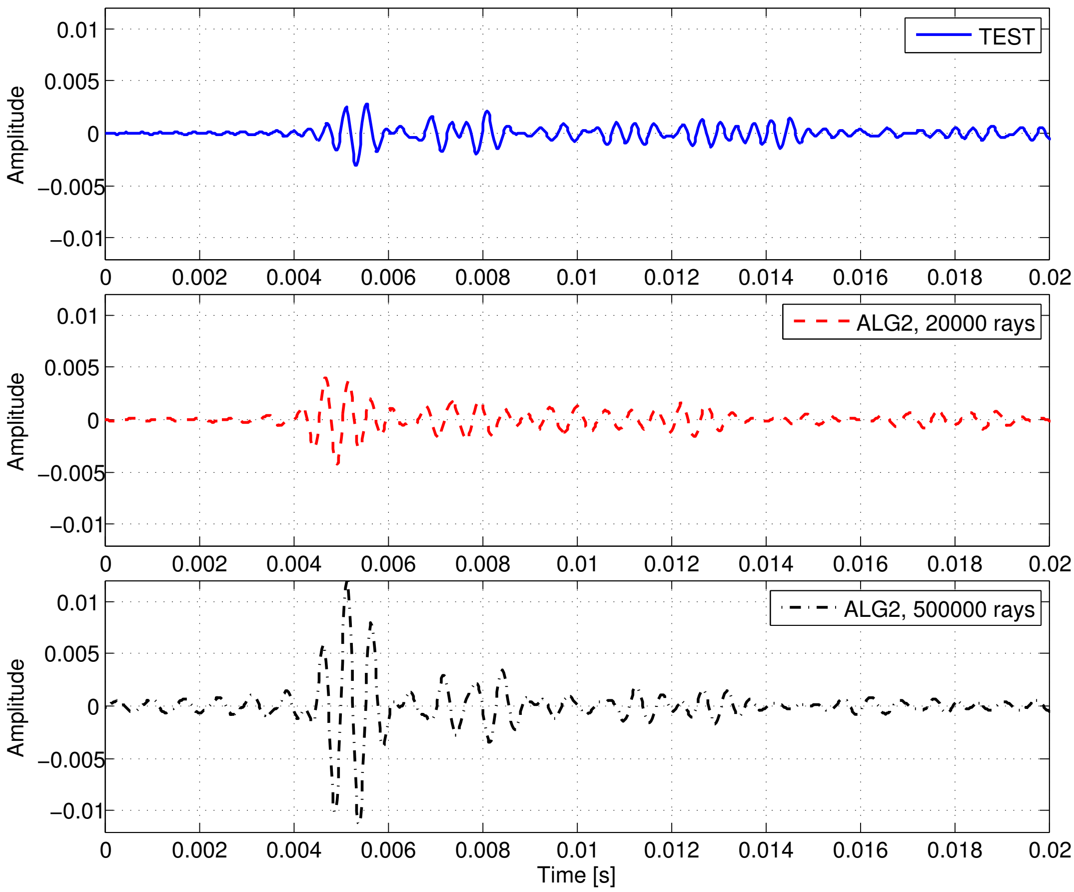

Figure 6.28.: IR B2xMic5 for 1000 Hz octave band: test, simple simulations ALG2 20000 rays and 500000 rays.

the comparison between measurements and models at higher frequencies. *TUCT* calculation module enables an option to see how the first rays reach the receiver in ISM module. Apparently, Mic5 is the receiver that gets early reflections from a left front B pillar. In the model with higher number of rays statistically more rays hit the B pillar so the contribution is higher. It is captured in Figure 6.28 presenting the measured and modelled IRs for the tweeter. The strong early reflections reaching the Mic5 come as the reflection from B pillar.

Since the correlation for both number of rays was very good, apart from the special case of Mic5, the other models were run with ALG2 and 20000 rays as they seemed to be enough to provide repeatable and reasonable results.

Additionally, the problem for Mic5 could be solved using the *auto-edge* scattering provided in GA software. The B pillar could be then modelled better and the difference between the models with different number of rays would not be seen. That is because the *auto-edge* scattering improves the diffraction modelling of small elements modelled in the software [13]. It is a simplified energy-based compensation that grasps the diffusing effects of the diffraction behind the obstacle. It is also believed that using this diffraction model would improve the results in general.

Different levels of detail

Similarly as for the case without seats, the study on different LOD of the models was conducted. Generally, the findings were the same as for the case without seats. The more complex model does not give much more reliable results for most of the receiver positions. The general behaviour of the two models for midrange is presented in Figure 6.29. The models were run with 20000 rays. The simple model took 00:34:27 minutes and the detailed 5:56:02 hours. The detailed model seems to give reliable results mainly at higher frequencies, which is logical for GA.

The interesting discrepancy occurred for the midrange case for Mic7 position. Figure 6.30 presents the results of measurements and two models. High discrepancy between the measurements and simple model is caused by the early reflections coming to the receiver. It was checked in *TUCT* ISM module where the first order rays come from. In the detailed model after the direct sound the most profound rays are reflected from the hard metal surface just above the armrest. In the simple model the door trim is averaged to one material which is more absorptive than the metal element.

It is also interesting to mention that the detailed model without seats gave the very similar pattern, although the match with the measurements was better. It is shown here in Figure 6.31. This means that the influence of the seats is not capture by the Mic7. In a new measurement the sound is attenuated at this receiver. As this problem occurs only for Mic7, that gets direct sound from the speaker, maybe only the geometry of the seats should be improved.

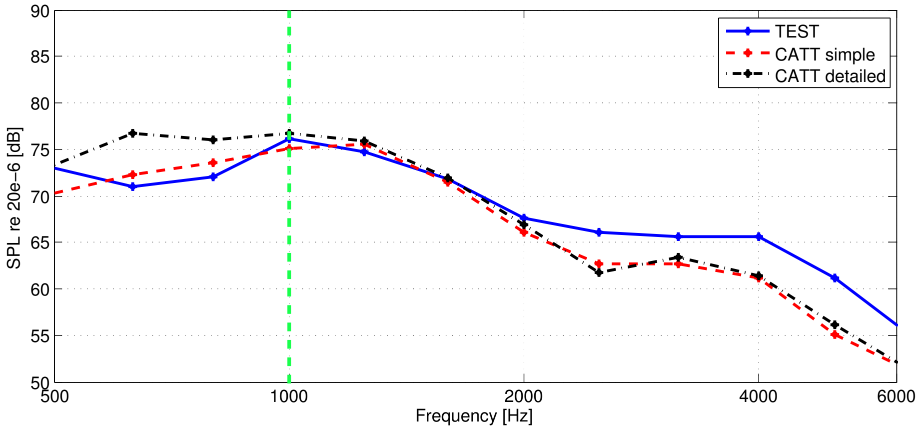

Figure 6.29.: FRF B1xMic5: test, simple and detailed simulations run with ALG2 with 200000 rays.

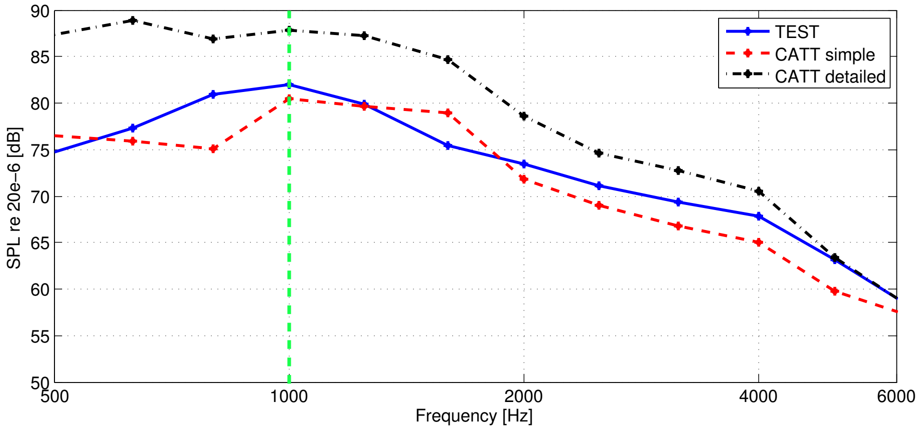

Figure 6.30.: FRF B1xMic7: test, simple and detailed simulations run with ALG2 with 200000 rays.

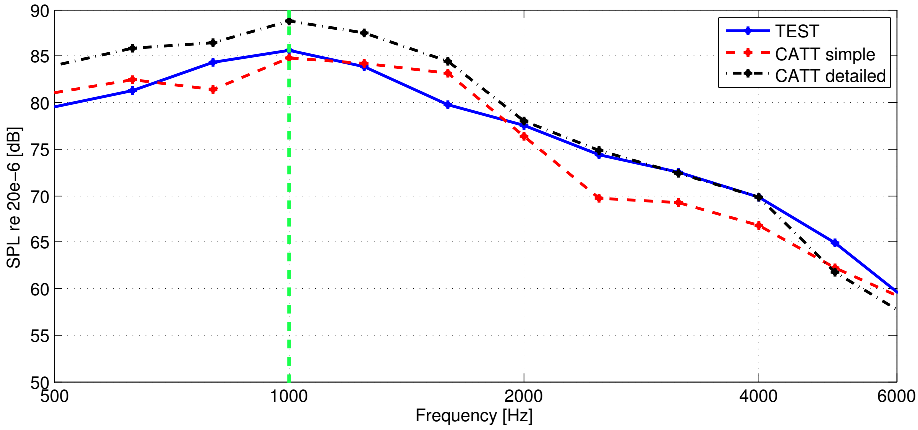

Figure 6.31.: FRF B1xMic7: The same comparison as in Figure 6.30 but for the case without seat.

For the tweeter the model with higher LOD appeared to improve the results only for very high frequencies. It may imply that the detailed model can give reliable results only for higher frequencies. The improved agreement between the measurements and two models is depicted for representative Mic5 in Figure 6.32. The two models compared were run with 20000 rays. The simple model computed for 01:18:37 minutes and the detailed one for 8:19:48 hours. The similar problem as at Mic7 for midrange source occurred as well for the tweeter at one position. This time it was Mic6 - the one behind the LF seat. The same conclusions were drawn for this case.

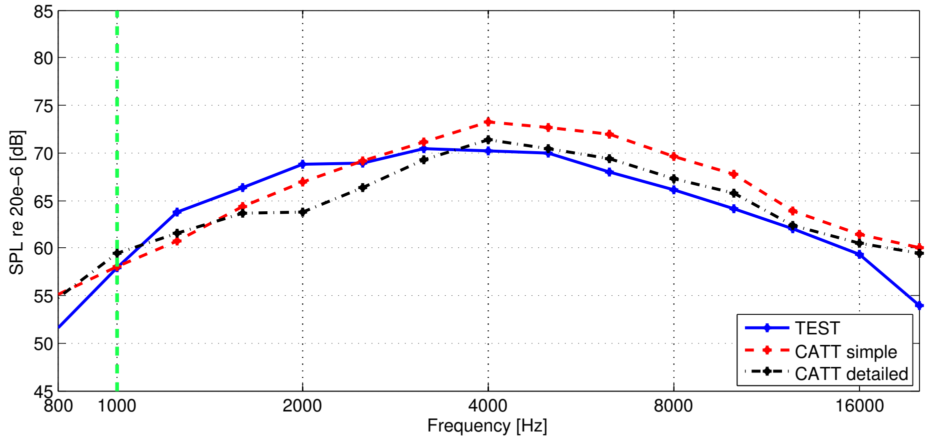

Figure 6.32.: Averaged FRF B2: test, simple and detailed simulations run with ALG2 with 200000 rays.

The main conclusions are that the detailed model can be used for higher frequency model e.g. for tweeter. It is also problematic to capture correctly the behaviour for all of the microphones at the back seats. For the modelled data improvement again the investigation on the *auto-edge* function is suggested. Also, the geometry of the seats could be revised.

New directivity

As it was already shown in the previous cases (for BIB and trimmed body without seats) the good match with the measurements can be obtained only if the input data is modelled carefully. The new directivity files were also tested in the trimmed body with seats. The overall responses look better when using the new data. Again, that is because the edge diffraction issues were no longer causing problems. The run times for both models were roughly 35:00 minutes for the midrange. Figure 6.33 presents the well matching case. Most of the other microphones gave better results for new directivity as well.

Although, there were two microphones that provided worse response for the new data. It was Mic1 and Mic2. The latter is depicted in Figure 6.34. The results show quite big mismatch for the frequencies between 400 and 1250 for an old model and above the shape follows the measurement curve, but the levels are too low. For the new model

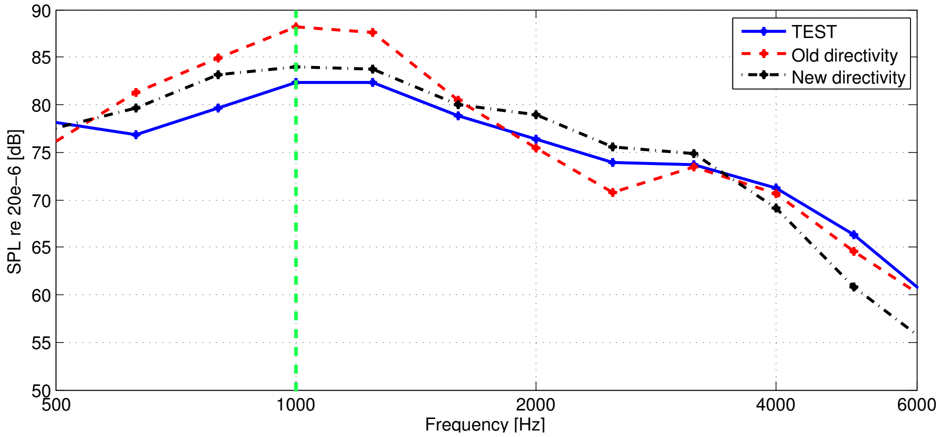

Figure 6.33.: FRF B1xMic4: test, simulations run with ALG2 with 200000 rays for old and new directivity data.

it seems that below 1000 Hz the agreement is better. Above 1000 Hz the shape of a curve is very similar to the measurements. It may mean that new directivity is better modelled, but the sensitivity data is too low above 1000 Hz. This explanation would also match the BIB and trimmed body without seats cases.

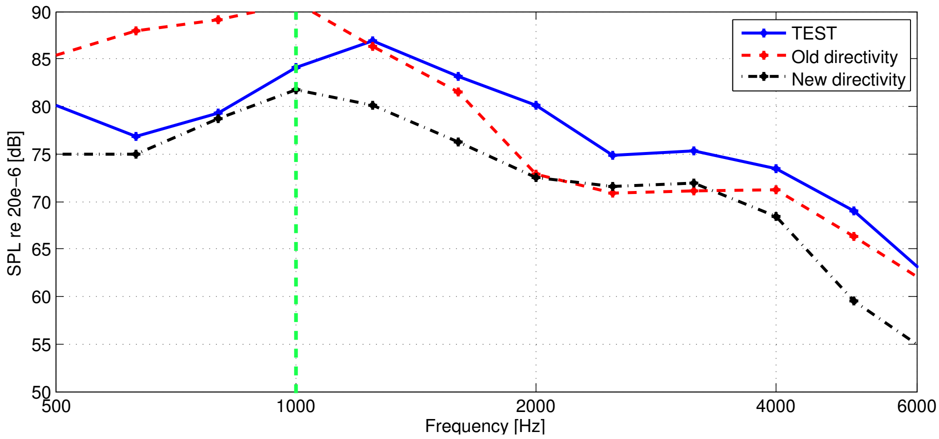

Figure 6.34.: FRF B1xMic2: test, simulations run with ALG2 with 200000 rays for old and new directivity data.

Additionally it is interesting to present the behaviour of the Mic7. The results for this receiver are depicted in Figure 6.35. The similar drop occurs around 1000 Hz as for the simple case presented in Figure 6.30. That could mean that the model would benefit if the door trim panel is modelled with more precision or with better absorption coefficient and if the right front seat is represented better.

For the tweeter source the models with new and old directivity data were compared as well. Both models were run with ALG2 and 20000 rays. The run times for both models were roughly 47:00 minutes. On average the small improvement was seen for the new data set. Even for the receivers that do not include the direct path. Figure 6.36

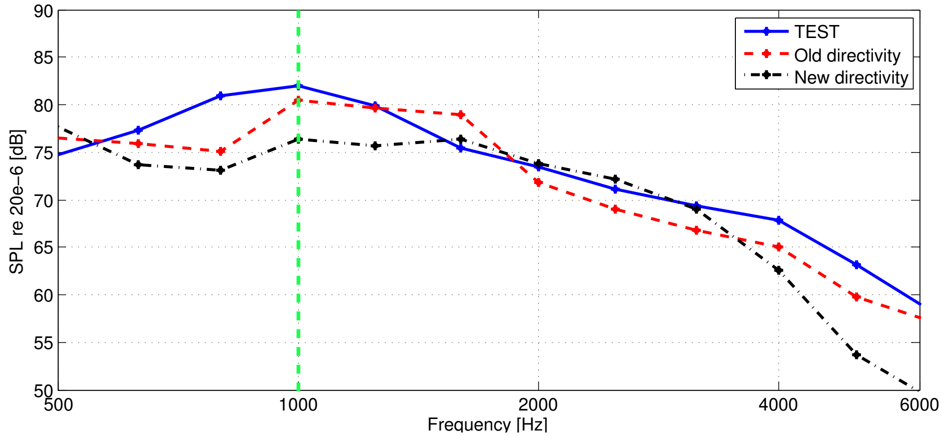

Figure 6.35.: FRF B1xMic7: test, simulations run with ALG2 with 200000 rays for old and new directivity data.

presents the receiver example without the direct path. The new curve follows the measurements better than the old one. Still, the FRF is overestimated below 1000 Hz and underestimated at high frequencies. Since for all the microphones above 6300 Hz the overestimation occurs for old directivity data and underestimation for the new data, it is believed that the problem is due to modelling of a source. So, it is again important to state that the accuracy of the simulation relies greatly on the input data details and quality.

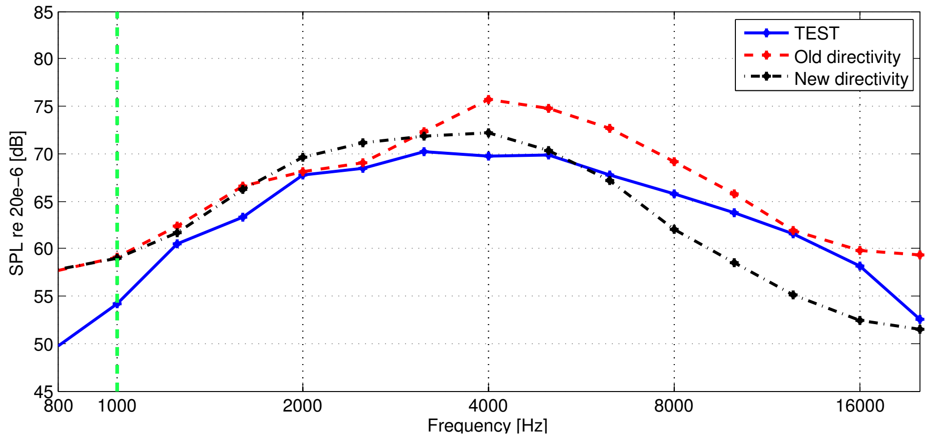

Figure 6.36.: FRF B2xMic6: test, simulations run with ALG2 with 200000 rays for old and new directivity data.

Tuning procedure

As shown in the previous section the new directivity data was tested in order to obtain better matching results. The obtained data was really good for all three trim levels, especially if one takes into account the number of uncertainties about the input data and the fact that it was a first trial with GA simulation at Volvo.

Finally, the tuning trial was conducted to see if the match with the measurements can be improved. And tuning in this case means changing the absorption coefficient. This was conducted only for a trimmed body with seats case, as it was the most interesting case for the company. Also, the other two cases without seats gave very satisfying results already. In the new model the two materials were altered. The plastic elements on the pillars and IP were modelled using much lower absorption values found in the literature. Also the panorama roof was changed to lower values at 8 and 16 kHz octave bands since around this frequencies the modelled FRFs seemed to be underestimated. Also, the *auto-edge* scattering was assigned to all of the surfaces. Before, it was assigned only to the seats.

For the midrange case the following procedure improved the results only slightly for several position. The example of Mic2 is shown in Figure 6.37. The model with changed absorption data computed for 23:17 minutes, as the echogram was set to 50 ms. The general shape of the FRF is captured better also for the frequency range below 1000 Hz, but still the overall levels are lower than measured. The suggestion would be to conduct the tuning procedure carefully studying what materials influence the response.

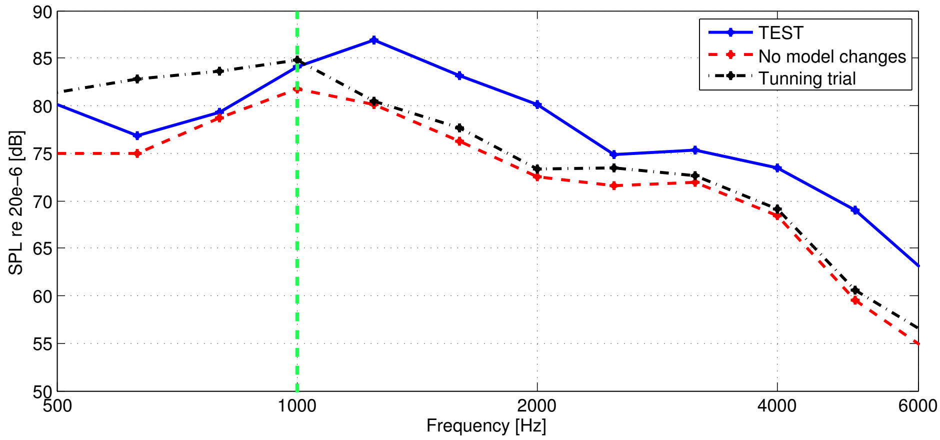

Figure 6.37.: FRF B1xMic2: test, simulations run with ALG2 with 200000 rays for old and new absorption coefficient values.

Figure 6.38 presents the response for Mic1 for the tweeter source. The models compared were run with ALG2, 20000 rays. In both the new directivity data was used, meaning the one obtained from the measurements in baffle with absorption on the edges. The model with old material parameters run for 47:15 minutes as the echogram length was set to 200 ms. The model with new absorption took 23:17 minutes as the echogram was set to 50 ms to lower the calculation time.

In the figure it is seen that generally lowering absorption increased the level, but the shape of the curve remained more or less the same. That means that the improvement of directivity data would be an advantage. For better tuning the further investigation on absorption coefficient could also be suggested. The controlled and well-though error and trial method might be a solution to tune the model to the measured values. Also, if the computation time is not a problem for the tweeter simulations the detailed models could be used as they generally created better results at higher frequencies.

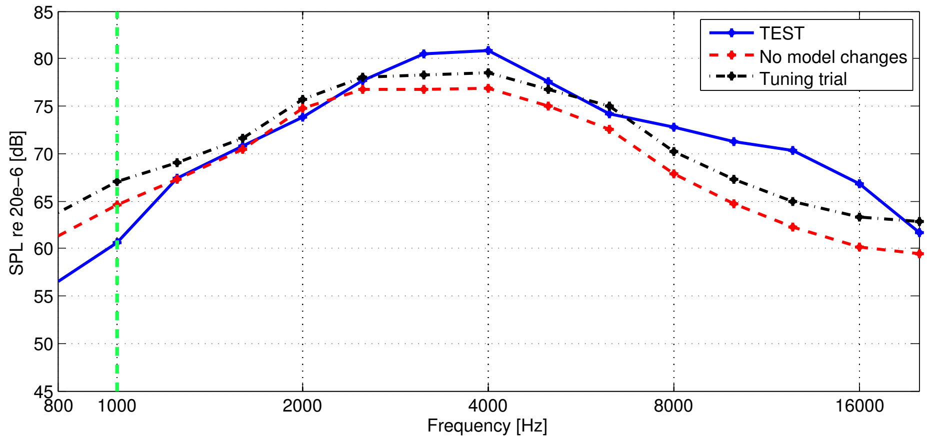

Figure 6.38.: FRF B2xMic1: test, simulations run with ALG2 with 200000 rays for old and new absorption coefficient values.

7. Findings

The three main parts of the thesis project were measurements and evaluation of the material paramaters, the source directivity investigation and the GA simulations evaluation. In this chapter the general findings on all three are reported.

The material parameters were obtained using the Microflown PU probe. The following conclusions on the absorption coefficient were drawn:

- The PU probe enables the user to measure the normal incidence impedance *in-situ* that is a big advantage over Kundt's tube and reverberation chamber method.
- The acquired data includes phase information that can be used in FE modelling when needed.
- The GA software requires the random absorption coefficient values in octave bands so the post-processing of Microflown PU data has to be done.
- The Microflown PU probe has its limitations. It works best for the flat specimen of size 30x30 cm, also it does not give reliable results for highly reflective surfaces.
- For curved surfaces the user has to make sure that the reflections after direct impulse do not contribute to the impedance calculation. It can be checked and sometimes corrected manually in the windowing option in the *Impedance 3.2* software.
- For the reflective surfaces (e.g. windows) the literature values can be used, as they provide more reasonable result. Also, another measurement method could be introduced.
- In the car compartment, that is a small enclosure, many close reflection apart from direct impulse can contribute to the impedance values. Again, it is beneficial to window them out manually in the software.

General points on the directivity measurements of the tweeter and the midrange are:

- The measurement of directivity data of a speaker requires a good understating of measurement method and of the directivity file format the data is to be used.
- The directivity measurement designed for CF2 file format (full 5 ° and 1/3 octave resolution) turned out to be a big project in itself. During the work it was decided to use a simpler directivity format. It was SD0 format that gives the data in octave bands with 15 ° resolution and is an approximation of the source directivity.
- For improving the simulation quality the CF2 format should be used. Such data can be measured or requested from the manufacturer, as it is format commonly used by the loudspeaker producers.

- When using SD0 format the measurements of speakers mounted in a baffle approximate the response of the speakers mounted in the car door on the agreeable level.
- In case of independent measurements of directivity it is good to bear in mind the issues with diffraction on the edges - especially for the midrange. If the measurement is conducted in a baffle the absorption should be put on the edges or the baffle should be big enough. If the measurement is conducted in a car door it would be a benefit to put some absorption on the car door edges as well.
- When measuring the tweeter in the car door the comb filtering effects were noticed. It was not a problem for the measurement conducted in the baffle. Thus, it is believed that the problem occurs due to door structure. This problem could be studied in the future for better understanding of tweeter behaviour.

The most important part of the thesis includes the comparison of the measured and modelled in *CATT-Acoustic* FRFs and IRs. The following outcomes of the evaluation are:

- In such a small and highly damped room as car compartment the shape of the IR is dominated by the direct sound and first reflections. Therefore it is of high importance to model the surfaces close to the loudspeakers with special care, meaning geometry, absorption coefficients and scattering coefficients.
- It also means that if the modelled receivers are misplaced in relation to the measurement positions the errors may occur. Each small discrepancy in location leads to different IR results as shown in scattering study. Thus, it is good to be sure that model represents reality as good as possible. If it is not the case, all tuning attempts of the model can be incorrect.
- The higher LOD for BIB case did not improve the results noticeable. Thus, it is suggested that BIB can be properly simulated using the simple LOD models.
- For a trimmed body case (both without and with seats) the results were slightly better for high LOD at high frequencies. Thus, it can be of interest to use simple models to simulate the midrange behaviour and detailed models to run the tweeter predictions.
- For the BIB case ALG1 can be successfully used to model the sound field, when the short computation time is of interest.
- In the trimmed body cases ALG2 is suggested as more complex and reliable. 20000 rays was proved to be a sufficient number of rays.
- The use of higher number of rays in trimmed body showed that front B pillar geometry and coefficient values should be rethought and improved.
- The comparison of the old and new directivity data models proved that the quality of the simulations relies greatly on the loudspeakers input data. Even though the SD0 format used in the project allowed to capture the general behaviour of the car compartment it would be beneficial to use more detailed file format, for example CF2.

- As proved during simulations evaluation the properly measured and modelled directivity data provides much better results for all three cases.
- Tuning the models of trimmed body by editing the absorption coefficients values should be well planned and aimed to correctly predict the FRFs in both cases (without and with seats).
- Generally, the trimmed body case with the seats was more difficult case to model. Still, the results were satisfying, especially if it is taken into account that it was the first use of GA at Volvo. The discrepancies between the measured and modelled data fell into +/- 5 dB range. Also, the use of *auto-edge* scattering provided by the GA software is suggested in order to improve the results.

When it comes to the simulations of the real audio system loudspeakers, the best results for each trim level were obtained for the new directivity data. In case of BIB model the best response was obtained for Mic5 for the midrange and Mic3 for the tweeter. The FRFs are presented in Figure 7.1.

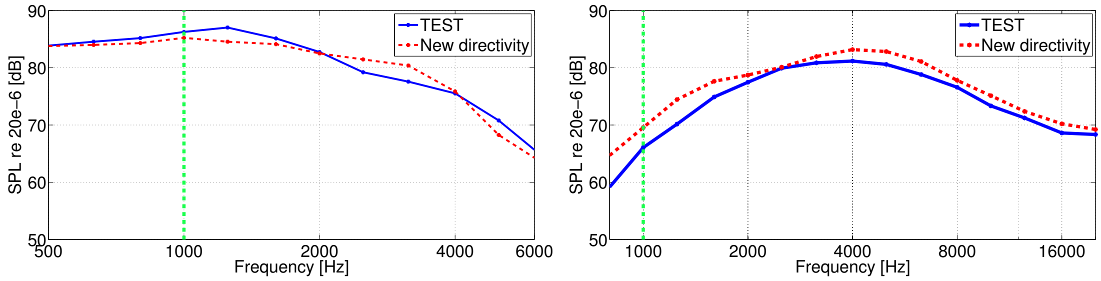

(a) (b)

Figure 7.1.: The best matching results for BIB: FRF B1xMic5, FRF B2xMic3.

The same combinations of source and receiver gave the best match in trimmed body without seats. The results are presented in Figure 7.2.

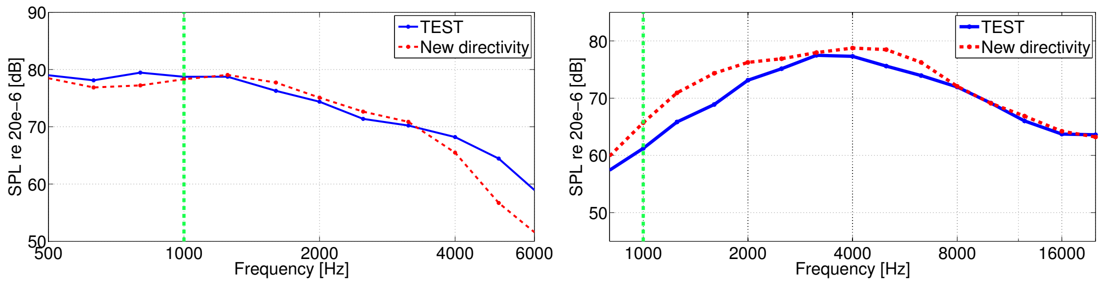

(a) (b)

Figure 7.2.: The best matching results for trimmed body without seats: FRF B1xMic5, FRF B2xMic3.

For the trimmed body with seats the best results were obtained when the new directivity data was used and additionally the tuning trial was conducted. The tuning included the alternation of absorption coefficient as described in Section 6.3.3. Also, the *auto-edge* scattering was assigned to all the surfaces in the model. Mic10 exhibit the best match for the midrange source and Mic9 for the tweeter. Figure 7.3 presents the FRFs.

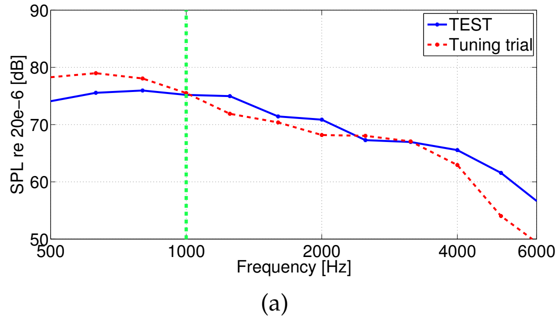

Figure 7.3.: The best matching results for trimmed body without seats: FRF B1xMic10, FRF B2xMic9.

Finally, it is good to emphasize that the data obtained out of the GA simulations could be expressed in time domain. The example of IR for the best BIB case excited with midrange is presented in Figure 7.4. Modelled and measured IRs are both filtered for octave band centered at 1000 Hz.

In the long term the scope of the work could be prediction and export of the IRs for the receivers located in the middle of the potential passengers' heads. Using convolution and HRTF data the sound files could be created out of any input sound signals. But before getting to this stage of the project the further small improvements of GA models could be done. Even though, the shape of the IRs differ, the subjective evaluation of the sound files could still lead to better design. That is because subjective listening is essentially different from the curve to curve comparison.

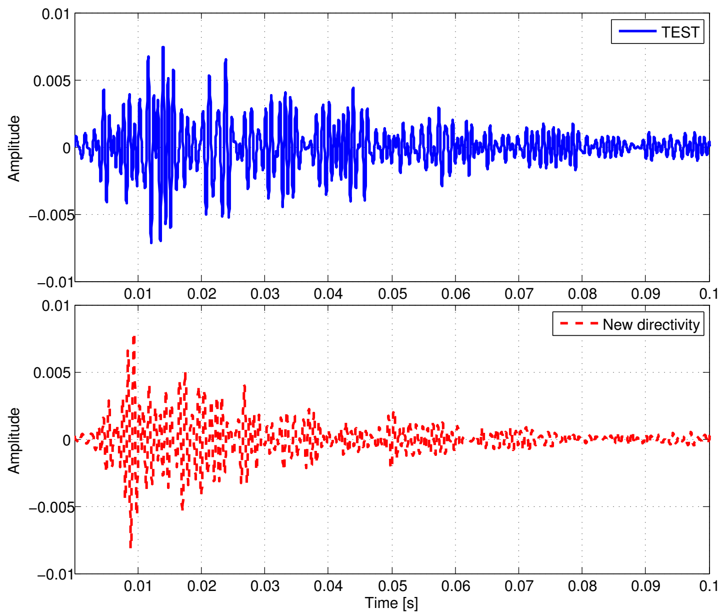

Figure 7.4.: IR B2xMic5 for 2000 Hz octave band: test and the best simulation for BIB.

8. Summary

Generally, the company has developed the broad use of the FE based methods in most of designing processes. The numerical methods basically support the design process of the low frequency audio system speakers and the high frequency speakers are tested in prototype vehicles with restricted availability. The need of high frequency modelling arose, since the virtual environment testing is planned for all the car components.

In the scope of the thesis the investigation on GA method used for high frequency simulation of the car compartment sound field was done. The method was newly used at Volvo and it was tested because the FE methods require a lot of time to simulate the sound field for higher frequencies due to great modal overlap. Also, the FE method would require extremely fine mesh to model very high frequencies. At some point the detail of mesh would have to include even the porosity of the materials. The simplified energy-based GA method allows to simulate the high frequency behaviour in much lower time. Also, it allows to capture the physical aspects of the source, such as its directivity, and of the material parameters, such as their absorption and scattering.

For the project a world widely used GA based software developed in Göteborg was chosen. The models were built manually in *ANSA* from the fine mesh FE models. The three trim levels of car compartment were modelled and for all of them the two models with low and high LOD were created:

- Body-in-Blue - glass and metal empty cavity of a car
- Trimmed body without seats - final trim level with removed seats
- Trimmed body with seats - final trim level

The input data needed for modelling, that was measured during the scope of the thesis, included the random absorption coefficient and the source directivity. Obtaining a good quality and reliable input data is of a high importance for good simulation results as proved in the report. And it is not an easy task in itself. There were several uncertainties about the methods that were tested and discussed. Also, some of the measurements had to be repeated. At the end it was a learning process how to obtain good input data and it is known that the measurement methods can be further investigated and improved.

Microflown PU probe was used to measure the normal incidence impedance, that later was converted to the random absorption coefficient needed for the GA software. Generally, the Microflown PU is a method that can be used *in-situ*, but has its limitation. Most of the measured absorption coefficient had to be extrapolated due to unreasonable shape of the curves. For materials that gave most unreliable results the literature data was used instead. Such approximation of absorption coefficient still provided satisfying GA results.

The directivity was measured in order to obtain the data supported by SD0 format file. It interpolates the data from values given in octave bands entered for a horizontal and vertical polar with resolution of 15 °. It was shown that carefully conducted measurements of directivity provided better results than the ones that exhibited edge diffraction issues. Therefore, the high quality data determines the accuracy of the GA simulations. Also, use of more complex directivity file format CF2 could be beneficial. Such files could be requested form the manufacturer side.

For BIB the Volvo HF speaker as well as Volvo audio system loudspeakers were successfully simulated with ALG2, 20000 rays and echogram length of 3000 ms. However, if the short run time is of interest the echogram could be lower to 1000 ms. Also, it was proved for Volvo HF speaker case that the simpler and more random ALG1 can be used for modelling BIB. It gives good results in shorter time than more deterministic ALG2. The suggested number of rays for ALG1 is at least 1000000.

For the trimmed body without seats the Volvo audio system loudspeakers were successfully simulated. The several small issues showed that the improvement of the front door trim modelling could be beneficial. Also, the use of the *auto-edge* scattering for further simulations would be suggested. The trimmed body with seats case was more difficult to simulate. Still, the results are very good. The improvement of the seats geometry and absorption is important for further predictions. Generally, ALG2 with 20000 rays and echogram length of 50 ms is enough to capture the behaviour of the trimmed body excited with different sources.

Eventually, it was shown that the GA based methods can be used for car compartment prediction. However, it is important to bear in mind all the limitations of the method. Good quality data provides better results. Also, the placement of the receivers in the GA models should reflect the measurement locations as good as possible, since the response relies greatly on the direct sound and first reflections in such a damped room. Generally, it is believed that the GA based simulations could be in the future used in the high frequency audio designing process. Merging the results with low frequency FE based simulation would allow to auralize the signals and provide the sound files that could be assessed subjectively during the listening tests in the virtual environment.

Possible further work could cover the following problems:

- Further investigation on influence of scattering coefficient
- Investigation on the diffraction model in GA simulations and model tuning
- Merging results of GA with FEM covering the low frequency part
- Study on the influence of the passengers in the car on the sound field
- Auralization and listening tests to assess the quality of auralized signals

References

[1] Kuttruff H: *Room Acoustics*, 5th edition, Aachen, Germany, Spon Press, 2009.

[2] Krokstad A, Strom S, aSorsdal S. *Calculating the acoustical room response by the use of a ray tracing technique*, Journal of Sound and Vibration, 8(1):118125, 1968.

[3] Kleiner Mendel, Jiri Tichy: *Acoustics of Small Rooms Oscillations*, CRC Press, Taylor & Francis Group, 2014.

[4] ISO 3382-1:2009, *Acoustics - Measurement of room acoustics parameters. Part 1: Performance spaces.*

[5] Granier Emmanuel: *Acoustical Prediction of Car Compartments. Monoaural Simulation*, Chalmers Univerity of Technology, December 1993.

[6] Aretz Marc: *Combined Wave and Ray Based Room Acoustic Simulations of Small Rooms. Challenges and limitations on the way to realistic simulation results*, PhD dissertation, RWTH Aachen Univeristy, 2012.

[7] Aretz M, Vorländer M: *Combined FE-GA simulations in a car compartment. Part II: Boundary and source data*, Applied Acoustics, 2012.

[8] Aretz M, Vorländer M: *Combined FE-GA simulations in a car compartment. Part II: Comparison of simulations and measurements*, Applied Acoustics, 2012.

[9] Aretz M, Vorländer M: *Efficient modelling of absorbing boundaries in room acoustic FE simulations*, Acta Acust Acust 2010; 96(6):104250.

[10] Muller-Trapet M, Dietrich P, Aretz M, Gemmeren van J, Vřlander: *On the in-situ impedance measurement with PU probes - Simulation of the measurement setup*, RWTH Aachen Universit, J. Acoust. Soc. Am. 134 (2), August 2013.

[11] Summers J, Takahashi K, Shimizu Y, Yamakawa T: *Assessing the accuracy of auralizations computed using a hybrid geometrical-acoustics and wave acoustics method*, J. Acoust. Soc. Am. 2004; 115(5):25145.

[12] *CATT-Acoustic v 9.0*, Users Manual, CATT-Acoustic^{TM} v 9.0, Sweden, January 2011.

[13] *TUCT TM v 1.0 g*, Users Manual, CATT-Acoustic^{TM} v 9, Sweden, 2011.

[14] Pelzer S, Aretz M, Vorländer M: *Quality assessment of room acoustic simulation tools by comparing binaural measurements and simulations in an optimized test scenario*, Forum Acusticum Aalborg, Denmark; 2011.

[15] Aretz M, Knutzen J:*Sound field simulations in a car passenger compartment using combined wave- and ray-based simulation methods*, EURONOISE, Edinburgh, Scotland; 2009.

[16] Granier E, Klainer M, Dalenbäck B-I, Svensson P: *Experimental auralization of car audio installations*, Journal of the Audio Engineering Society, 44(10):835-849, 1996.

[17] Vorländer M, Auralization: *Fundamentals of Acoustics, Modelling, Simulation, Algorithms and Acoustics Virtual Reality*, RWTH Aachen Univeristy, Springer 2008.

[18] Svensson P, Savioja L: *Overview of geometrical room acoustic modelling techniques*, J. Acoust. Soc. Am. 138 (2), August 2015.

[19] London A: *The Determinantion of Reverberant Sound Absorption Coefficients from Acoustic Impedance Measurements*, J. Acoust. Soc. Am., Vol. 22 (2), March 1950.

[20] Microflown Technologies Manual: *Impedance Setup*, V2.0 2013 - 10, Arnhem, The Netherlands.

[21] Microflown Technologies Manual: *Impedance 3.2*, M.V1.0 2014 - 04, Arnhem, The Netherlands.

[22] Microflown Technologies: *The Microflown E-book, Chapter 6: Impedance*, November, 2008, Arnhem, The Netherlands.

[23] International Standard *IEC 60268 5:2003 + A1:2007: Sound system equipment Part 5: Loudspeakers*, third edition, 2003-05.

[24] *www.clfgroup.org*, last visited: 2016-06-07.

[25] *http://blog.bowers-wilkins.com/speakers/car-audio/announcing-a-new-audio-system-for-volvo/*, last visited: 2016-05-25.

[26] *https://mediatech.aalto.fi/en/research/virtual-acoustics/research/room-acoustics-modeling/69-geometrical-acoustics*, last visited: 2016-06-02.

A. Absorption coeffiecient values

A.1. Body-in-Blue

In the GA models of BIB the following absorption coefficient was ascribed to the surfaces, given for octave bands 125 to 16000 Hz (the values are presented in %):

Reflective surface (from Sabine)	19.5	17.9	18.4	14.9	12.1	8.6	:	5.4	3.1

A.2. Trimmed body

In the GA models of trimmed body the following absorption coefficient was ascribed to the surfaces, given for octave bands 125 to 16000 Hz (the values are presented in %):

Laminated glass (from literature)	18.0	6.0	4.0	3.0	2.0	2.0	:	-	-
Material above windows	58.7	53.4	54.0	50.2	54.1	60.3	:	-	-
Front car below IP	59.2	59.2	59.2	55.7	52.6	72.2	:	72.2	72.2
Floor under front seats	18.2	18.2	18.2	17.7	37.7	46.3	:	-	-
Floor under IP	16.6	16.6	16.6	16.6	45.6	88.7	:	-	-
Carpet material in front	19.9	22.2	26.5	36.2	50.3	54.5	:	80.3	80.3
Carpet material at the back	23.3	23.3	23.3	27.4	51.2	52.9	:	64.8	70.0
Floor under back seat	15.6	15.6	15.9	15.9	13.3	26.7	:	49.7	55.0
Tailgate door trim	51.2	51.2	51.3	50.0	45.4	51.3	:	-	-
Door trim - back left	43.0	39.1	45.0	51.0	43.4	50.9	:	59.8	65.0
Headliner with window	35.8	37.4	40.4	47.6	61.3	70.2	:	-	-
Pillar	19.8	19.8	19.8	19.8	16.3	39.4	:	-	-
Tailgate walls material	41.0	41.0	41.0	42.0	41.6	13.2	:	-	-
Gear tunnel material (side)	19.8	21.1	22.1	22.9	23.8	13.2	:	13.2	13.2
Gear tunnel material (top)	31.7	31.7	31.7	32.8	40.9	66.8	:	70.0	75.0
Rear of the seat	35.3	35.3	35.3	38.7	27.3	21.5	:	31.1	31.1
Seat - head rest	54.0	54.0	54.0	54.0	54.0	32.0	:	-	-
Seat - back rest	79.0	79.0	79.0	83.0	83.0	62.0	:	-	-
Seat - seating	90.0	90.0	90.0	90.0	90.0	74.0	:	-	-
Plastic chairs (from [17])	6.0	10.0	10.0	20.0	30.0	30.0	:	20.0	20.0
Material above armrest	7.5	9.6	12.6	18.0	28.5	33.3	:	-	-
Armrest material	26.5	28.7	33.0	42.6	55.5	47.9	:	-	-

When the values for 8000 and 16000 Hz are not provided, they are extraolated from 2000 and 4000 Hz values in GA.

For a tuning trial the two materials were altered. The plastic elements on the pillars and IP were modelled using much lower absorption values found in the literature. Also the panorama roof was changed to have lower values at 8 and 16 kHz octave bands. The absorption coefficient fot the tuning was set to:

New headliner with window	35.8	37.4	40.4	47.6	61.3	70.2	:	67.8	67.0
Plastic (from literature)	3.0	3.0	3.0	3.0	5.0	5.0	:	-	-

B. Directivity polars

The chapter includes the information on directivity data used in GA software. The directivity function at any angle $D(\theta, \gamma)$ is defined as a ratio of frequency response at this angle to the on-axis emission, when both are determined at the same distance from the source in a far field [6]. The directivity data was modelled using SD0 file format that is used by the software. In the polard the directivity index is presented:

$$DI = 10 \cdot log_{10}(D) \tag{B.1}$$

The sources are presented in the SD0 format for the following measurement cases:

- Midrange measured in a clean baffle
- Midrange measured in a car door
- Midrange measured in a baffle with mineral wool on the edges
- Tweeter measured in a clean baffle
- Tweeter measured in a car door
- Tweeter measured in a baffle with acoustic foam on the edges

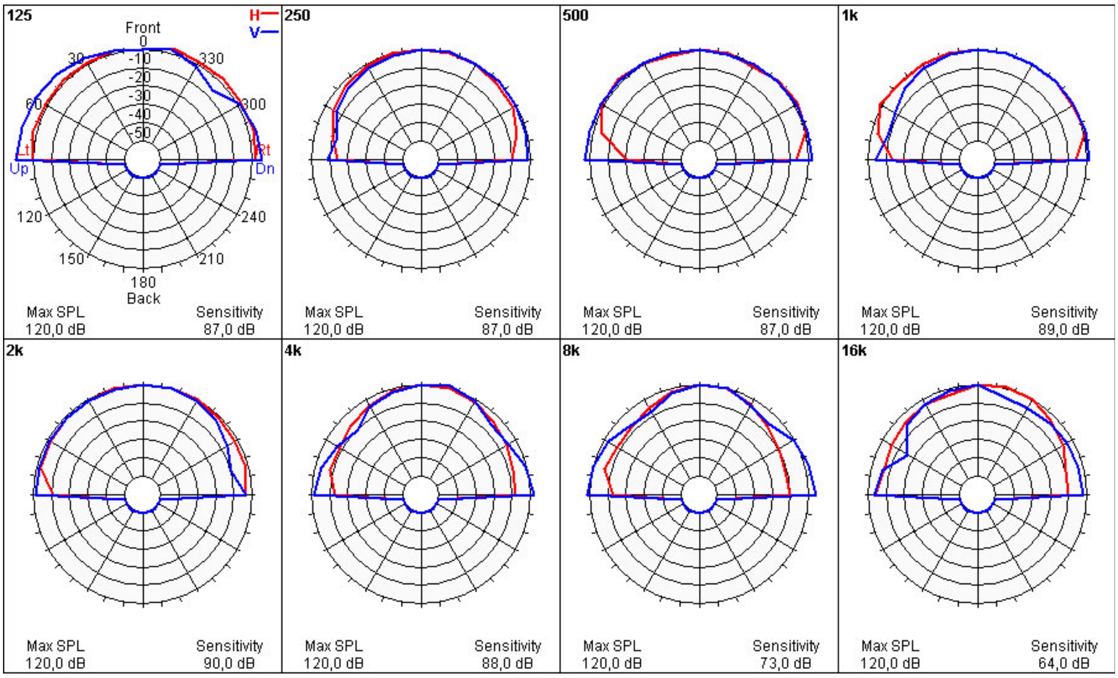

Figure B.1.: Polar diagrams: horizontal and vertical directivity function for midrange measured in a clean baffle.

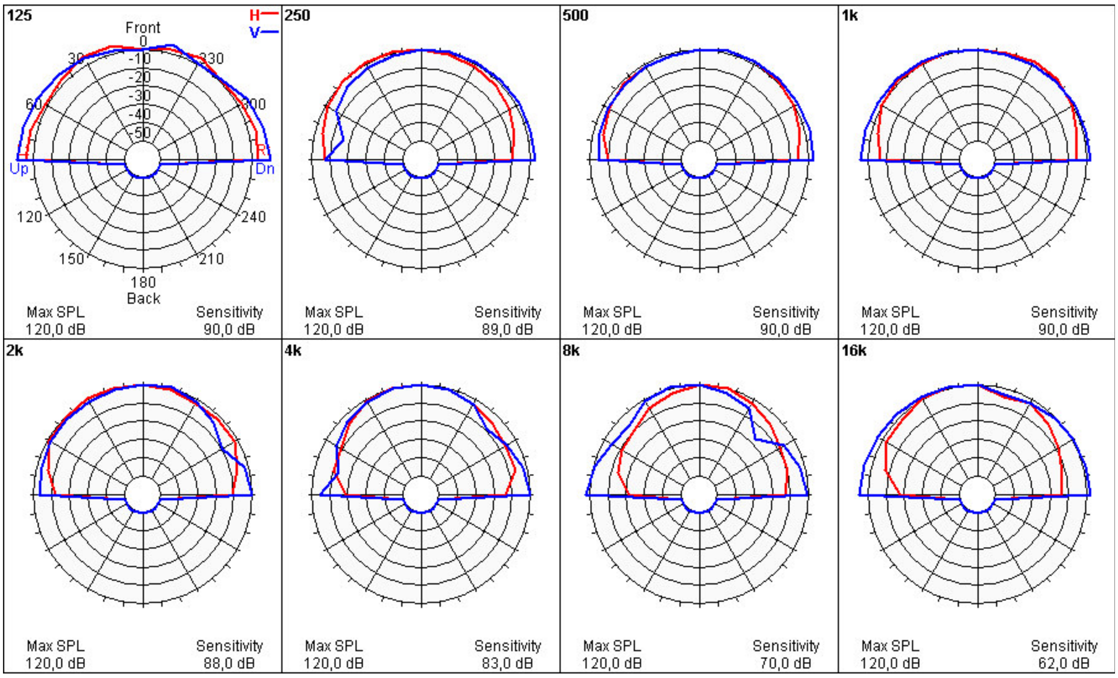

Figure B.2.: Polar diagrams: horizontal and vertical directivity function for midrange measured in a car door. Also, referred as "old directivity data" in Section 6.

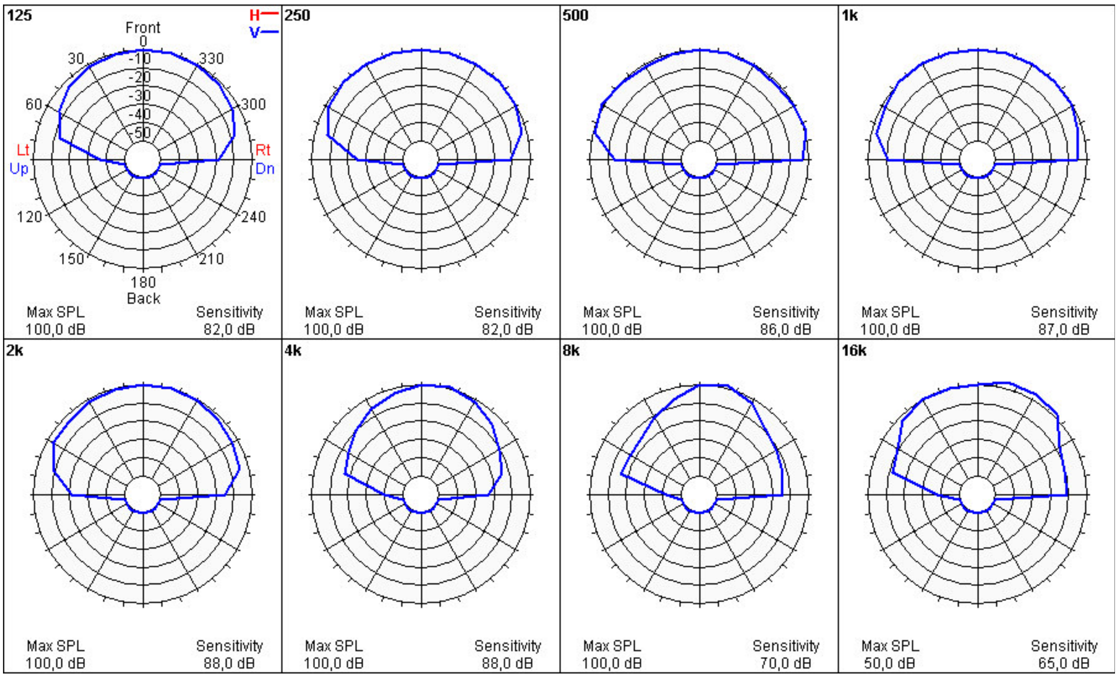

Figure B.3.: Polar diagrams: horizontal and vertical directivity function (symmetric) for midrange measured in a clean baffle with mineral wool on the baffle edges. Also, referred as "new directivity data" in Section 6.

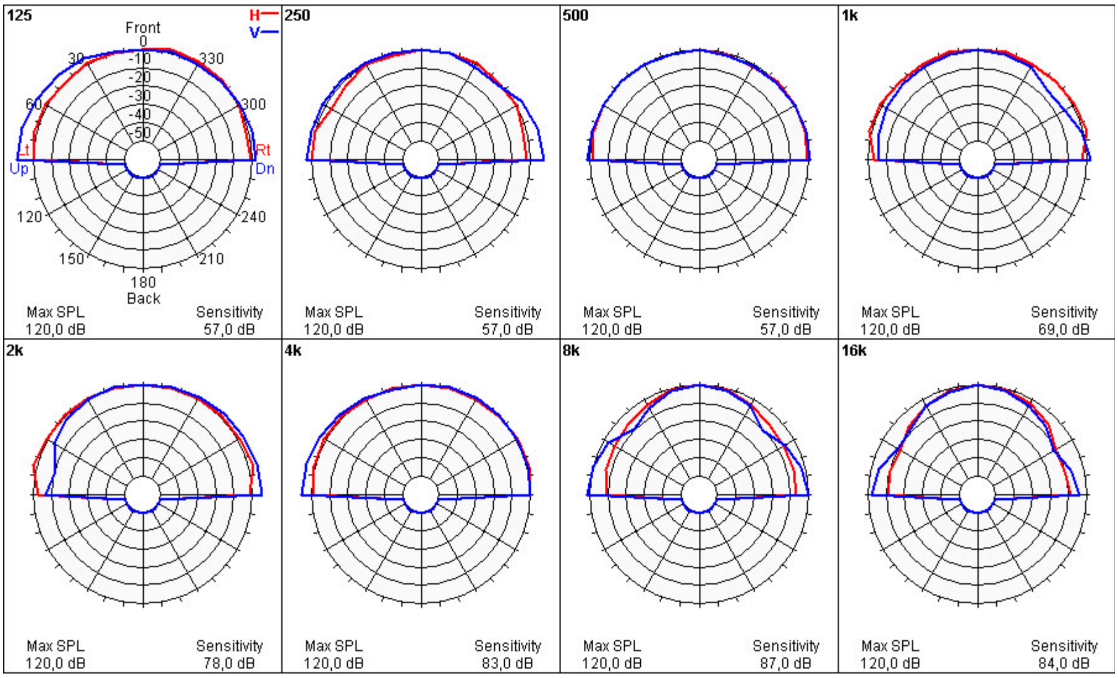

Figure B.4.: Polar diagrams: horizontal and vertical directivity function for tweeter measured in a baffle. Also, referred as "old directivity data" in Section 6.

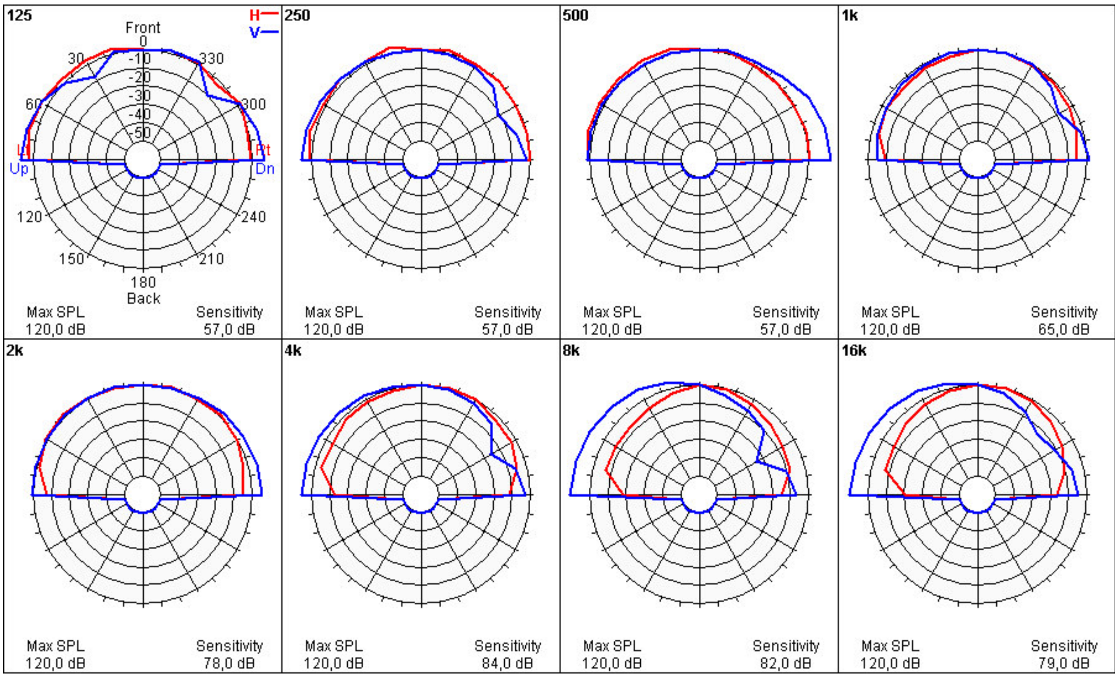

Figure B.5.: Polar diagrams: horizontal and vertical directivity function for tweeter measured in a car door.

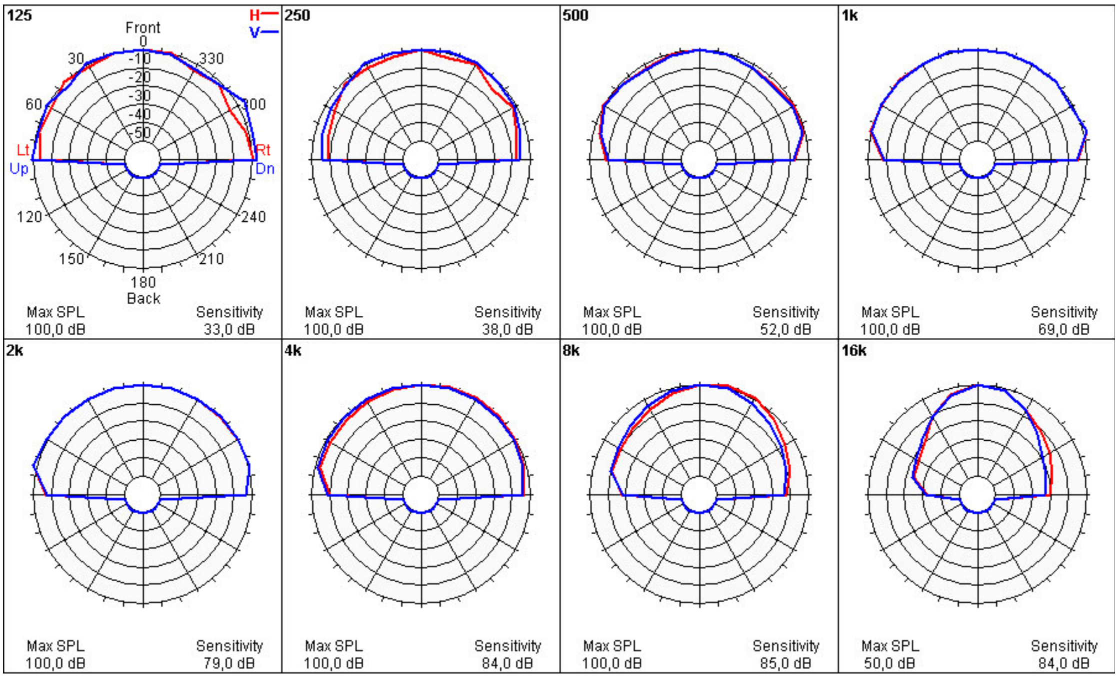

Figure B.6.: Polar diagrams: horizontal and vertical directivity function (symmetric) for tweeter measured in a baffle with acoustic on the baffle edges. Also, referred as "new directivity data" in Section 6

C. Models comparison

Below there are presented all the models that were compared in Section 6. The computer CPU was E5-2620 v2 (12 cores). It is worth to mention that some very long computation times could be caused by the fact that several different simulations were running at the same machine at the same time.

C.1. Resolution study

The trimmed body without seats model was studied for LF midrange for $d = 5$ cm:

Model	Source	Algorithm	Rays	Echogram	LOD	Run time
Model, $d = 5$ cm	B1	ALG2	200000	100 ms	simple	00:19:02

The trimmed body without seats model was studied for LF midrange for $d = 2$ cm:

Model	Source	Algorithm	Rays	Echogram	LOD	Run time
Model, $d = 2$ cm	B1	ALG2	200000	100 ms	simple	00:17:52

C.2. Body-in-Blue

Different levels of complexity

The following two models were compared to measurements for Volvo HF speaker:

Model	Source	Algorithm	Rays	Echogram	LOD	Run time
Model 1	A1	ALG1	2000000	3000 ms	simple	01:46:02
Model 2	A1	ALG1	2000000	3000 ms	detailed	18:18:07

Different algorithms

The following two models were compared to measurements for Volvo HF speaker:

Model	Source	Algorithm	Rays	Echogram	LOD	Run time
Model 1	A1	ALG1	2000000	3000 ms	simple	01:46:02
Model 2	A1	ALG2	20000	3000 ms	simple	01:18:21

New directivity

The following two models were compared to measurements for LF midrange:

Model	Source	Algorithm	Rays	Echogram	Directivity	Run time
Model 1	B1	ALG2	20000	3000 ms	car door	similar as below
Model 2	B1	ALG2	20000	3000 ms	absorptive baffle	01:02:38

The following two models were compared to measurements for LF tweeter:

Model	Source	Algorithm	Rays	Echogram	Directivity	Run time
Model 1	B2	ALG2	20000	3000 ms	car door	02:25:35
Model 2	B2	ALG2	20000	3000 ms	absorptive baffle	similar as above

C.3. Trimmed body without seats

Different number of rays

The following two models were compared to measurements for LF midrange:

Model	Source	Algorithm	Rays	Echogram	LOD	Run time
Model 1	B1	ALG2	20000	200 ms	simple	00:31:16
Model 2	B1	ALG2	500000	200 ms	simple	02:18:11

Different levels of complexity

The following two models were compared to measurements for LF midrange:

Model	Source	Algorithm	Rays	Echogram	LOD	Run time
Model 1	B1	ALG2	20000	200 ms	simple	00:31:16
Model 2	B1	ALG2	20000	200 ms	detailed	15:28:15

The following two models were compared to measurements for LF tweeter:

Model	Source	Algorithm	Rays	Echogram	LOD	Run time
Model 1	B2	ALG2	20000	200 ms	simple	00:48:08
Model 2	B2	ALG2	20000	200 ms	detailed	06:59:38

New directivity

The following two models were compared to measurements for LF midrange:

Model	Source	Algorithm	Rays	LOD	Directivity	Run time
Model 1	B1	ALG2	20000	simple	car door	similar as below
Model 2	B1	ALG2	20000	simple	absorptive baffle	00:21:01

The following two models were compared to measurements for LF tweeter:

Model	Source	Algorithm	Rays	LOD	Directivity	Run time
Model 1	B2	ALG2	20000	simple	car door	similar as below
Model 2	B2	ALG2	20000	simple	absorptive baffle	00:21:01

C.4. Trimmed body with seats

Different number of rays

The following two models were compared to measurements for LF midrange:

Model	Source	Algorithm	Rays	Echogram	LOD	Run time
Model 1	B1	ALG2	20000	200 ms	simple	00:34:27
Model 2	B1	ALG2	500000	200 ms	simple	01:15:23

The following two models were compared to measurements for LF tweeter:

Model	Source	Algorithm	Rays	Echogram	LOD	Run time
Model 1	B2	ALG2	20000	200 ms	simple	01:18:37
Model 2	B2	ALG2	500000	200 ms	simple	01:14:08

Different level of complexity

The following two models were compared to measurements for LF midrange:

Model	Source	Algorithm	Rays	Echogram	LOD	Run time
Model 1	B1	ALG2	20000	200 ms	simple	00:34:27
Model 2	B1	ALG2	20000	200 ms	detailed	05:56:02

The following two models were compared to measurements for LF tweeter:

Model	Source	Algorithm	Rays	Echogram	LOD	Run time
Model 1	B2	ALG2	20000	200 ms	simple	01:18:37
Model 2	B2	ALG2	20000	200 ms	detailed	08:19:48

New directivity

The following two models were compared to measurements for LF midrange:

Model	Source	Algorithm	Rays	LOD	Directivity	Run time
Model 1	B1	ALG2	20000	simple	car door	00:34:27
Model 2	B1	ALG2	20000	simple	absorptive baffle	similar as above

The following two models were compared to measurements for LF tweeter:

Model	Source	Algorithm	Rays	LOD	Directivity	Run time
Model 1	B2	ALG2	20000	simple	car door	similar as below
Model 2	B2	ALG2	20000	simple	absorptive baffle	00:47:15

Tunning procedure

The following two models were compared to measurements for LF midrange:

Model	Source	Algorithm	Echogram	Directivity	Absorption	Run time
Model 1	B1	ALG2	200 ms	absorptive baffle	old	00:34:27
Model 2	B1	ALG2	50 ms	absorptive baffle	new	00:23:17

The following two models were compared to measurements for LF tweeter:

Model	Source	Algorithm	Echogram	Directivity	Absorption	Run time
Model 1	B2	ALG2	200 ms	absorptive baffle	old	00:47:15
Model 2	B2	ALG2	50 ms	absorptive baffle	new	00:23:17